Identification of the SNARE proteins involved in the postsynaptic membrane trafficking

Julia Krapivkina

université de BORDEAUX

THÈSE

Pour le
DOCTORAT DE L'UNIVERSITE DE BORDEAUX

Ecole doctorale Sciences de la Vie et de la Santé
Mention : Sciences, Technologie, Santé
Option : Neurosciences

Présentée et soutenue publiquement
Le 29 novembre 2016

Par **Julia Krapivkina**
Né le 20 juillet 1988 à Essentouki

Identification of the SNARE proteins involved in the postsynaptic membrane trafficking

---

Sous la direction de : David PERRAIS

Co-directeur : Camin DEAN

Membres du jury

M GARRET Maurice, Université de Bordeaux	Président du Jury
Mme DESNOS Claire, Université Paris Descartes	Rapporteur
M El Far Oussama, Université Aix Marseille	Rapporteur
Mme DANGLOT Lydia, Université Paris Diderot	Examinateur
M LANG Jochen, Université de Bordeaux	Examinateur
M PERRAIS David, Université é de Bordeaux	Directeur de thèse

To my husband
and my little Sunrise

Acknowledgements

I want to thank Claire Desnos (Université Paris Descartes) and Oussama El Far (Université Aix Marseille) for kindly accepting to read and evaluate the manuscript. I thank other jury members: Lydia Danglot (Université Paris Diderot), Maurice Garret (Université de Bordeaux) and Jochen Lang (Université de Bordeaux) for agreeing to judge my work. I am very honoured by your presence.

I would like to thank Daniel Choquet for welcoming me in his group and giving the opportunity to work with cutting edge imaging technics. It was a pleasure to be a part of Choquet's team, and I thank all past and present members that form its incredible scientific diversity. I would like to express my most sincere gratitude to my PhD supervisor, David Perrais, who has literally taught me the biology and the research. Thank you for your passion for research and knowledge, for your patience and your trust in me, but also for warm parties at your home, delicious and the most original cakes and all fun that we had together in "les Perrais" minigroup.

I am grateful to Damien Jullié, who has initiated this project, coached me in confocal microscopy and always remembered that to do a good job one should also know how to have fun. Many thanks to Jennifer Petersen, who was always there for any immunocytochemistry problem and with whom I shared interesting discussion about anything, to Kalina Haas, for giving me the place to live during the first months of my PhD and whom I admire a lot for her deep dedication for science. I am grateful to Andrew Penn and Mathieu Letellier, who have shared their experience and eased my conversion to electrophysiology. I thank Sebastien Marais and the BIC team for their help and support in very difficult moments of microscopy breakdown. I thank culture-BM team: Emeline Verdier, Natacha Retailleau, Christelle Breillat, Béatrice Tessier, Zeynep Karatas, IINS would be impossible without you. I am very grateful to Delphine Bouchet and Pauline Durand, who has kindly taught me organotypic slice

preparation. My very sincere thanks to all people who worked and work in the endo-exo team and especially to Morgane Rosendale for her vibrant spirit and warm talks around a cup of tea, Thi Nhu Ngoc Van for her strong character, love for parties and an example of a woman who “can it all”, Magalie Martineau for her enigmatic smile and invaluable support during the last weeks of my thesis writing, Léa Claverie for her vivacity and amazing sociability capacities. I thank all IINS people that I met during my PhD, for your smiles, for little and big discussions, for making the Institute a unique place where cultures from all over the world meet around the table at lunchtime.

My dear mother, thank you for everything you did to me, for you love, support and understanding throughout my life. I would not be the person I am without you. My poor husband, I hope that my PhD years did not make you regret marrying this crazy woman. You supported my back every single day and granted me with too much love. And I thank my little daughter, who is covering the apartment with drawings while I’m finishing my manuscript, for all the happiness and joy that she brought to my life.

Abstract

Membrane trafficking is a universal process that is essential for neuronal function in a wide spectrum of applications. From neuronal growth and morphological development to neurotransmitter release and synaptic plasticity, it supports neuronal activity and gives countless questions that drive today's neurobiology research. Notably, the trafficking of recycling endosomes (REs) in somatodendritic compartments participates in synaptic transmission and plasticity, such as long-term synaptic potentiation (LTP). However, the fusion machinery mediating RE exocytosis is still unclear. To identify the vesicular SNAREs (v-SNAREs) involved in different forms of postsynaptic RE exocytosis, we first imaged neuronal VAMP proteins fused with pH-sensitive pHluorin in cultured hippocampal neurons, and found that only VAMP2 and VAMP4, but not VAMP7, underwent somatodendritic exocytosis in mature neurons. After identifying these two candidate proteins, we used a combination of different downregulation techniques to chronically or acutely deactivate their function and observe consequences on REs exocytosis, basal synaptic transmission and LTP. Our results suggest that VAMP2 is involved in activity-regulated exocytosis important for LTP, but not constitutive postsynaptic AMPARs exocytosis, supporting basal transmission. VAMP4 is required for constitutive exocytosis of at least a large proportion of REs, but the functional implication of these endosomes still need to be explored, as VAMP4 downregulation did not alter basal synaptic transmission.

Keywords: exocytosis, LTP, fluorescent microscopy, electrophysiology, SNARE, VAMP2, VAMP4, recycling endosomes.

Resumé

Le trafic membranaire est un processus universel qui est essentiel pour la fonction neuronale dans un large spectre de fonctions. De la croissance neuronale et le développement morphologique à la libération des neurotransmetteurs et la plasticité synaptique, il prend en charge l'activité neuronale et donne d'innombrables questions qui animent la recherche sur la neurobiologie d'aujourd'hui. Notamment, l'exocytose des endosomes de recyclage (ER) dans les compartiments somatodendritiques participe à la transmission synaptique et à la potentialisation synaptique à long terme (PLT). Cependant la machine moléculaire sous-tendant l'exocytose des ER reste encore méconnue. Afin d'identifier les protéines SNAREs vésiculaires (v-SNARE) impliquées dans les différentes formes d'exocytose des ER postsynaptiques, nous avons d'abord imagé les protéines VAMP neuronales fusionnées avec la pHluorine, une GFP mutée sensible au pH dans les neurones de l'hippocampe en culture. Nous avons constaté que seulement VAMP2 et VAMP4, mais pas VAMP7, rapportaient des événements d'exocytose somatodendritique dans les neurones matures. Après avoir identifié ces deux protéines candidates, nous avons utilisé la combinaison de différentes techniques de régulation négative chronique ou aiguë pour désactiver leur fonction et observer les conséquences sur l'exocytose des ER, la transmission synaptique basale ou la PLT. Nos résultats suggèrent que VAMP2 est impliqué dans une forme d'exocytose régulée importante pour la PLT, mais pas l'exocytose constitutive des récepteurs AMPA, qui stabilise la transmission basale. VAMP4 est nécessaire pour l'exocytose constitutive d'une grande partie des endosomes, mais l'implication fonctionnelle de ces endosomes doit encore être explorée, car la régulation négative de VAMP4 ne modifie pas la transmission basale.

Mots-clés: exocytose, PLT, microscopie à fluorescence, électrophysiologie, SNARE, VAMP2, VAMP4, endosomes de recyclage.

.

Publications and communications list

Publications:

Julia Krapivkina, Damien Jullié, Jennifer Petersen, Natacha Retailleau, Daniel Choquet & David Perrais. The identity if vSNAREs involved in recycling endosomes exocytosis in neuronal dendrites (in preparation).

Presentations and communications:

2013,-15 ENC Network Annual meeting (2013 Bordeaux, 2015 Coimbra).
Oral Presentation and Poster.

2013, -15 European Neuroscience Conference by Doctoral Students (2013 Bordeaux, 2015 Sesimbra).
Poster presentations.

2013,-14,-15 12th, 13th, 14th scientific meeting for PhD students of the Ecole Doctorale des Sciences de la Vie et de la Santé), Arcachon, France.
Poster presentation (2014, 2015)

2013 4thEuropean Synapse Meeting, Bordeaux, France.
Participant

2013 European Synapse Summer School, Bordeaux.
Instructor in the project “Studies of presynaptic function in a mouse model of intellectual disabilities”.

2015 18th "Exocytosis-Endocytosis club" congress, Evian les Bains, France.
Oral report and poster presentation

2016 10th FENS Forum of Neuroscience, Copenhagen, Denmark.
Poster presentation.

List of abbreviations

AA	Amino acid
ACPD	(1S, 3R)-1-amino-1, 3-cyclopentanedicarboxylic acid
aCSF	Artificial cerebral spinal fluid
AMPA	α-amino-3-hydroxy-5-methylisoxazole-4-propionic acid
AMPAR	α-amino-3-hydroxy-5-methylisoxazole-4-propionic acid receptors
BDNF	Brain derived neurotrophic factor
BoNT	Botulinum neurotoxin
BSA	Bovine serum albumin
DIV	Days in vitro
EGTA	Ethylene glycol-bis (β-aminoethyl ether)-N,N,N',N'-tetraacetic acid
EPSC	Excitatory postsynaptic current
EPSP	Excitatory postsynaptic potential
ER	Endoplasmic reticulum
ESC	Extracellular solution
FN3	Fibronectine3
GAP	GTPase-activating protein
GDF	GDI displacement factor
GDI	Rab GDP dissociation inhibitor

GDP	Guanosine diphosphate
GEF	guanine nucleotide exchange factor
GFP	Green fluorescent protein
GGT	Geranylgeranyl transferase
GTP	Guanosine triphosphate
IgG	Immunoglobulin G
HEPES	4-(2-hydroxyethyl)-1-piperazineethanesulfonic acid
IPSP	Inhibitory postsynaptic potential
KD	Knock-down
KO	Knock-out
LTP (cLTP)	Long-term potentiation (chemical long-term potentiation)
mEPSC	miniature Excitatory postsynaptic current
MVB	Multivesicular bodies
NMDA	N-Methyl-D-aspartic acid
NMDAR	N-Methyl-D-aspartic acid receptor
NSF	N-ethylmalmeimide-sensitive factor
PBS	Phosphate-buffered saline
PM	Plasma membrane
RE	Recycling endosome
REP	Rab escort protein
RNA	Ribonucleic acid
ROI	Region of interest
RRP	Readily releasable pool
RT	Room temperature
SCE	Single cell electroporation

SD	Standard deviation
SDCM	Spinning disk confocal microscope
SEM	Standard error of the mean
SEP	Super-ecliptic pHluorin
SM	Sec1/Munc18-like
SNAP	Soluble NSF attachment protein
SNAP-25	25-kDa synaptosome-associated protein
SNAREs	Soluble N-ethyl maleimide (NEM)-sensitive factor attachment protein receptor protein family
SR	Surrounding region
SV	Synaptic vesicle
TeNT	Tetanus neurotoxin
TGN	*Trans*-Golgi network
TIRF	Total internal reflection fluorescence
TTX	Tetrodotoxin
VAMP	Vesicle associated membrane protein
Vti1a	Vps10p tail interactor 1a

List of figures

Table of contents

Introduction

Exocytosis is a universal process of vesicular membrane fusion with the plasma membrane (PM) and the final step in intracellular transport of proteins and molecules inside vesicles to the cell exterior. In neurons, exocytosis has core role in such neuron-specific processes like neurotransmitter release, receptor delivery and plasticity.

Soluble N-ethyl maleimide (NEM)-sensitive factor attachment protein receptor protein family, or SNAREs, are part of the molecular machinery that mediate membrane fusion during trafficking and exocytosis. Different SNARE isoforms are involved in different types of exocytosis in neurons. While extensive studies have already described quite in detail the SNARE machinery mediating membrane fusion in presynaptic compartments, little is known about SNARE isoforms involved in postsynaptic exocytosis. The aim of this study is to reveal SNARE proteins engaged in recycling endosomes (RE) exocytosis in the postsynaptic compartments.

1 Neuronal cells

In the first part of the introduction, I would like to or introduce basic background notions, necessary for the understanding of the research subject. Provided information is based on two fundamental works, which are “Principles of Neural Science” by Eric R. Kandel, James H. Schwartz, Thomas M. Jessell (2000) and “Synapses” by W. Maxwell Cowan and Thomas C. Südhof, Charles F. Stevens (2001).

1.1 Basic units of the Nervous System

The nervous system is mainly formed with two types of cells: neuronal and glial cells. Neuronal and glial cells, or glia, are in roughly the same numbers in adult rat and humain brains (Azevedo et al. 2009; Bandeira et al. 2009), with an estimate of 86 billion neurons and 85 billion non neuronal cells in the adult human brain (Azevedo et

al. 2009). Glia surround neurons and their processes and support neuronal functioning by playing some fundamental roles like providing brain with structure, insulating neurons and neuronal groups from each other, removing debris after neuronal death, cleaning extracellular space by taking up chemical transmitters and different molecules released during synaptic transmission, and other. Recent evidence shows that glia cells, notably astrocytes, are also suspected to participate in information processing (Araque & Navarrete 2010; Croft et al. 2015).

Neurons, on the other hand, are considered as principal cells, which receive, process, transmit and store information. They are further classified in thousands of types that share, nevertheless, similar structural organisation consisting of three parts: cell body (soma), dendrites, and axon (Figure 1). The cell body serves as metabolic center, it has nucleus that contains genes and the machinery for RNA and proteins, although some of it can be deported to dendrites and axons. Dendrites are neuronal cell compartments that branch out in a tree-like manner and receive incoming signals from other nerve cells. Axon is a long and thin tubular protrusion arising from the cell body; it conducts electrical signals, or action potentials, to other neurons.

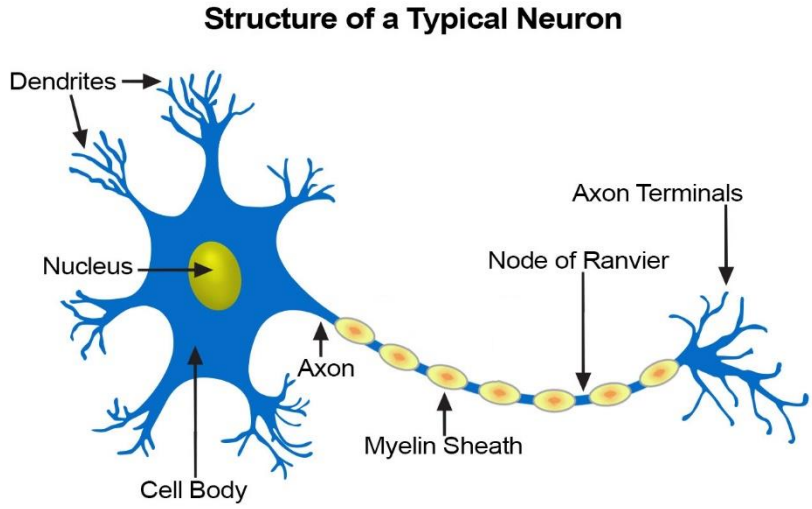

Figure 1 Neuronal architecture
Most neurons share same common features. The cell body contains the nucleus with genetic information and endoplasmic reticulum. Basal and apical dendrites receive incoming signals. Action potentials are generated in the axon's initial segment and propagated towards its terminals, contacting other neuronal cells. Most axons are insulated with fatty myelin sheaths alternated with nodes of Ranvier. Image is taken from U.S. National Cancer Institute's Surveillance, Epidemiology and End Results Program training web site.

Action potentials are rapid, all-or-none transient impulses of about 1 ms duration and an amplitude of about 100 mV. They are initiated in the axon's initial

segment. In the peripheral nervous system, special type of glia cells, named Schwann cells, tightly wrap their processes around the axon and cover it with insulating myelin sheaths alternated with the nodes of Ranvier. Uninsulated nodes of Ranvier are located at regular distances from each other and serve to regenerate action potential propagation in long motor and sensory neurons. In central nervous system, another type of glial cells called oligodendrocyte forms myelin sheaths. In white matter, they provide neurons with myelin, and in grey matter, oligodendrocytes support neuronal cell bodies. Axon myelination increases the propagation speed and signal regeneration maintains the amplitude of the action potential constant during its travel.

The axon divides into fine branches near its end and forms communication sites with other neurons. These sites are known as synapses and I will further discuss their structure in more detail.

1.2 Neuronal transmission

1.2.1 Synapse: the interface of neuronal connection

Synapse, neuron communication site, is an intercellular junction, allowing signal propagation between two cells. Synapses can be formed between two neurons or between a neuron and another excitable cell. Synapses are defined as electrical or chemical. In electrical synapses, transmission occurs via direct propagation of the electrical signal through the gap junction between neurons. Such type of transmission is very rapid, with the delay less than a millisecond, and usually can occur in both directions. Electrical synapses are found in all nervous systems, but they are a minority and have general role of synchronizing neuronal activity. Chemical synapses are sites of discontinuity of neuronal network where signal propagation occurs through a chemical intermediate called neurotransmitter. They are slower, due to the delays imposed by signal transmission through extracellular space, typically 0.5-1 ms, but possess important property of signal amplification and modulation. Most of the neuronal connections in the nervous systems are realised through chemical synapses and I will be referring to those when mentioning synapses.

In the context of a given synapse, the signal-transmitting cell is called presynaptic, and the receiving cell is called postsynaptic. Postsynaptic sites are located on the dendrites, but they also can be found on the soma or, very rarely, at the beginning or end of the axon of the receiving neuron. The electrical signal propagating in the axon triggers the exocytosis of the synaptic vesicles containing chemical neurotransmitters. Neurotransmitter is thus subsequently released into the little space of 20 – 40 nm separating the opposed membranes called synaptic cleft (Figure 2). After diffusion across the synaptic cleft, neurotransmitter binds to specific receptors located on the postsynaptic membrane and that opens or closes ion channels, and thus changes postsynaptic membrane conductance and potential. The most common neurotransmitters are glutamate for excitatory synapses and GABA or glycine for inhibitory synapses. In the hippocampus, which is the structure I will focus my work on (see 1.3), glutamatergic synapses on pyramidal cells are formed mainly on dendritic spines, small protrusions arising from dendrites, whereas inhibitory GABAergic synapses are found mainly on the dendritic shaft, as well as on the soma.

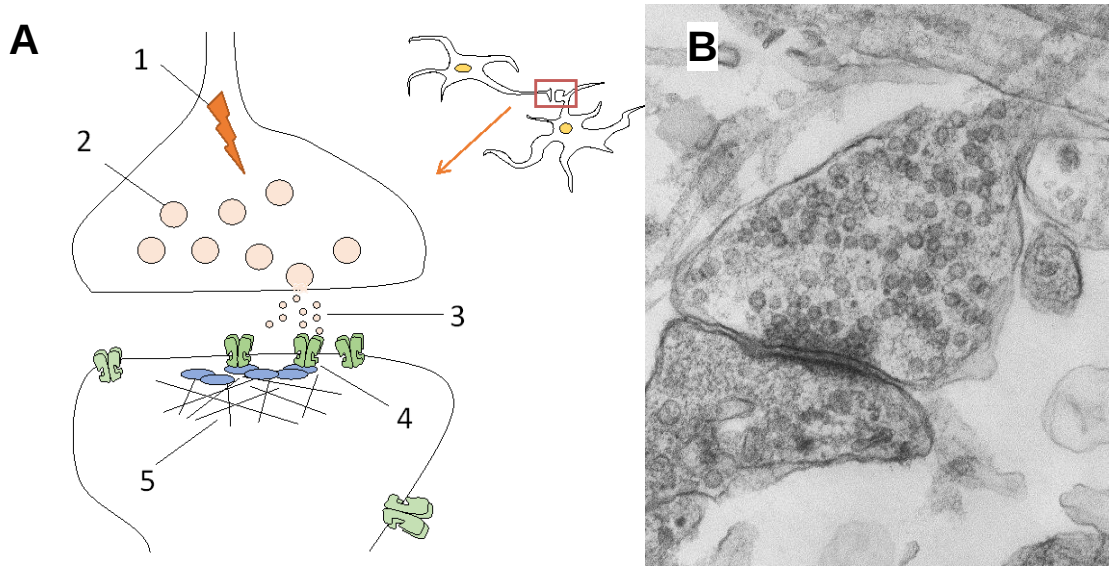

Figure 2 The structure of chemical synapses
A, the presynaptic axon is opposed to the postsynaptic membrane and separated from the latter by synaptic cleft. When action potential (1) arrives, it triggers the exocytosis of the presynaptic vesicles (2) containing neurotransmitter molecules. Released neurotransmitter (3) binds to the postsynaptic receptors (5) anchored on the postsynaptic density (5) and induces ion channel opening and postsynaptic cell depolarisation. **B**, electron microscopy image of a synapse; image source: http://neuralnoises.com/wp-content/uploads/2014/03/synapse.jpg

The transmission step in the synapse communication is rapid and highly focused. This is possible due to the active zones, a specialized secretory machinery in the presynaptic terminal. When transmitter is released into the synaptic cleft, it acts directly on neighbouring cells in a fast and precise manner; it can also be released out of the active zone as a modulator with diffuse effect, or even in the blood stream as a neurohormone.

The postsynaptic response depends on the properties of the receptors that recognizes a given transmitter. The receptors for chemical transmitters are membrane-spanning proteins. Their extracellular region recognizes and binds the transmitter. Receptors fulfil effector role for ion channels of the target cell. In the case where receptors gate ion channels directly, they are called ionotropic receptors. Ionotropic receptors are single macromolecules comprised of several domains. The extracellular domain is the transmitter receptor and the membrane-spanning domain is an ion channel. Receptors that are distant from ion channels they affect are called metabotropic receptors, since they alter intracellular metabolic reactions. Activation of metabotropic receptors frequently leads to the production of second messengers, which in their turn usually activate protein kinases, phosphorylation enzymes that very often directly phosphorylate ion channels.

Every synaptic vesicle released for transmission contains thousands of transmitter molecules. Usually 2 to 4 molecules of neurotransmitter bind to open a single ion channel at the postsynapse, but their affinity is quite low. This way, a single synaptic vesicle will generate a large but transient rise in the concentration of neurotransmitter, which will activate a fraction of the ion channels located in the postsynaptic density. Therefore, changes in the quantity of neurotransmitter or their diffusion away from release site could potentially affect synaptic transmission, as well as the number and properties of postsynaptic receptors.

1.2.2 Neurotransmitter release

It was demonstrated by Bernardo Katz and Ricardo Miledi that neurotransmitter release is regulated by depolarization of the presynaptic terminal membrane (Katz et al. 1967). Voltage-gated Na^+ and K^+ channels provide Na^+ influx and K^+ efflux that depolarizes the presynaptic membrane from its resting potential, eventually resulting in action potential generation. Action potential triggers transmitter release and propagation of a large synaptic potential in the postsynaptic cell. The quantity of the released transmitter depends on the presynaptic potential amplitude, as shown by progressive Na^+- channel blocker (tetrodotoxin) application and following measurements of the postsynaptic potentials.

Neurotransmitter release can occur even during complete Na^+/ K^+ channels blockade if the membrane depolarization is induced artificially via a current-passing electrode. This means that it is not the Na^+/ K^+ ion flow that is important to trigger the release, but rather the potential it creates. Rodolfo Llinas and his colleagues showed that voltage-gated Ca^{2+} influx in the presynaptic terminal results in the release of transmitter (Llinás & Heuser 1977). Voltage-gated Ca^{2+} channels are sparsely distributed along the axon and specifically abundant in the active zone. They are activated upon action potential depolarization and allow Ca^{2+} efflux from the extracellular space. Gradual presynaptic membrane depolarization leads to gradual inward Ca^{2+} current and following gradual neurotransmitter release, as judged by the postsynaptic potential recordings. Interestingly, the Ca^{2+} dependency of the transmitter release is not linear, thus a 2 times Ca^{2+} current increase can increase the transmitter release up to 16-fold.

Fast and synchronous neurotransmitter release happens only when Ca^{2+} concentration increases largely and rapidly, up to a thousand fold within a few hundred microseconds. Such an increase is possible only in the active zone, where Ca^{2+} channels are highly abundant. Moreover, as the Ca^{2+} sensor has low affinity, release only takes place in the narrow region surrounding Ca^{2+} channel. Ca^{2+} channels, in their turn, open a little bit slower than Na^{+} channels and Ca^{2+} raise starts on the descending phase of the action potential, see Figure 3. Slower Ca^{2+} dynamics contributes to the delays in the synaptic transmission.

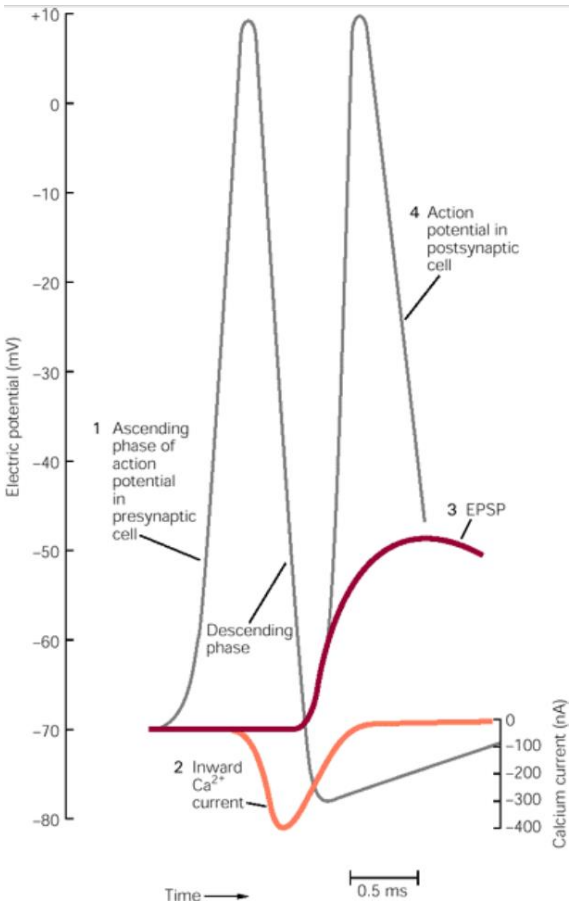

Figure 3 Synaptic transmission onset with regards to Ca^{2+} current influx
Voltage-gated Ca^{2+} channels in the presynaptic cell open upon activation by action potential depolarization (1). Inward Ca^{2+} current (2) starts only on the descending phase of the action potential due to the delays in channel opening. Incoming Ca^{2+} triggers neurotransmitter release, and shortly after the excitatory postsynaptic potential (EPSP) rises (3), and if large enough, induces action potential in the postsynaptic cell (4). Image from "Principles of Neural science" by Eric R. Kandel, James H. Schwartz, Thomas M. Jessell (2000).

Apart from fast synchronous release of neurotransmitter, which is accountable for most neuronal communication, neurons also exhibit slower evoked asynchronous as well as spontaneous releases. If synchronous release occurs within several milliseconds after action potential, asynchronous release continues from tens of

milliseconds to tens of seconds after an action potential, or series of action potentials. Spontaneous release occurs randomly in the absence of any action potential. Three types of release are shown on the Figure 4.

Different types of releases play physiologically distinct roles and have different Ca^{2+} dependence and kinetics (Kaeser & Regehr 2014), and they rely on different molecular machinery (Crawford & Kavalali 2015) that I will discuss in more detail in 2.2. Remarkably temporally precise synchronous release is driven by high local Ca^{2+} concentration raise near open Ca^{2+} channels. Time course of the Ca^{2+} current is very brief, due to the Ca^{2+} channels short opening time, and corresponds to the duration of the synchronous release (Chen & Regehr 1999; Kaeser & Regehr 2014). Artificially prolonged AP repolarization prolongs Ca^{2+} entry and affects the synchrony of the release (Geiger & Jonas 2000). Furthermore, to insure high release synchrony, molecular fusion machinery must react rapidly on Ca^{2+} increase and be able to abort its function immediately when local Ca^{2+} level returns to the basal values.

Asynchronous release is also triggered by Ca^{2+}, but there are some essential differences between both mechanisms of the evoked transmission. Slow Ca^{2+} chelator EGTA abolishes asynchronous release, but has little influence on the synchronous release (Atluri & Regehr 1998; Van der Kloot & Molgó 1993; Cummings et al. 1996). These findings suggested that Ca^{2+} sensor for asynchronous release is withdrawn further away from the Ca^{2+} source and responds to bulk cytosolic Ca^{2+} alterations rather than to local Ca^{2+} increase.

Ca^{2+} dependency of the spontaneous release is more complex, and the associated SV fusion can be possibly mediated by multiple mechanisms. Studies have shown that spontaneous release machinery may be Ca^{2+} independent as well as it may be influenced by high local Ca^{2+} or bulk cytosolic Ca^{2+} (Kaeser & Regehr 2014)

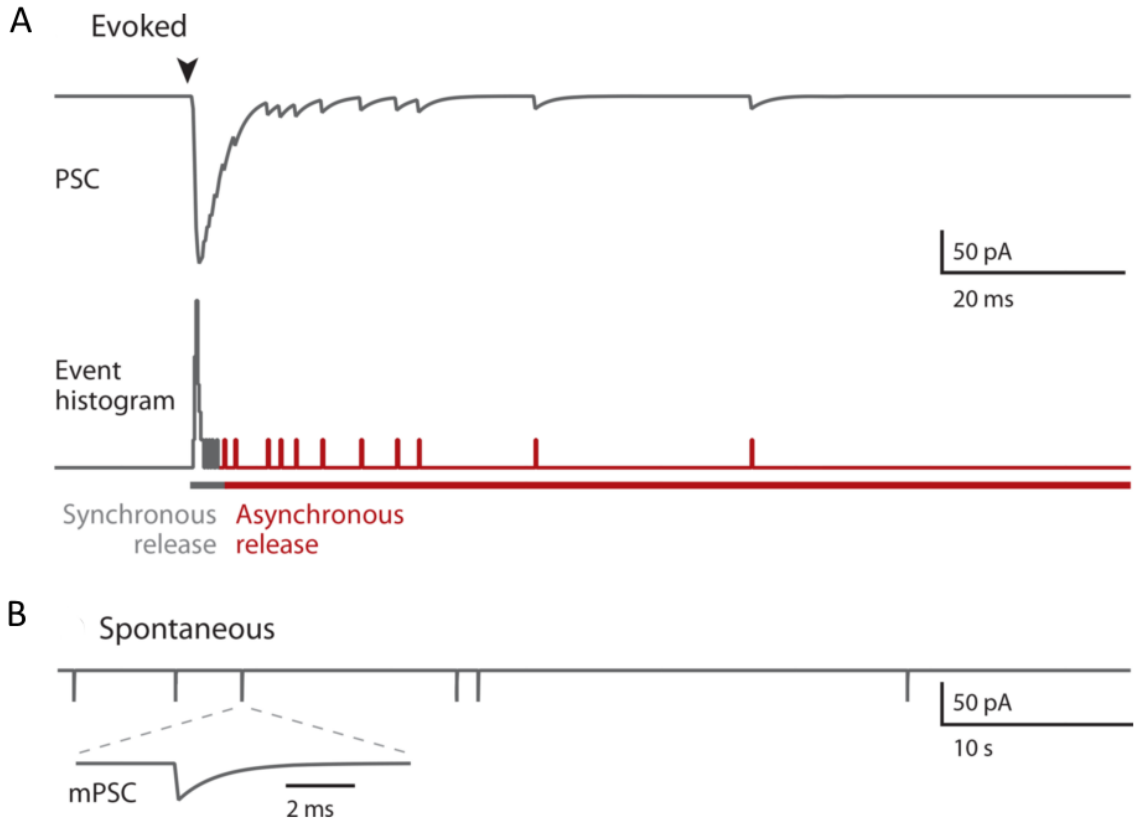

Figure 4 Different types of neurotransmitter release
A, Two types of evoked neuronal transmission: synchronous release that happens within milliseconds after presynaptic depolarization and slow, only loosely correlated with the action potential onset, asynchronous release. B, Spontaneous miniature postsynaptic currents (mPSC) occurring without presynaptic depolarization are shown. Data simulation from (Kaeser & Regehr 2014)

By studying spontaneous activity at the frog neuromuscular junction, Paul Fatt and Bernard Katz showed quantal nature of synaptic transmission (Fatt & Katz 1952). They observed random spontaneous voltage fluctuations of a fixed size near the nerve innervation sites. These fluctuations showed characteristic sensitivity to nerve denervation, osmotic pressure and cholinergic agents. They were called miniature end-plate potentials after end-plate potential, the synaptic potential at vertebrate nerve-muscle synapse. Central neurons also exhibit the same kind of miniature activity, but the amplitude distribution of events is often quite variable and skewed towards larger values. Nevertheless, careful statistical analysis is compatible with a model where miniature events reflect the release of neurotransmitter from single vesicles (Bekkers & Clements 1999) and evoked synaptic currents are composed of an integral number of unit responses called quantum of synaptic transmission.

What accounts for a quantum of transmitter release is the way neurotransmitter is stored and released. As it can be seen on the electron microscopy images of the

presynaptic boutons (Figure 2, B), the presynaptic terminal is filled with small synaptic vesicles. Neurotransmitters are stored in those vesicles and released into the synaptic cleft through exocytosis. Synaptic vesicles can be classified in different "pools", depending on their ability to fuse with the plasma membrane with presynaptic stimulation (Rizzoli & Betz 2005; Denker & Rizzoli 2010; Crawford & Kavalali 2015). First, the readily releasable pool (RRP) consists of vesicles primed in the active zone and they are the first to exocytose in response to a stimulation. During strong and prolonged stimulation, the vesicles containing in the recycling pool are recruited, providing additional source of neurotransmitter. It is very hard to elucidate the exocytosis of the reserve pool and its physiological implications still need to be explored (Rizzoli & Betz 2005). However, in conditions of mild stimulation frequencies eventually all the vesicles seem to participate in synaptic transmission (Ikeda & Bekkers 2009), questioning the existence of a significant reserve pool.

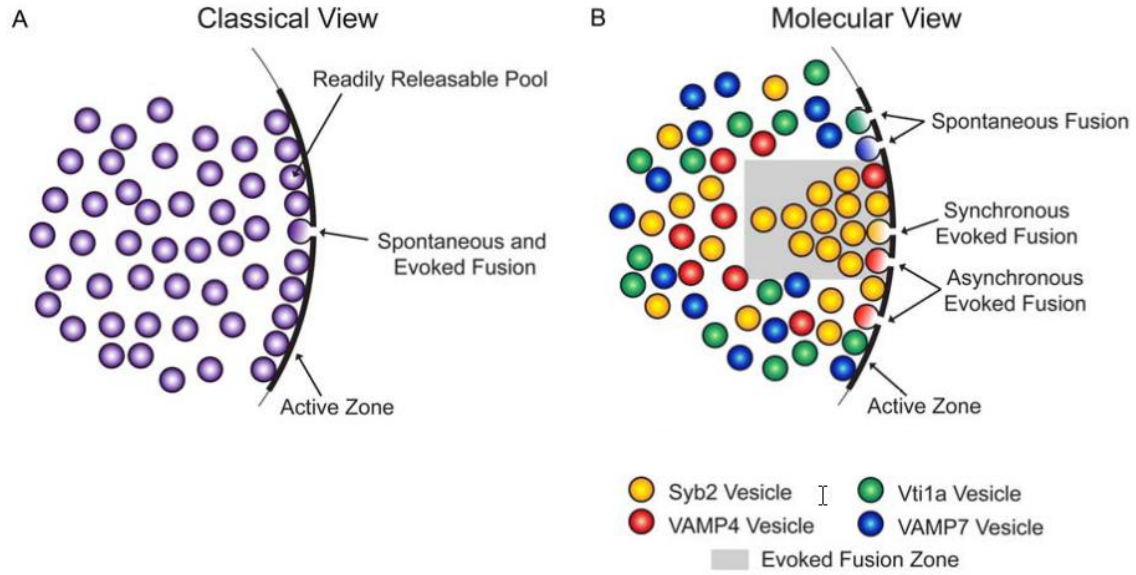

Figure 5 Presynaptic vesicle pools
A, Classical model of the presynaptic vesicle pool, where all vesicles are considered a homogenous population. Acording to this model, evoked synchronous, asynchronous and spontaneous releases originate from the same population of vesicles. Factors like distance from the active zone determine whether a given vesicle belongs to readily releasable, recycling or reserve pool. **B**, SV pool model suggesting heterogeneity of the presynaptic vesicle populations, arising from different v-SNARE proteins mediating their fusion and thus determine their kinetics, Ca^{2+} dependency and functional implication. For instance, VAMP2 –containing vesicles drive fast synchronous transmission, VAMP4 vesicles primarily participate in asynchronous transmission and VAMP7 vesicles mostly undergo spontaneous fusion. Image source: (Crawford & Kavalali 2015)

More recent studies classify vesicles by their molecular exocytosis machinery (Crawford & Kavalali 2015), as the latter defines whether the vesicular content will be

released synchronously, asynchronously or spontaneously (Figure 5). The molecular role of the proteins involved in presynaptic vesicular exocytosis are described in the part 2 of the Introduction, Trafficking and exocytosis in neurons.

1.2.3 Inhibitory and excitatory transmission

Hundreds or even tens of thousands of neurons innervate a central nerve cell. The inputs it receives from the presynaptic neurons can be both inhibitory and excitatory. These incoming signals are mediated by multiple neurotransmitters that modify the activity of multiple types of ion channels. Therefore, the postsynaptic potential and eventual action potential in the postsynaptic cell is a result of numerous diverse signals integration.

For triggering an action potential, the membrane potential of a nerve cell needs to reach a certain threshold. Excitatory postsynaptic potentials, or EPSPs, are the ones that depolarize cell membrane from its resting membrane potential (V_{rest}) towards the threshold, consequently increasing the action potential generation probability. Conversely, inhibitory postsynaptic potentials (IPSPs) hyperpolarize the postsynaptic membrane and decrease the likelihood of action potential generation. Example EPSP and IPSP curves are shown on the Figure 6.

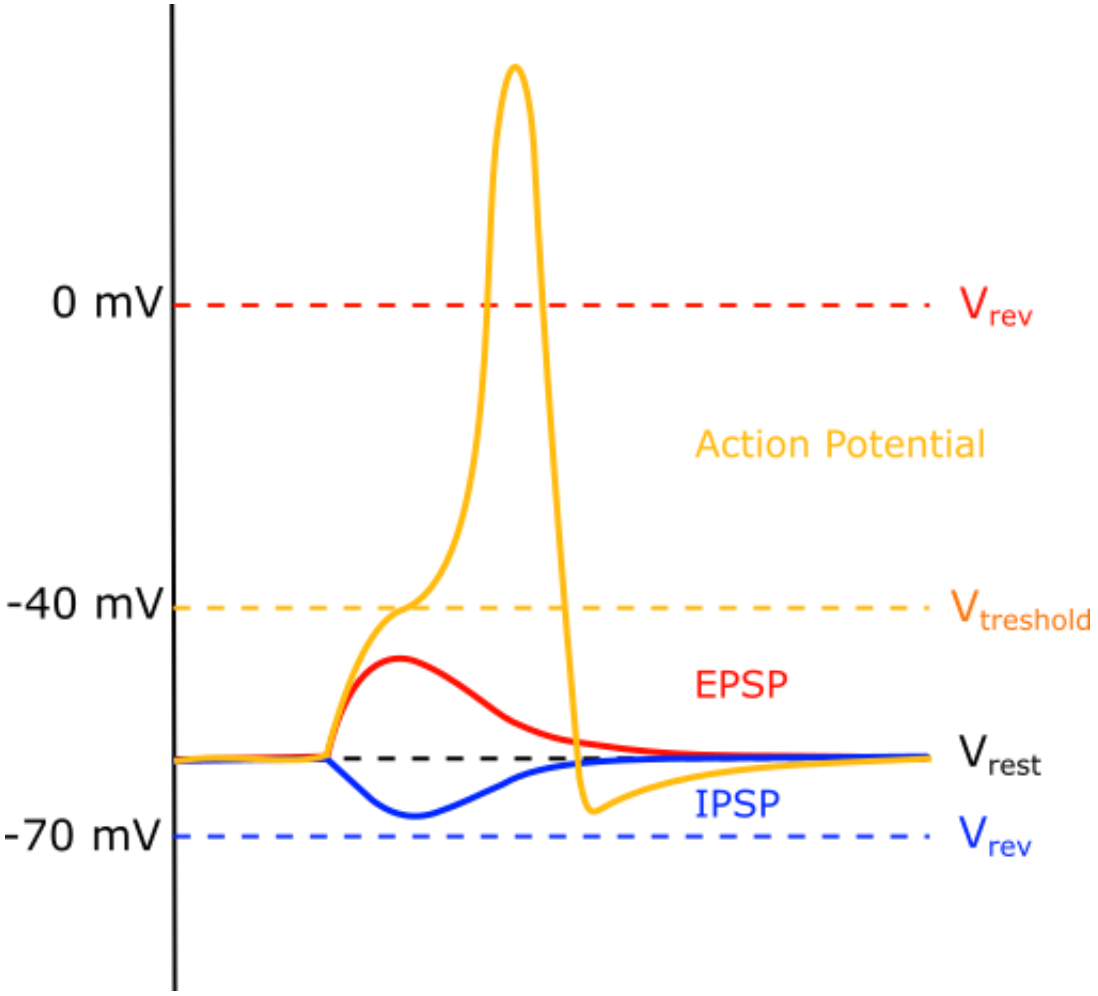

Figure 6 Excitatory and inhibitory postsynaptic potentiation.
In red, an example curve of depolarizing EPSP, which is generated if synaptic reversal potential V_{rev} is superior to the cell's membrane potential, which is equal to neuronal resting potential V_{rest} in this example. If V_{rev} is inferior to the neuronal membrane potential, the postsynaptic cell will generate a hyperpolarizing IPSP, shown in blue. When generated EPSP depolarizes neuronal membrane above the $V_{threshold}$, the postsynaptic cell generates an action potential, shown in yellow. Curves do not represent real data, but illustrate typical forms of discussed potentials.

Inhibitory or excitatory action of the synaptic connection is not defined by the type of released neurotransmitters, but by the type of ionic channels that they activate on the postsynaptic cell. Even though most transmitters are recognized either by inhibitory or excitatory signals mediating receptors, part of them primarily gates receptors of certain type. Hence, the principal excitatory neurotransmitter in the CNS is amino acid L-glutamate and the major inhibitory amino acid neurotransmitters are γ-aminobutyric acid (GABA) and glycine.

Glutamate-gated excitatory transmission

Glutamate-gated channels that mediate excitatory action conduct K^+ and Na^+ ions. Their reversal potential (a membrane potential, at which there is no net current

through the given channel) is equal to 0 mV, as they are equally permeable to both Na^+ and K^+. Ionotropic glutamate receptors always produce excitatory action upon glutamate activation and have three major subtypes, named after their synthetic agonists: AMPA (α-amino-3-hydroxy-5-methylisoxazole-4-propionic acid), kainate and NMDA (N-methyl-D-aspartate) receptors. Finally, metabotropic glutamate receptors, or mGluRs, are activated by the agonist trans-(1S, 3R)-1-amino-1, 3-cyclopentanedicarboxylic acid (ACPD). They are formed by homo- or heterodimers of mGluR1-8 subunits and can be classified in three groups depending on their coupling to secondary messengers.

Ionotropic glutamate receptors are tetramers, which bear four agonist binding, sites. AMPA receptors are mostly heteromers composed of GluA1-4 subunits, and most AMPA receptors in cortical and hippocampal pyramidal neurons are impermeable to Ca^{2+} due to the presence of the edited GluA2 subunit. They contribute to the largest part of EPSPs. Kainate receptors are composed of GluK1-5 subunits but they do not seem to contribute to only a very specialized subset of excitatory synapses such as mossy fibre synapses between dentate gyrus granule cells and CA3 pyramidal cells in the hippocampus. NMDA receptors are obligate heteromers composed of the GluN1 subunit and at least one of the GluN2A-D or GluN3A-B subunits. NMDA receptor-channel contributes to the late phase of the EPSP and exhibits some feature that distinguish it among other glutamate receptors. NMDA receptor activation opens cation channel with high conductance (50 pS), that is permeable to Ca^{2+} ions as well as to Na^+ and K^+. The channel opening requires presence of extracellular glycine, which binds to the GluN1 subunit, as a cofactor. Finally, the channel has voltage-dependent Mg^{2+} block. At resting conditions, with membrane potential around -65 mV, extracellular Mg^{2+} binds to the site in the pore of the open channel, obstructs the channel and prevents the current flow. During membrane depolarization Mg^{2+} is ejected by electrostatic repulsion and Na^+ and K^+ can enter the channel. As NMDA receptors are blocked at resting membrane potential, their contribution to the EPSP generated at the resting levels is not substantial, while the non-NMDA glutamate receptors play primary role. With membrane depolarization, more NMDA receptors open, allowing more current to flow through them. Moreover, NMDA receptor-channels have slow opening kinetics, and thus contribute to the late phase of EPSP. This late EPSP phase becomes significant after repeated presynaptic stimulations, when postsynaptic membrane becomes depolarized to - 20 mV or more. The increased

late-phase current is carried essentially by Ca^{2+}. The inward Ca^{2+} flow into the postsynaptic cell activates calcium-dependent enzymes and second messenger-dependent protein kinases. The activated reaction cascade triggers signal transduction pathway, that produces long-lasted changes in the synapse associated with learning and memory. I will further consider those changes in 1.3

Inhibitory action mediated by GABA- and glycine gated chloride channels.

The major inhibitory neurotransmitter in the CNS is GABA. GABA is gated by two types of receptors: $GABA_A$ and $GABA_B$. $GABA_A$ receptors is an ionotropic receptor gating Cl^- channel. $GABA_B$ receptor is a metabotropic receptor; its second-messenger cascade commonly opens a K^+ channel or inhibit voltage-gated Ca^{2+} channels. Glycine is another inhibitory transmitter, it is less common in the forebrain and acts on ionotropic receptors gating to Cl^- channel.

Cl^- conducting ionotropic receptor-channel reverse potential corresponds to the Cl^- equilibrium potential. The membrane potential of a typical neuron (V_{rest} = -65 mV) is more positive then Cl^- equilibrium potential (E_{Cl} = -70 mV). Therefore, Cl^- -channel opening upon receptor activation leads to outward current, carried by the influx of Cl^- ions and driven by positive electrochemical force ($V_{rest} - E_{Cl}$). Such current results in the negative charge accumulation on the inside of the plasma membrane and neuron's hyperpolarization towards the E_{Cl}. In some neurons, V_{rest} is equal to E_{Cl}. For those, the opening of Cl^- channels does not change the postsynaptic membrane potential, but still provides an inhibiting effect by increasing the resting membrane conductance. One of the ways to understand such inhibitory synaptic input outcome is to consider how it will affect a simultaneous EPSP. The magnitude of the generated EPSP depends on the excitatory postsynaptic current I_{EPSP} and the magnitude of the resting conductance channel (g_i), that includes contributions from inhibitory synaptic channels. According to the Ohm's law, the amplitude of depolarization during an EPSP is given by

$$\Delta V_{EPSP} = \frac{I_{EPSP}}{g_i}$$

Thus, the opening of the inhibitory channel will increase the resting conductance and diminish the size of the EPSP, what is known as a short-circuiting or shunting effect of the inhibitory inputs.

There are some cell types, like the ones with $GABA_B$ receptors, where inhibition is also driven through the opening of the K^+ channels. K^+ equilibrium potential, which is equal to -80 mV in neurons, is even more negative than Cl^- equilibrium potential and is always below the membrane resting potential.

Signal integration

Depolarization produced by one synaptic input is almost never sufficient to trigger an action potential. Each input signal, inhibitory or excitatory, has different impact strength on the final decision of whether the action potential will be generated. Two passive parameters define how the competing input signals will be integrated: cell membrane's time and length constants. Time constant defines postsynaptic potential decay time and is critical for temporal signal summation. Neurons with long time constant have slow decay time of the postsynaptic potentials and high probability of the algebraic summation of two consecutive potentials. Length constant defines the extent to which the signal is decreased when it spreads passively. In neurons with large length constant, signals propagate to the trigger zone with little diminution and the summation of signals arising from distant regions is facilitated. Synaptic location is also a factor that influences its efficacy. Synaptic currents generated in the axosomatic area have stronger signal and greater impact on the resulting effect at the trigger zone.

Excitatory synapses are often formed on the dendritic spines. Spine is a small protrusion arising from the dendrite's main shaft, like on synapse, represented on the Figure 2. Every spine participates in at least one synaptic connection. The postsynaptic receptors on the spine are anchored in the material called the postsynaptic density, as it appears dense in electron microscopy images. Each spine forms a distinct biomechanical compartment with finicky regulation.

Inhibitory synapses arise from distinct GABAergic neurons: some target mainly the cell body while others target neuronal dendrites. Inhibitory synapses on the cell body control neuronal excitability globally because EPSPs, as they propagate towards the initial axon segment from various dendritic compartments, inevitably pass through the cell body. Inhibitory input on the soma opens Cl^- channels, increase membrane resting conductance and shunt the excitatory current spreading through the soma. An inhibitory synapse at the membrane compartments far from the cell body will control more specifically excitatory inputs in distant zones.

1.2.4 Role of non-neuronal cells in synaptic transmission

Glial cells were previously considered to play only supportive role, are also implicated in synaptic transmission (Araque et al. 1999; Auld & Robitaille 2003). Emerging evidence suggests that glial cells, in particular astrocytes, have multiple ways of interacting with neurons and modifying synaptic transmission, which gives the neuronal networks even more adaptive mechanisms. Very frequently, glial cells closely enwrap synapses with their processes, which gives them an advantageous position to sense neurotransmitter release. In the majority of the peripheral nervous system neuromuscular junctions, extent processes of the presynaptic Schwann cells lie in close opposition to the presynaptic terminal and have finger-like protrusions approaching the active zone (Auld & Robitaille 2003). In the CNS, the presence of glial cells at the synaptic sites is more heterogeneous. In hippocampus, for instance, astrocytic processes adjacent to pre- and postsynaptic elements are obvious on part of the synapses in the stratum radiatum of the CA1 hippocampus area (Ventura & Harris 1999).

Glia processes in the proximity of the synapses express high concentration of glutamate transporters such as GLAST and GLT-1. Glia glutamate transporters bind or up-take glutamate and in this way regulate glutamate activity at the synapse, carry out glutamate clearance and prevent glutamate spillover that is predisposed to affect neurotransmission at neighbouring synapses.

Glial cells in the proximity of the synapses demonstrate certain sensitivity to the synaptic activity. One of the most fundamental astrocyte reactions to the neuronal transmission is the neurotransmitter-induced elevation of the cytosolic Ca^{2+} levels, which can be in forms of long duration Ca^{2+} spikes or Ca^{2+} levels oscillations (Araque et al. 1999). In response to internal Ca^{2+} elevation, glial cells can in their turn release neurotransmitters (also called gliotransmitters) that modulate synaptic transmission. It was first shown in cultured neurons that activation of astrocytes with bradykining leads to the APV-sensitive intracellular Ca^{2+} increase in the neighbouring neurons, suggesting that activated astrocytes release glutamate that acts on neuronal NMDA receptors (Parpura et al. 1994). Now it is known that astrocytes in the hippocampus can release a wide palette of gliotransmitters, like glutamate, ATP, GABA, D-serine, adenosine, prostaglandins, brain-derived neurotrophic factor (BDNF), and many others (Perea & Araque 2010). Astrocytes could thus with gliotransmitters modulate

neuronal excitability, regulate synaptic transmission, firing frequency and induce long-term synaptic plasticity (Perea & Araque 2010).

Gliotransmitter release

Despite the apparent physiological importance of the gliotransmitter release, its underlying molecular mechanisms are still under investigation. There are two main types of gliotransmitter release under investigation: 1) Ca^{2+}- and SNARE protein-dependent molecular machinery, 2) non vesicular release (Sahlender et al. 2014). Proposed non-vesicular gliotransmitter release pathways are the following: reversal of glutamate uptake, connexin hemichannels, pannexin hemichannels, cystein glutamate exchanger system, pore-forming p2x7 receptors and volume regulated anion channels (Perea & Araque 2010). However, for principal gliotransmitters (Glutamate, ATP and D-serine) SNARE-dependent exocytosis is proposed as major release mechanism (Sahlender et al. 2014; Harada et al. 2015).

1.3 Synaptic Plasticity

The nervous system constantly adapts to the changing environment and changes itself to be able to respond adequately and efficiently to the challenges it faces in its everyday functioning. Brain's capacity to change is often referred to as plasticity. Neuroplasticity expresses itself in various ways: when immature brain organizes itself during early childhood, after an injury when the nervous system compensates the loss of function and during learning and memorizing.

It is now commonly accepted that the brain realizes the function of learning and information storage through modification of synaptic efficiency of particular synapses and resulting changes in firing patterns that are brain's representations of the external events (Bliss & Collingridge 1993; Malenka et al. 1994; Nabavi et al. 2014). In my work part of the experiments were based on the participation of postsynaptic exocytosis in specific type of long-term synaptic changes that I will briefly expose in the current section.

1.3.1 Potentiation and depression of synapses

Neurons are capable of strengthening or weakening their synaptic connections in response to particular patterns of activity. Two forms of such activity-dependent synaptic plasticity have been extensively studied and believed to stand for the cellular correlates of learning and memory: long-term potentiation (LTP) and depression (LTD). As we shall see later in Section 2.3.3 of the Introduction, postsynaptic exocytosis is directly involved in LTP expression, so I will further concentrate on the LTP model introduction.

Synaptic plasticity has been most extensively studied in the hippocampus, a cortical structure responsible for the conscious memory storage in man. Hippocampal slices possess well-ordered anatomical arrangement that facilitate the study of its connectivity. In addition, several hippocampal pathways appear to be very plastic. Consequently, the hippocampal activity-induced NMDA receptor-dependent LTP of the glutamatergic connection between CA3 and CA1 pyramidal neurons (see Figure 7) became the dominant model of synaptic plasticity and this is the model I will be referring to in the present work.

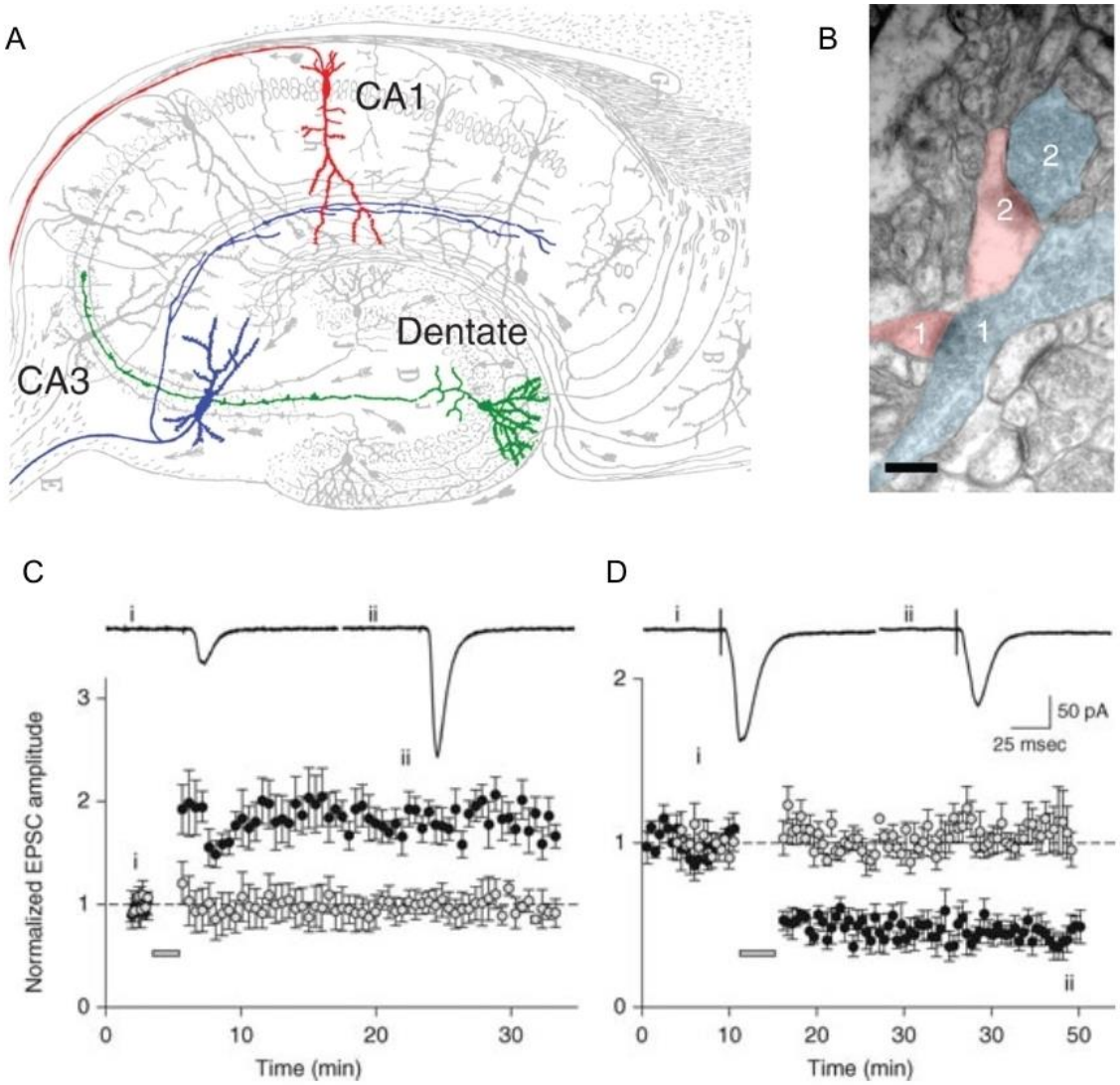

Figure 7 Long-term potentiation and depression in the hippocampal slices
A, drawing of the trisynaptic pathway in the hippocampus by Ramon y Cajal. The potentiation or depression were induced by activation of the NMDA receptors between pyramidal neurons of the CA3 and CA1 regions (blue and red respectively). **B**, electron microscopy image of two synapses (highlighted) on the CA1 neuronal dendrites by Schaffer collaterals from CA3 neurons. Scale bar, 200 nm. **C**, LTP induced by the pairing protocol, bar: 450 stimuli; 3 Hz; 0 mV (filled circles). The same protocol was unable to potentiate the synaptic response in the presence of 50 µM AP5 (white circles). **D**, LTD, induced with a pairing protocol: 1 Hz for 6 min, Vh =−40 mV. Stable control recordings were obtained where plasticity induction protocols were not applied (white circles). Images A and B were adapted from (Lüscher & Malenka 2012). C and D demonstrate data from (Bortolotto et al. 2011).

1.3.2 LTP induction and expression

LTP can be induced with specific patterns of activity that can be achieved in the experimental conditions by various protocols (Bliss & Collingridge 1993; Malenka et al. 1994; Chen et al. 1999). These protocols include high frequency stimulation (N stimulations at 100 Hz), theta burst stimulation (e.g. Nx M groups of stimulations), which mimic theta wave activity recorded in the hippocampus in vivo. In addition, when the postsynaptic cell membrane potential can be controlled, the pairing of

postsynaptic depolarization (e.g. to 0 mV) with synaptic stimulation, or evoking a postsynaptic action potential a few milliseconds after stimulation also evokes LTP. In all cases, LTP induction can only happen when both the presynaptic and the postsynaptic parts of the synapse are activated. The postsynaptic membrane needs to be depolarized enough to relieve the voltage dependent Mg^{2+} block from the postsynaptic NMDA receptors. NMDA receptors, unlike AMPA receptors, are permeable to calcium and their opening will generate a large but transient Ca^{2+} influx to the postsynaptic neuron. Ca^{2+}, in its turn, will activated intracellular second-messenger pathways ultimately leading to the enhancement of the synaptic strength.

The question whether synaptic strengthening was due to the presynaptic increase in neurotransmitter release or to the postsynaptic changes provoked considerable debates for a couple of decades. Now it seems clear that even though the presynaptic bouton can be very plastic (Castillo 2012), signal changes during NMDA receptor-dependent LTP is mostly due to an increase in the number of AMPA receptors at the postsynaptic membrane, as well as their subunit composition and degree of phosphorylation (Huganir & Nicoll 2013; Malenka et al. 2004; Isaac et al. 1995).

Multiple signaling cascades have been implicated in the induction of LTP, depending on the induction protocol or the developmental stage (Malenka et al. 2004). However, calcium/calmodulin-dependent protein kinase II (CaMKII) seems to be absolutely required for NMDA receptor-dependent LTP induction independently of the protocol (Lüscher & Malenka 2012; Malenka et al. 2004). CaMKII is enriched in dendritic spines and activated when intracellular Ca2+ levels increase sufficiently. CaMKII activation leads to phosphorylation AMPA receptors and other proteins (Huganir & Nicoll 2013). The phosphorylation of AMPA receptors can increase their conductance and probably participates in the early stages of LTP (Lüscher & Malenka 2012; Ehlers et al. 2000). LTP is also accompanied by a fast enlargement of spines which partly depends on CaMKII activation, but also directly on Rho GTPases which regulate the actin cytoskeleton (Bosch & Hayashi 2012). Finally, CaMKII regulates at least in part the exocytosis of GluA1 containing vesicles during LTP (Patterson et al. 2010), a phenomenon I will focus on in part 2.3.3 of the Introduction.

LTP has been mainly studied in *ex vivo* brain slices or *in vivo* with specific patterns of synaptic stimulation, as seen above. Moreover, cultures of dissociated

hippocampal neurons can also experience LTP following the same pairing protocols (Tao et al. 2000). One can thus take advantage of the ability to manipulate cultured cells and the high resolution optical imaging allowed by this preparation to examine the molecular and cellular mechanisms of LTP in great detail. However, one would need protocols that are simpler that protocols based on electrophysiology. The rationale is to provide a way to activate NMDA receptors strongly but transiently which would activate CaMKII preferentially and avoid the activation of other calcium dependent pathways which require prolonged NMDA receptor activation and evoke the opposite of LTP, long term depression. One such "chemical" LTP protocol (chemLTP or cLTP) has been developed: the application of a solution without Mg^{2+} and with the NMDA co-agonist glycine (100 μM) provokes a very high degree of NMDA receptor activation during synaptic glutamate release and a long lasting increase in the amplitude and frequency of spontaneous EPSCs, even in the presence of tetrodotoxin (TTX). This chemLTP protocol has thus been used in cultured hippocampal neurons with various readouts such as increase in miniature EPSC amplitude and frequency (Lu et al. 2001; Petrini et al. 2009; Jurado et al. 2013; Menna et al. 2013), surface staining of AMPA receptors (Lu et al. 2001; Ahmad, J. S. Polepalli, et al. 2012; Jaafari et al. 2012; Jurado et al. 2013) or spine volume and density (Kopec et al. 2006; Menna et al. 2013).

2 Trafficking and exocytosis in neurons

2.1 SNARE complex as exocytosis machinery

In eukaryotic cells, many essential processes such as communication between membrane-enclosed intracellular compartments, protein and membrane trafficking as well as neurotransmitter or hormones secretion rely on membrane fusion. Intracellular fusion reaction are highly specific and vary a lot in size, shape and content of fusing organelles. Regardless of high diversity of the fusing compartments, almost all intracellular budding and fusion reactions are realised by SNARE proteins families, with the notable exception of mitochondrial fusion and fission (Jahn & Scheller 2006; Südhof & Rothman 2009; Südhof 2013a). During membrane fusion, SNAREs localized on the opposing membranes form four-helix bundle. The fusion is driven by the free energy released during the four-helix bundle formation. The recycling of SNAREs through the dissociation of the helical bundle is mediated by N-ethylmalmeimide-sensitive factor (NSF) protein with the assistance of SNAPs (Soluble NSF attachment proteins, different from SNAP type SNARE described further).

2.1.1 SNAREs structure

SNARE proteins are small proteins that exhibit simple domain structure. The key characteristics of the SNARE superfamily is the SNARE motif, a section of 60-70 evolutionary conserved amino acids arranged in heptad repeats. Most of the time a short linker connects the SNARE motif to the single transmembrane domain at the C-terminal end. SNAREs lacking the transmembrane domain, like neuronal SNAP-25, are subject to hydrophobic post-translational modification mediating membrane anchoring (Jahn & Scheller 2006). In addition to the SNARE motif, SNAREs usually have an independently folded additional domain. This motif varies between subgroups of SNAREs and is positioned closer to N-terminal. However, some of the SNARE proteins, such as VAMP2, may lack the N-terminal domain.

SNARE proteins have been classified in two ways. The first terminology relies on the assumption that there is a strict separation between SNAREs found on the vesicular or ‘donor’ membrane (v-SNAREs), and SNAREs found on the target or ‘acceptor’ membrane (t-SNAREs). v-SNAREs comprise the vesicle associated membrane protein (VAMP)1 and 2 (also called synaptobrevin1 and 2), VAMP3 (also

called cellubrevin), VAMP4, 5, 7 (also called tetanus toxin insensitive or TI-VAMP) and VAMP8 (called endobrevin), as well as the mammalian homolog of Sec22. However, some SNAREs can form complexes with different partners in various intracellular steps, like some of the *S. cerevisiae* SNAREs that may mediate fusion in retrograde and anterograde traffic (Jahn & Scheller 2006). In addition, v-/t-SNARE terminology can be misleading in describing homotypic fusion reaction, when both fusing membranes have all four SNAREs.

Another classification is based on the highly conserved molecular structure of the SNARE complexes (Jahn & Scheller 2006; Fasshauer et al. 1998). In their monomeric form, SNAREs have unstructured SNARE motif. Nevertheless, if a complete corresponding set of SNAREs is combined, their SNARE motifs spontaneously form very stable helical bundle, the SNARE complex. As seen on the crystal structure of combined SNARE motifs of the neuronal SNAREs VAMP2, syntaxin1a and SNAP25B (Antonin et al. 2002; Brunger et al. 1998), the SNARE core complex consist of elongated coiled coils out of four intertwined, parallel α-helices, each provided by a different SNARE motif , see Figure 8. This structure was very similar for other combinations of SNARE motifs, such as syntaxin7/syntaxin8/Vti1b/VAMP8 involved in the fusion of late endosomes (Antonin et al. 2002), and confirmed and extended to the transmembrane domains for the synaptic vesicle SNARE complex. The internal layers of the bundle are formed by 16 side chain layers interacting with each other, which explains the very high stability of this complex that can resist treatments by strong detergents such as SDS. With the exception of the central layer, internal layers of the bundle remain hydrophobic. The central layer (or 0 layer) is a highly conserved structure that is composed of three glutamine residues (Q) and one arginine residue (R): the corresponding SNAREs are classified as Q_a-, Q_b-, Q_c- and R-SNARE, respectively (Jahn & Scheller 2006; Fasshauer et al. 1998). The v-SNAREs described above (VAMPs and Sec22) correspond to the R-SNAREs. Most syntaxins are Q_a-SNAREs while Q_b and Q_c-SNAREs are either other syntaxins (6 and 8) or are found in a single protein of the SNAP (synaptosome-associated protein) subfamily (SNAP25, 23 and 47).

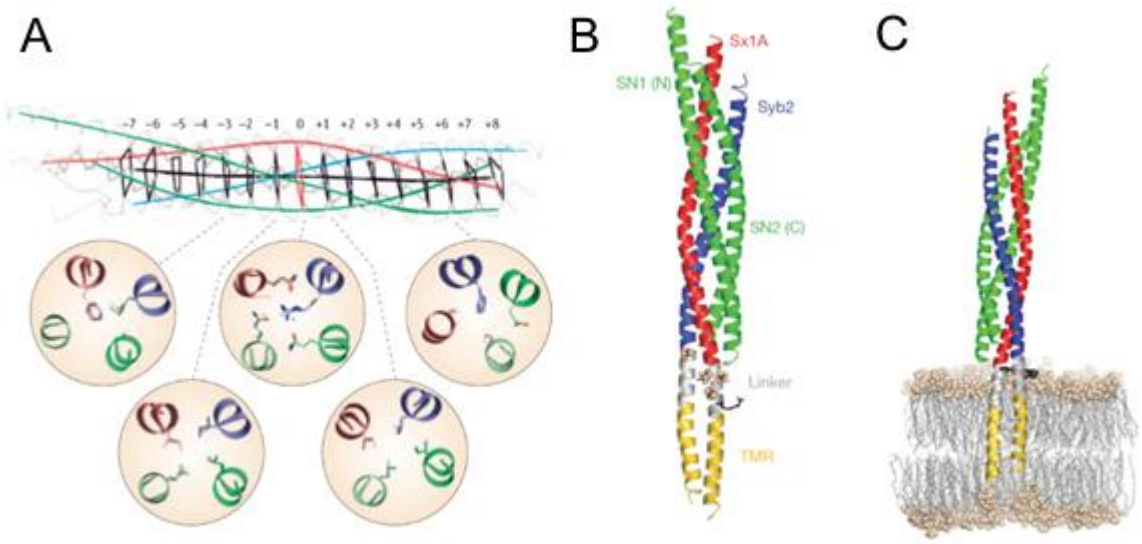

Figure 8 Structure of the SNARE complex
A, Skeleton diagram of the neuronal SNARE complex indicating the position of the central layers of interacting side chains. Q_a- SNARE (syntaxin1) is shown in red, Q_b and Q_c SNARE motifs are both green (SNAP-25) and R-SNARE (VAMP2) is blue. Image from (Jahn & Scheller 2006) **B**, Synaptic SNARE complex ribbon plot including linkers and TMRs. **C**, Model of the synaptic SNARE complex inserted in a membrane. B and C images source: (Stein et al. 2009).

N-terminal domain of Q_a- SNAREs and certain Q_b-, Q_c-SNAREs contain an antiparallel three-helix bundles (Figure 11, A, B). R-SNAREs N-terminal domain often has profilin-like folds that are also referred as longin domain, see Figure 9 B. Some Q_a-SNAREs, like syntaxin-1, can adapt reversible 'closed' conformation, where three-helix bundle type N-terminal domain associates with fraction of its own SNARE motif.

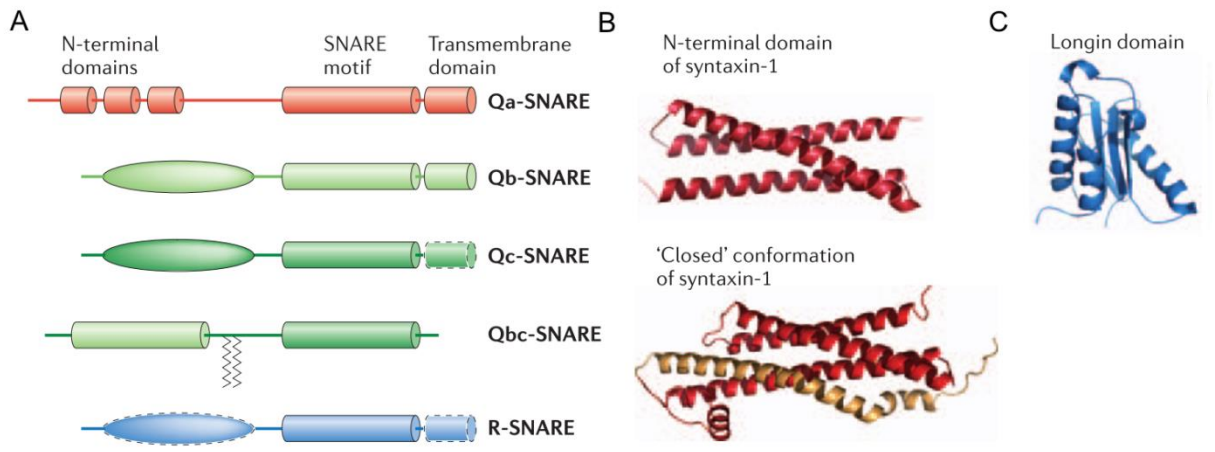

Figure 9 Domains of SNARE proteins

A, SNARE subfamilies domain structure. Domain with dashed borders are absent in some subfamily proteins. Q_a SNAREs or syntaxins have antiparallel three-helix bundles at their N-terminal domain. Different variations of Q_b- and Q_c-SNARE N-terminal domains are represented by an oval shape. Small subfamily of SNAP-25 or Q_{bc}- SNAREs contains two SNARE motifs. Zigzag lines represent possible palmitoylation of the linker between the Q_b- and Q_c- SNARE motifs. **B**, Three-dimensional structure of the synaptic SNARE syntaxin-1 isolated N-terminal domain in open and closed conformation. Three-helix bundle at the N-terminal on the upper-panel is representative for the Q_a-SNAREs subfamily. Lower panel illustrates syntaxin-1 closed conformation where its N-terminal domain (red) is reversibly associated with part of its own SNARE motif designated in beige. **C**, three-dimensional longin or profilin-like domain at the N-terminal of the R-SNARE Ykt6 is shown. Figure adapted from (Jahn & Scheller 2006). Same colour code is used on the Figure 10.

2.1.2 SNARE cycle

According to the SNARE model, SNARE complex formation requires the participation of at least one SNARE protein with a transmembrane domain on each of the two fusing membranes. In the case of synaptic vesicle exocytosis, it would be VAMP2 on synaptic vesicles and syntaxin1A on the presynaptic plasma membrane. The remaining SNAREs contribute to the complex formation in various configurations: either both fusing membranes are equipped with a pair of SNAREs, or the complex is formed from a SNARE triplet on one membrane interacting with a single membrane-anchored SNARE of the other membrane (Jahn et al. 2003). For synaptic vesicle exocytosis, to complement VAMP2 located on synaptic vesicles and syntaxin1A on the plasma membrane, SNAP25 bears both remaining SNARE domains and is located on the plasma membrane as well.

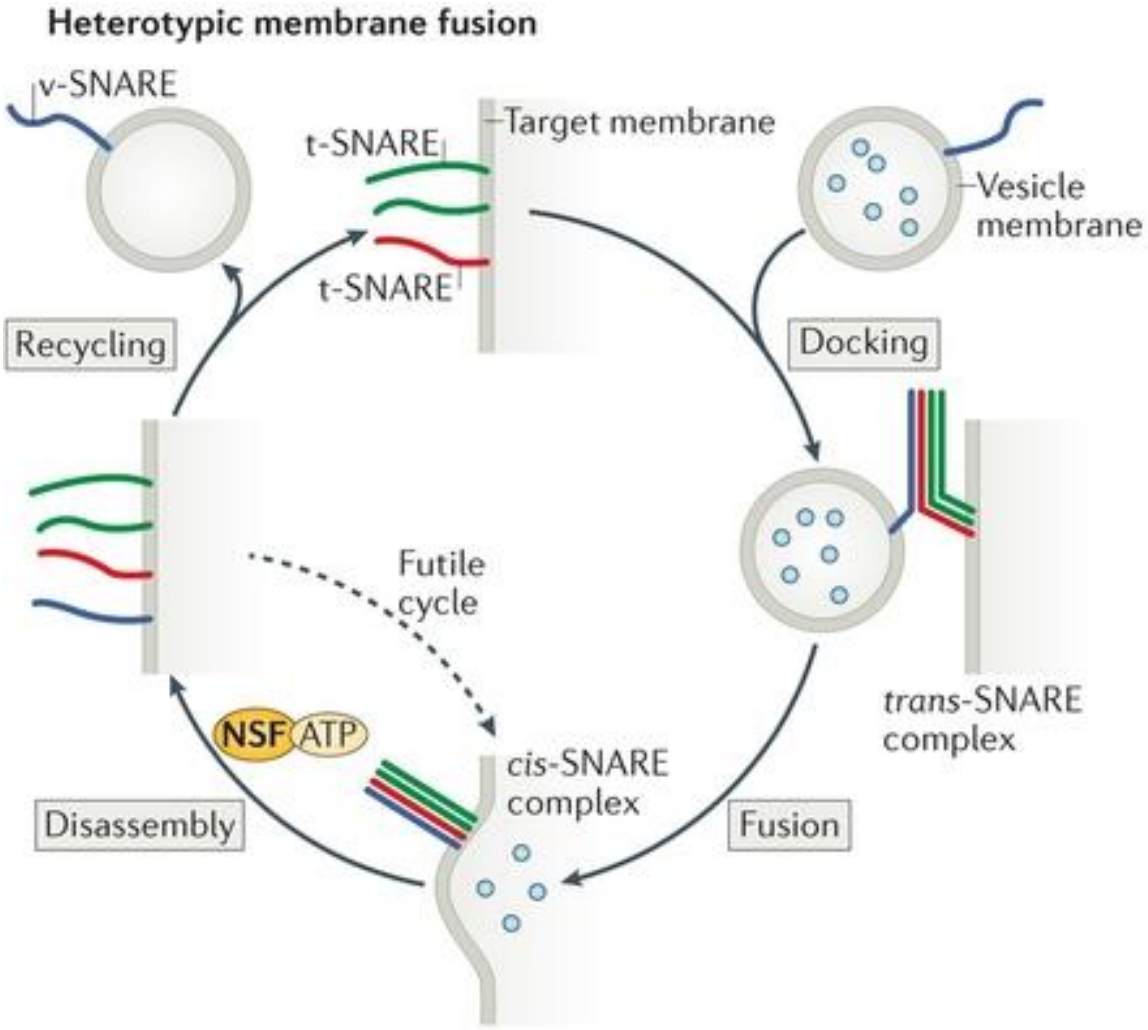

Figure 10 Heterotypic membrane fusion.
In heterotypic membrane fusion, vesicle containing v-SNARE on its membrane fuses with the acceptor membrane having three t-SNAREs. Vesicular docking and consecutive fusion is driven by *trans*-SNARE complex formation. Fusion and cargo delivery ends with *cis*-SNARE complex formation. *Cis*-SNARE complex is subsequently disassembled by NSF ATPase SNAP assistance, after disassembly v-SNARE protein has to be recycled back to the donor membrane in order to be mediate new fusion reactions. If reassembly proceeds before v-SNARE recycling, that leads to *cis*-SNARE complex formation and recurrent disassembly without membrane fusion catalysis (futile cycle). Image from (Baker & Hughson 2016)

SNAREs localized on the opposite membranes associate into core complexes through their SNARE motifs interaction. SNARE-motifs associate in a zipper-like fashion from their N-terminal domains toward the C-terminal domains, proximal to the lipid membranes. Such association would bring the fusing membrane in close apposition and liberate enough energy to overcome the fusion energy barrier (Hanson et al. 1997; Lin et al. 1997). For such reaction to happen, interacting SNARE complex formation must proceed through trans configuration (Jahn & Scheller 2006). Prior to fusion, SNAREs are considered to form binary Q_{abc} acceptor complex on the target membrane that is prepared to receive the R-SNARE for docking and fusion. After

association with R-SNARE, vesicle is docked and SNAREs form *trans*-SNARE complex or SNAREpin (Figure 10, *trans*-SNARE complex formation on the example of v- and t-SNAREs in heterotypic fusion).

Trans-SNARE complex is highly reactive and in vitro experiments on neuronal synaptic SNAREs showed that Q_{abc}-complex quickly recruits second Q_a and acquires a dead-end Q_{aabc} conformation, complicating its structural characterization (Jahn & Scheller 2006). Q_{abc} structure of yeast *trans*-SNARE complex was characterized by NMR. The study revealed well-structured N-terminal region while the C-terminal region was frayed (Brunger et al. 1999). In vivo, the acceptor complex is stabilized by SM (Sec1/Munc18-related) proteins that interact with SNAREs in various states (Südhof & Rothman 2009; Baker & Hughson 2016). Recent advances demonstrated that SNAREs assemble in multiple steps with characteristic energy levels (Lou & Shin 2016). Lately, it was possible to capture and describe *trans*-SNARE complex with 'nanodisk sandwich' technique, giving strong support for the 'zippering' assembling hypothesis (Shin et al. 2014). The transition states are regulated by various proteins that include small helical proteins complexins and synaptotagmins (Jahn & Scheller 2006; Baker & Hughson 2016; Südhof 2013c). Complexins bind to the surface of SNARE complexes; they are involved in Ca^{2+} triggering of the presynaptic exocytosis (Mohrmann et al. 2015). Synaptotagmins form a family of 17 proteins best known for their Ca^{2+}-sensor role in fast neurotransmitter release(Esteves da Silva et al. 2015), see 2.2.2 below.

Membrane fusion implies the conversion of the pre-fusion *trans*-SNARE complex into a *cis*-SNARE complex (Figure 10). In this conformation, all four SNARE partners are located on the same membrane. *Cis*-complex disassembly is mediated by NSF ATPase and SNAPs (Block et al. 1988; Clary et al. 1990). NSF provides the necessary energy needed for the dissociation, since *Cis*-SNARE complex configuration has low potential energy. SNAPs acts as NSF cofactors in dissociation that binds to the SNARE complex surface. After the dissociation, t-SNAREs are readily available for a new fusion cycle, while v-SNAREs have to be recycled to the donor membrane in order to engage to a new docking and fusion cycle (Baker & Hughson 2016). In addition, SNAREs, disassembled by NSF after a fusion reaction, can assemble into *cis*-SNARE complexes before they are recycled back to the donor compartment. Resulting *cis*-SNARE complex has to be disassembled by the ATPase NSF in order to be available for

subsequent reuse in fusion. This physiologically disadvantageous interaction is called a futile cycle (Figure 10 Heterotypic membrane fusion.). Irrelevant interactions are likely prevented by SNARE chaperones and tethering factors that coordinate membrane tethering, organize SNARE acceptor complex formation and core complex assembly (Baker & Hughson 2016).

2.1.3 SNARE specificity

SNAREs form a large superfamily that contains 36 members in humans and 24 members in yeast. Such variety of proteins serves for mediating numerous reactions that occurs on the highly organized routes of the membrane trafficking pathway. Some SNAREs seem to be highly specialized in mediating one fusion step with particular set of partners, others can be more versatile and participate in a variety of fusion events.

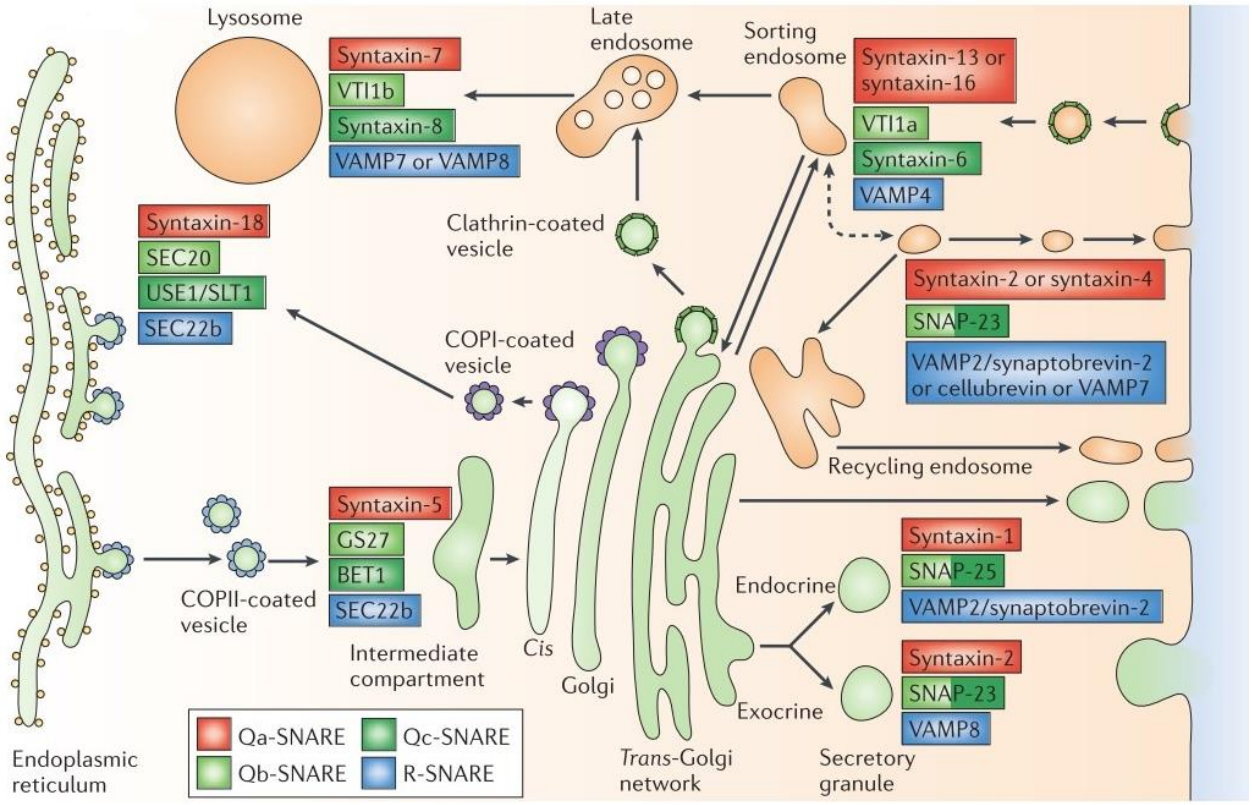

Figure 11 Mammalian membrane trafficking pathways and associated SNARE proteins.
Figure illustrating SNARE sets assigned to individual fusion reactions along trafficking pathways in mammalian cells. Heterotypic fusion reactions are indicated with arrows. Dashed double-headed arrow denotes homotypic fusion reaction between sorting endosomes. Image source: (Jahn & Scheller 2006)

How is a particular set of SNAREs assigned to a given fusion reaction (Figure 11)? SNAREs are often enriched in the compartments of their implication. It is the case of syntaxin-1/2 and 4, SNAP-25 that are abundant on the plasma membrane (Hong

2005) where they participate as t- SNAREs in fusion during exocytosis (Fasshauer & Margittai 2004). Nonetheless, SNAREs recycle and can be located in different intracellular compartments during different stages of their proteic life: biosynthesis, fusion, recycling, etc. Even though SNARE localization is a good indicator of its physiological role, it is not sufficient to deduce all of the proteins implications. VAMP2, for example, that is enriched on synaptic vesicles (Hong 2005) and most known for its R-SNARE role in neurotransmitter release (Chapman 2002), has recently been shown to participate in postsynaptic forms of exocytosis (Jurado et al. 2013).

Vesicular traffic connects membrane-enclosed intracellular compartments by multiple routes of secretory pathway. Intracellular transport organization implies that the membrane of the donor compartment finds its way to the specific acceptor membrane. By what extent do SNARE proteins participate in the specificity of vesicular localization is still an open question. Well-known membrane contact coordinator is the family of Rab GTPases (Stenmark 2009). Rab GTPases switch between GTP- and GDP- bound states (Figure 12). In their GTP bound form they associate with membranes by geranylgeranyl groups, GDP bound Rab form soluble complexes with GDP dissociation inhibitor. GTP bound Rabs also interact with SNAREs, motors or coat components and form effector complexes that coordinate tethering and docking between the fusion partners.

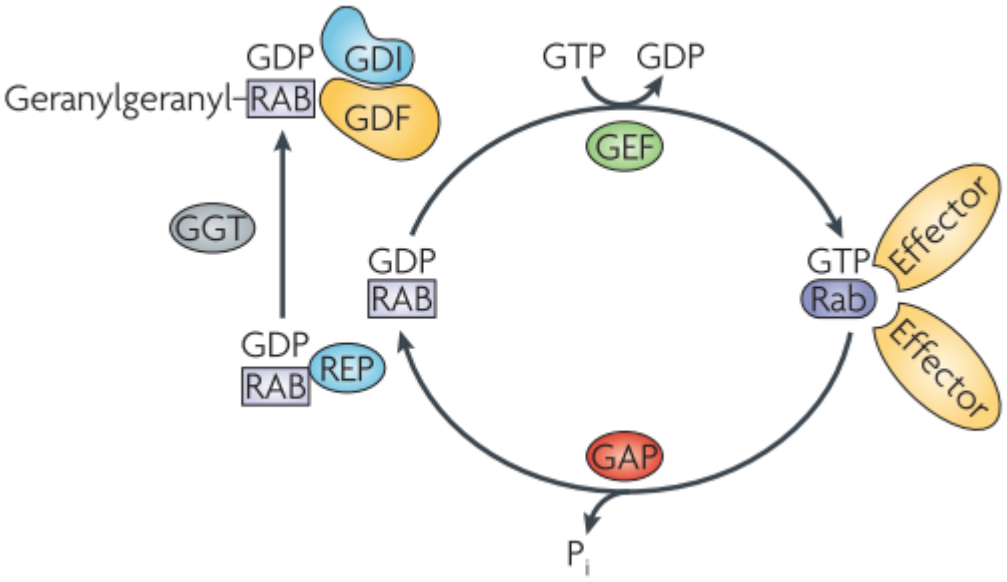

Figure 12 Rab circuitry
Guanine nucleotide exchange factor (GEF) catalyses the exchange of GDP for GTP, this causes the conversion of the GDP-bound ('inactive') Rab into its GTP-bound ('active') conformation. Rab in its active conformation is recognized by various effector proteins. GTPase-activating protein (GAP) stimulates GTP hydrolysis and Rab's conversion to its GDP-bound inactive form accompanied by the release of an inorganic phosphate P_i. Rab escort protein (REP) recognizes newly synthesized Rab proteins in its GDP-bound form and presents it to geranylgeranyl transferase (GGT). Rab is geranylgeranylated on one or two C-terminal Cys residues. Rab GDP dissociation inhibitor (GDI) recognizes GDP-bound, geranylgeranylated Rab and regulates Rab membrane cycle. GDI displacement factor (GDF) mediates Rab-GDI complex targeting to specific membranes. Illustration from (Stenmark 2009)

In our work, we were particularly interested in the identification of v-SNAREs that would be implicated in postsynaptic forms of exocytosis. Mammalian R-SNAREs that are Sec22b, Ykt6 and the seven proteins of the VAMP family (VAMP1, VAMP2, VAMP3/cellubrevin, VAMP4, VAMP5, VAMP7/Ti-VAMP, VAMP8/endobrevin). While Sec22b and Ykt6 are mainly enriched between endoplasmic reticulum and Golgi, the seven isoforms of VAMP family are found on diverse post-Golgi compartments and participate as R-SNAREs in fusion reactions with *trans*-Golgi network (TGN), endosomes and PM. With the exception of VAMP5, all VAMP isoforms can form fusogenic complexes with t-SNAREs SNAP-25 and syntaxin-1 or -4, found on the PM (Hasan et al. 2010) and can probably be implicated in exocytosis. VAMP1 and VAMP2 are very homologous isoforms differentially distributed in the rat brain (Raptis et al. 2005) that are implicated in Ca^{2+}-dependent synaptic vesicle exocytosis in neurons (Söllner et al. 1993; Brunger et al. 1998) and other forms of regulated exocytosis in non-neuronal cells (Rossetto et al. 1996). In neurons, VAMP2 is highly polarized to axons (Sampo et al. 2003), but is also present on dendrites and was recently reported

to be involved in dendritic exocytosis during LTP (see (Jurado et al. 2013) and section 2.3.3). VAMP3, also known as cellubrevin, is localised in endosomes (Jović et al. 2014). It was shown to participate in alpha-granule exocytosis in platelets (Feng et al. 2002), integrin trafficking (Proux-Gillardeaux, Gavard, et al. 2005) and transferrin receptor recycling to the PM (Galli et al. 1994) as well as retrograde transport of mannose-6 phosphate receptor (Ganley et al. 2008). Remarkably, VAMP3 is not expressed in brain (Susanne; Schoch et al. 2001), but can rescue transmission in VAMP2 knock-out (KO) cells (Deák et al. 2006). VAMP1, 2 and 3 share a lot of structural similarities, and, unlike other isoforms they are sensitive to clostridial neurotoxins (Pellizzari et al. 1999), see 2.2.1 below.

VAMP4 is a broadly expressed protein, particularly enriched in the brain (Advani et al. 1998; Steegmaier et al. 1999). It is abundant on the TGN structures and was reported to participate in early and recycling endosomes transport to TGN (Steegmaier et al. 1999; Mallard et al. 2002), as well as in the homotypic fusion of the early endosomes in complex with syntaxin13, Vti1a and syntaxin6 (Brandhorst et al. 2006; Zwilling et al. 2007). VAMP4 targeting to TGN is due to the dominant autonomous signal located on its N-terminal extension and consisting of a double-leucine motif followed by an acidic cluster (Zeng et al. 2003; Peden et al. 2001; Tran et al. 2007). The targeting signal allows VAMP4 binding to the adaptor complex AP1 and consecutive specific targeting to TGN. VAMP4 cycles though PM, where it is internalized back through clathrin-dependent endocytosis and transported to the sorting and recycling endosomes and finally concentrated in the Golgi (Tran et al. 2007). Immunolabeling of hippocampal slices showed VAMP4 presence in a perinuclear compartment in the soma as well as in apical and basal dendrites (Raingo et al. 2012). In axonal terminals, VAMP4 maintains bulk Ca^{2+}-dependent asynchronous release (Raingo et al. 2012), and appears to be an important cargo molecule for activity-dependent bulk endocytosis, a type of endocytosis which is triggered only with intense neuronal activity (Nicholson-Fish et al. 2015). VAMP4 is present on the membrane of enlargeosomes (Cocucci et al. 2008). These organelles are small vesicles that undergo rapid exocytosis upon cytosolic Ca^{2+} concentration rise and induce enlargement of the PM in pheochromocytoma (PC12) and neuroblastoma cell lines. Experiments with the corresponding small interferering RNA (siRNA) demonstrated that the regulated exocytosis of enlargeosomes is mediated by VAMP4 in association with syntaxin-6 and SNAP23 (Cocucci et al. 2008).

VAMP7 is another tetanus neurotoxin insensitive R-SNARE protein, also referred as Ti-VAMP, that possesses versatile functions in secretory and endocytic pathways depending on the considered cell type (Chaineau et al. 2009). Among others, it mediates apical exocytosis of the polarized epithelial cells (Galli et al. 1998; Pocard et al. 2007) and vesicular protein transport from early endosomes to lysosomes (Advani et al. 1999) as well as lysosomal exocytosis. VAMP7 and VAMP2 are involved in glucose transporter Glut4 translocation to the PM in adipocytes (Williams & Pessin 2008). Lately, VAMP7 was reported to regulate constitutive membrane insertion of the TRPM8 channel (Ghosh et al. 2016). Neurite outgrowth in PC12 cells and neurons also depends on VAMP7 mediated exocytosis (Martinez-Arca, Alberts & Galli 2000; Martinez-Arca et al. 2001). Finally, VAMP7 mediates SV exocytosis during spontaneous presynaptic activity (Hua et al. 2011) which can be stimulated by Reelin (Bal et al. 2013). VAMP7 has an auto-inhibitory longin domain: when it is folded back onto the coiled-coiled domain, the SNARE-complex assembly kinetics is decreased. This auto-inhibition can be released by tyrosine phosphorylation in the longin domain (Burgo et al. 2013). Finally, the VAMP7 longin domain is also implicated in selective sorting of VAMP7 to its sites of action through interaction with coat components of clathrin-coated vesicles (Daste et al. 2015).

VAMP8 or endobrevin is particularly enriched in kidney (Advani et al. 1998) and is associated with late endosomes (Wong et al. 1998). VAMP8 is the v-SNARE for regulated exocytosis in pancreatic acinar cells and probably plays an important role in the secretion processes of the entire exocrine system (Wang et al. 2004; Wang et al. 2007).

2.2 SNARE proteins for synaptic vesicle exocytosis

The main function of the axonal presynaptic terminal is the signal communication to the postsynaptic neuron in form of neurotransmitter release. Neurotransmitter is stored in the synaptic vesicles (SVs), shown on the Figure 2, that fuse with the plasma membrane upon Ca^{2+} arrival or spontaneously. Fast and precise exocytosis of the SV relies on custom tailored fusion machinery. SNARE complex for SV fusion and associated proteins is the most studied exocytosis system. Consecutively, presynaptic SNARE proteins are currently one of the best characterized and neurotransmitter release became the reference model of exocytosis.

2.2.1 SV SNAREs are targets of clostridial neurotoxins

VAMP1, also named synaptobrevin, was the first synaptic v-SNARE protein identified (Trimble et al. 1988; Baumert et al. 1989). It was described as an important element of SV membrane, probably implicated in vesicular docking or fusion. Studies in the early nineties found that VAMP2 was a target of tetanus and botilinum-B neurotoxins, TeNT and BoNT-B respectively (Schiavo et al. 1992). TeNT and seven serotypes of BoNT (from A to G) belong to a family of structurally correlated toxin proteins produced by anaerobic bacterium Clostridium botulinum. Clostridial neurotoxins block exocytosis of the SVs and their activity results in clinical signs of botulism. Toxins consist of two chains connected by a disulphide bond. Their specific binding to nerve cells and subsequent penetration is mediated by the heavy chain (~100 kD). The light chain (~50 kD) is responsible for protease activity. Demonstration that TeNT and BoNT-B are zinc endopeptidases that cleave rat VAMP2 isoform at the peptide bond Gln76-Phe77 was the first evidence of VAMP's direct implication in SV exocytosis. Shortly after it was shown that BoNT-A and BoNT-C1 prevent synaptic transmission by cleaving presynaptic SNAP25 and syntaxin, respectively (Blasi, Chapman, Link, et al. 1993; Blasi, Chapman, Yamasaki, et al. 1993). Around the same time VAMP2/synaptobrevin-2, SNAP25 and syntaxin were identified as membrane receptors for SNAP, known as an essential element of the fusion machinery (Söllner et al. 1993). In their study, the group of JE Rothman introduced term v-SNARE, for SV membrane residing VAMP, and t-SNAREs, for PM residing syntaxin and SNAP-25 for the first time.

2.2.2 Other proteins involved in neurotransmitter release

We have seen that SNARE proteins are essential proteins for SV exocytosis. SNARE functioning is assisted by other protein families that play complementary role in fusion like docking, tethering and Ca^{2+}-sensitivity of the fusion. Studies of the SV exocytosis identified other proteins that are essential for the control of synaptic vesicle exocytosis that will briefly describe below.

SM (Sec1/Munc18-like) proteins interact with SNAREs in various ways (Figure 13) and organize SNARE complex spatially and temporally. They have an arch-shaped "clasp" structure adapted to clasp a four-helix bundle (Misura et al. 2000). It can be the four-helix bundle of a zippering SNAREpin (Shen et al. 2007; Dulubova et al. 2007) or individual t-SNARE syntaxin1 in the 'closed' conformation when its N-

terminal 'Habc' domain comprised of three helices is bound to the syntaxin's SNARE motif helice (Hata et al. 1993; Dulubova et al. 1999). Munc18-1 is a major synaptic SM protein and its deletion leads to severe exocytosis impairment (Verhage et al. 2000). It promotes fusion by adapting an 'open' conformation (Figure 14, B), where it is bound to a specific N-terminal sequence of the syntaxin. Open SM-protein – syntaxin complex leaves the arch-shaped SM-protein body available associate with the forming SNAREpin and clasp across the zippering SNARE complex (Figure 14, C). SM proteins also participate in Ca^{2+} exocytosis regulation, like presynaptic Munc13 (Chicka et al. 2016)(Shin et al. 2010; Calloway et al. 2015). In endosomal cycling, Munc13-4 was identified as Rab11 binding protein that participates in endosomal trafficking and docking at the PM (Johnson et al. 2016).

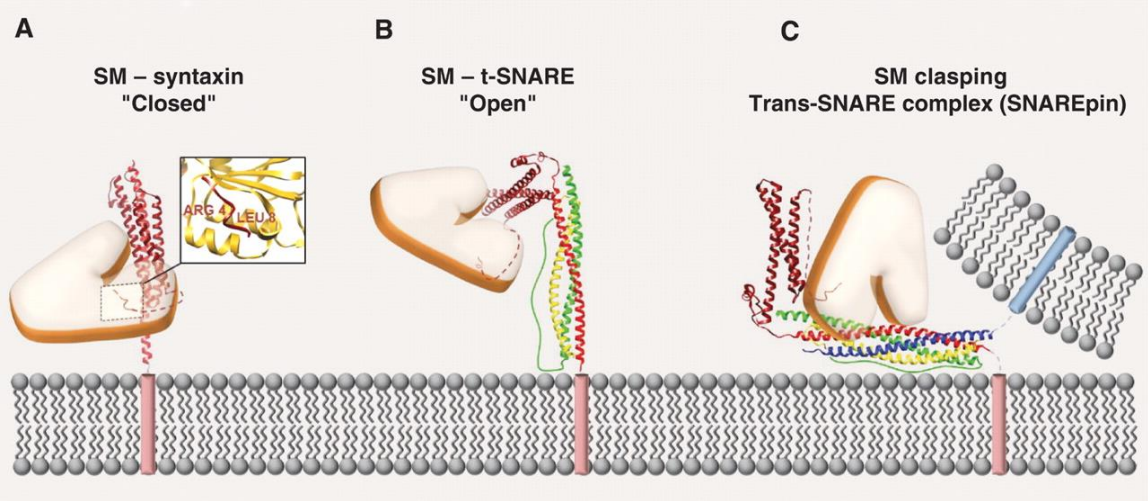

Figure 13 SM proteins binding to SNAREs
A, SM-protein bound to the closed closed conformation of syntaxin. **B**, open conformation of the SM protein-tSNARE complex, where SM protein is bound to the syntaxin Habc domain. **C,** SM-protein binding to the 'zippering' SNARE complex. Image from(Südhof & Rothman 2009)

As SNARE complex formation is thermodynamically spontaneous process of protein folding, it needs to be externally regulated to prevent excessive or physiologically irrelevant fusion. Precise timing and regulation of the fusion reactions is performed by complexins and synaptotagmins (Südhof & Rothman 2009). Complexin activates and clamps SNARE proteins, holding them in a prepared 'primed for fusion' state (Tang et al. 2006; Reim et al. 2001). Finally, the Ca^{2+} sensor synaptotagmin, upon binding to Ca^{2+}, reverse complexin action and thus triggers the fusion (Fernández-Chacón et al. 2001; Pang et al. 2006).

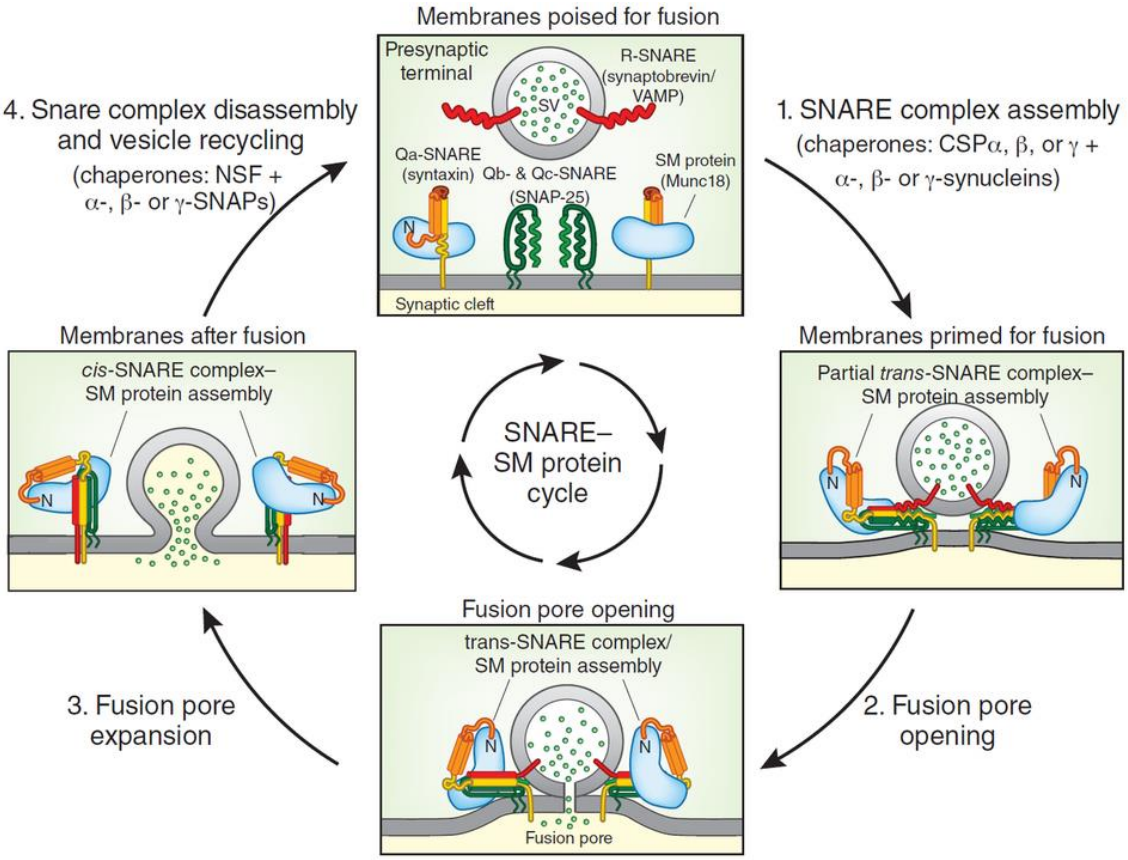

Figure 14 Synaptic SNARE-SM proteins cycle
SV fusion and the associated SNARE-SM protein cycle. In the first step, syntaxin adapts open conformation, Munc18-binding mode also opens its closed conformation and SVs are primed for fusion though the partial assembly of the *trans*-SNARE complex. During the second step, full *trans*-SNARE complex assembly opens the fusion pore. In the third step, *trans*-SNARE conversion to its *cis*- configuration is accompanied by the fusion pore expansion. In the fourth step, NSF and SNAP disassemble the SNARE complex. Image from (Südhof 2013b).

Synaptotagmins (syts) are secretory vesicle proteins containing two characteristic protein kinase C–like C2 domains. Many members of the 17 syts isoforms family act as Ca^{2+} sensors, promoting fusion in a Ca^{2+}-dependent manner. In the presynaptic terminal, fast synchronous release is promoted by syt1 and syt2 (Geppert et al. 1994; Fernández-Chacón et al. 2001). Fast synchronous release Ca^{2+} sensors react to the high local Ca^{2+} raise, preventing spontaneous fusion in the absence of presynaptic depolarization. Asynchronous release, that depends mostly on the bulk cytosolic Ca^{2+} alterations, is mediated by syt7 (Bacaj et al. 2013) which is also important for increase in NT release during paired-pulse facilitation (Jackman et al. 2016).

2.2.3 Vesicular pools for synaptic transmission

Neurotransmitter release at the presynaptic terminals can happen in various ways. Numerous molecular actors for SV trafficking and exocytosis have already been

identified, but their complex mechanisms and interactions are still have to be untangled.

SV have can be classified in different “pools” based on their functional or morphological properties. Conventional classification contains three main pools in regards to their exocytosis rates in response to a stimulation: the readily releasable pool (RRP), the recycling pool and the reserve or the resting pool (Rizzoli & Betz 2005; Südhof et al. 2000; Denker & Rizzoli 2010). In hippocampal glutamatergic boutons, there is a total of about 100 to 200 SVs (Schikorski & Stevens 1997). Vesicles from RRP form a subgroup of the recycling pool and correspond to SVs that are docked at the active zone and immediately available for release typically 5-10 SVs (Schikorski & Stevens 2001; Siksou et al. 2007; Watanabe et al. 2013). Consequently, they are the first to exocytose during the stimulation. The recycling pool, defined as the fraction of vesicles which recycle continuously under physiological levels of stimulation, was estimated by prolonged stimulation and either fluorescence imaging or subsequent electron microscopy. Depending on the method, it represents 20 to 50% of all vesicles, in cultured neurons (Harata et al. 2001; Kim & Ryan 2010) and in slices (Marra et al. 2012). Finally, a fraction of vesicles in synaptic terminals are distinct from the recycling pool and form the reserve pool. They are the most reluctant to release and would mediate release only after continuous high-frequency stimulations, after the depletion of the recycling pool. In the three-pools model, SV ability to recycle is defined mainly by its position relatively to the active zone and interaction with surrounding scaffolding proteins (Denker & Rizzoli 2010), which are modulated by phosphorylation/dephosphorylation of various substrates by Cdk5 and calcineurin(Kim & Ryan 2010; Marra et al. 2012). Reserve pool SV would be little mobile due to their tight connection to the scaffolding protein. Conversely, SV from recycling pool are highly mobile but can be transferred to the reserve pool through binding or scaffolding molecules and integrating vesicular cluster.

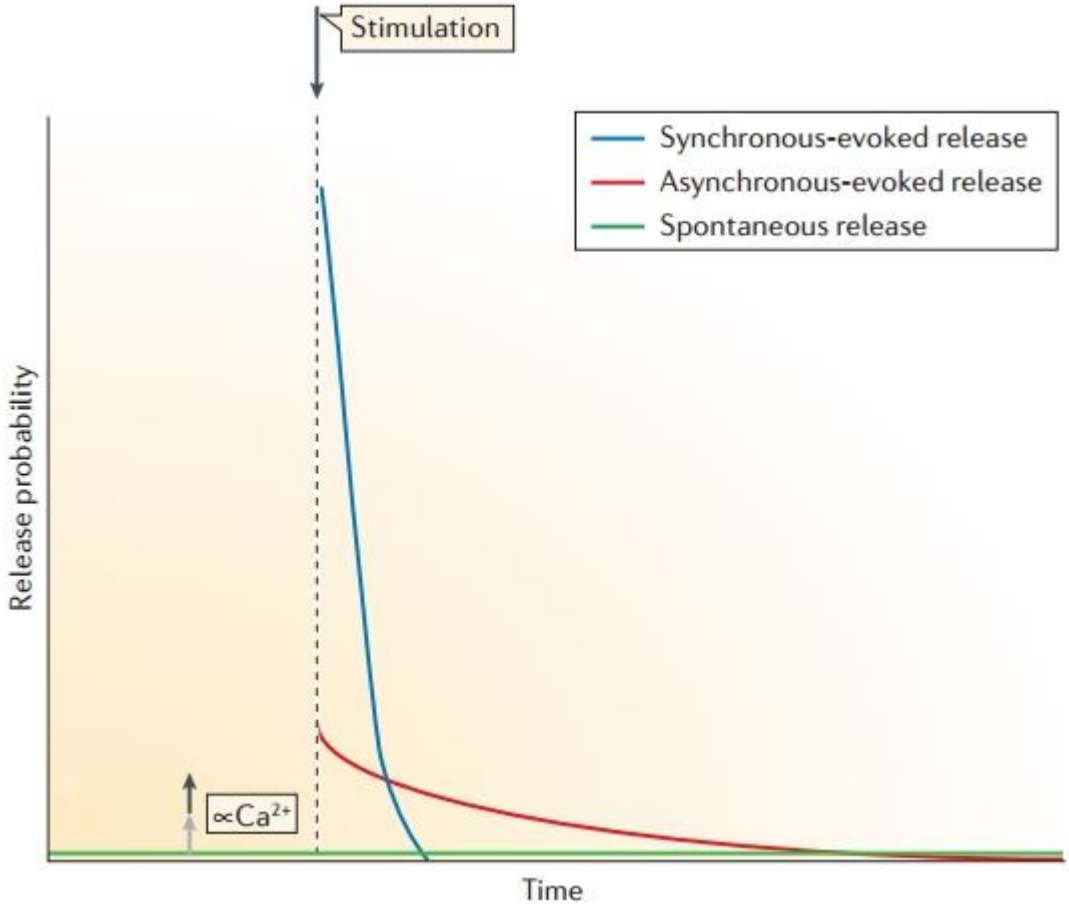

Figure 15 Time course of the probability for kinetically different types or release.
The probability of the synchronous release is highest during the 1 ms after stimulation and decreases rapidly. Asynchronous release is poorly coupled to stimulation and spontaneous release manifests independently of the presynaptic action potentials. Image source: (Crawford & Kavalali 2015)

In addition to their location relative to the active zone, SVs belonging to different pools could have a different composition of proteins and lipids. Studies in of the presynaptic exocytosis highlight that functional differences in vesicular exocytosis are based on vesicular molecular make-up and temporal dependency from the action potential arrival (Crawford & Kavalali 2015). As already discussed in 1.2.2, currently three main types of releases are distinguished: synchronous, asynchronous and spontaneous. They differ mainly in the time course of their appearing in relation to intracellular Ca^{2+} raise and amplitude. Synchronous release appears shortly after stimulation and has highest amplitude, asynchronous release is triggered with some delay after the stimulation and spontaneous release is not correlated with the Ca^{2+} raise and postsynaptic currents or potentials it provokes are identified as miniature (mEPSC or mEPSP). Another way of looking at the different releases is to consider the

probability of it's appearing after Ca^{2+} raise: asynchronous release has highest probability at the moment of stimulation that decreases rapidly with time, asynchronous release probability is not that high at the stimulation, but decreases slower and the spontaneous release probability is stable and does not depend on stimulation but its rate is proportional to basal Ca^{2+} levels, see Figure 15. Trafficking and exocytosis machinery most likely underlies differences in three types of releases.

VAMP1 and 2 are two of the most abundant SV proteins (Takamori et al. 2006; Raptis et al. 2005). VAMP1 is mostly expressed in the mesencephalon and spinal cord while VAMP2 is essentially expressed in the telencephalon (Susanne Schoch et al. 2001). They are mainly responsible for evoked synchronous neurotransmitter release (Susanne; Schoch et al. 2001; Liu et al. 2011). In VAMP2 KO mice, the spontaneous and evoked neurotransmission releases are severely decreased but still present. Noticeably, a VAMP2 mutant, with the addition of 12-residue insertion was able to rescue only spontaneous transmission, indicating mechanical differences in evoked and spontaneous SV exocytosis (Deák et al. 2006). Synchronous evoked fusion is also operated with synaptotamin-1, -2 and probably synaptotagmin-9 Ca^{2+} sensors (Maximov & Südhof 2005; Xu et al. 2007).

TeNT insensitive v-SNARE VAMP4 is implicated in evoked asynchronous release (Raingo et al. 2012). Knock-down (KD) of VAMP4 in cultured hippocampal neurons significantly decreased asynchronous component of the postsynaptic currents. Additionally, slow Ca^{2+} chelation by EGTA-AM impairs VAMP4 mediated current, after its overexpression in VAMP2 KO neurons. Finally, there are two v-SNAREs reported to be associated with spontaneous neurotransmitter release: vti1a, although a Qb SNARE, is directly involved in spontaneous SV fusion but does not mediate action potential dependent exocytosis (Ramirez et al. 2014). VAMP7 is also not involved in stimulation dependent exocytosis (Hua et al. 2011; Bal et al. 2013) but spontaneous EPSCs can be enhanced by Reelin in a VAMP7-dependent manner (Bal et al. 2013). In conclusion, even though VAMP2 is undoubtedly the major SV SNARE involved in synchronous neurotransmission, the other vesicular SNAREs, VAMP4, VAMP7 and Vti1A, which represent a small minority of this category of membrane proteins (Takamori et al. 2006), play a specialized role in SV fusion, during asynchronous and spontaneous neurotransmission. However, it remains to be determined if these particular SNAREs define separate populations of SVs or if they

are located on the majority of SVs, enabling these forms of neurotransmission, depending on the conditions of neuronal stimulation.

2.3 Dendritic exocytosis

Dendritic forms of exocytosis, although not so intensely studied as neurotransmitter release, are important for many aspects of the cellular life like molecular composition of the PM, cellular growth, release of soluble factors, and functional as well as morphological neuronal plasticity (Kennedy & Ehlers 2011).

2.3.1 Organelles for dendritic exocytosis

The variety of functions of dendritic exocytosis is supported by multiple types of organelles (Figure 16). Dendritic compartments contain the necessary machinery corresponding all stages of canonical secretory pathway for local constitutive trafficking of lipids and proteins. EM images demonstrate the presence of endoplasmic reticulum (ER), Golgi membranes, endosomal system and, in particular types of cells, dense core vesicles all over the dendritic arbor (Cooney et al. 2002; April C. Horton et al. 2005; Park et al. 2006; Spacek & Harris 1997). In addition, non-canonical secretory pathways may also be present in dendrites, like fusion of smooth ER-derived organelle spine apparatus found in some spines. Spine apparatus sometimes contain vesicular structures, raising the possibility of direct secretion from ER related compartments.

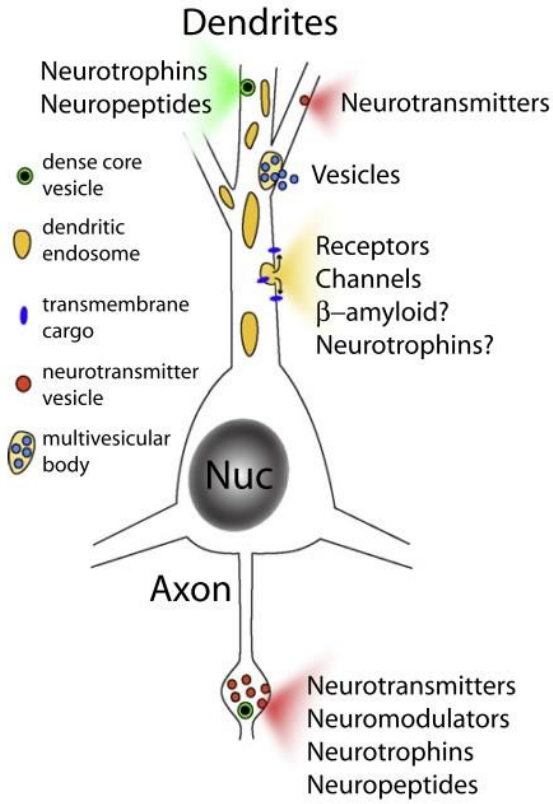

Figure 16 Dendritic organelles for exocytosis
Schematic neuronal representation illustrating exocytosis from dendrites and axons. Various organelles can be secreted from dendritic compartments. Dendrites are able to secrete soluble cargo like neurotransmitters, neuropeptides and neurotrophins in addition to transmembrane proteins. Image from (Kennedy & Ehlers 2011)

Dendritic compartments are rich in different types of endosomes (Cooney et al. 2002). Endosomes are intracellular membranous compartments that received

endocytosed vesicles. They sort membrane-associated molecules or ligands back to the PM or further down the endocytic pathway for degradation in lysosomes. Endosomal system consist of early/sorting endosomes, recycling endosomes (RE), late endosomes, and lysosomes (Maxfield & McGraw 2004). Membrane-bound endosomal compartments or multivesicular bodies (MVBs) carrying integral vesicles were observed in dendrites and axonal terminals (Cooney et al. 2002). Most of the MVBs content is forwarded to lysosomes for degradation. However, studies have shown that MVBs can also fuse with the PM. The intact vesicles released into the extracellular space are called exosomes and they can be taken up by the neighbouring cells and are used for intercellular transport of soluble proteins, membrane proteins and nucleic acids (Simons & Raposo 2009). They could constitute an important, yet still elusive, form of neuronal communication

2.3.2 Functionally different types of dendritic exocytosis

Neuronal growth during early development requires constant addition of the PM to the cell surface. In mature neurons, established shape and polarity can be maintained for months or years despite the constant renewal of the PM lipids and proteins. Dendritic growth can be prevented by ER-Golgi pathway disturbance through genetic or pharmacological techniques (April C Horton et al. 2005). In mature neurons, post Golgi traffic block leads to dendritic length reduction and dendritic arbour simplification (April C Horton et al. 2005). On the other hand, axonal morphology is not influenced by secretory pathway block, suggesting that canonical secretory pathway is important specifically for dendritic development and stability. Nevertheless, experiments with TeNT addition to cultured neurons revealed that the absence of functional VAMP-2 and other TeNT-sensitive VAMP proteins did not have a significant impact on dendritic arbour development (Harms & Craig 2005). Moreover, in VAMP2 knock-out animals, neuronal morphology is unaffected (Susanne; Schoch et al. 2001). These data indicate that other v-SNARE proteins should be important in trafficking for morphological development, like TeNT-insensitive VAMP7, that is involved in neurite outgrowth in PC12 cells (Martinez-Arca et al. 2001). However, VAMP7 knock-out animals also have minimal morphological neuronal defects (Danglot et al. 2012) suggesting redundancy in the molecular mechanisms of this essential feature of brain development.

Dendrites also possess secretory vesicles structurally resembling SVs and containing glutamate, dopamine, GABA and neuroactive peptides (Kennedy & Ehlers 2011). Such uniformly filled small vesicles are often packed in dense sites. These regions contact other dendrites that in their turn contain similar vesicle-rich areas, facing the site of the contact. Symmetrical structure suggest reciprocal nature of the dendrodendritic connection or dendrodendritic synapse. Electrophysiological data confirms that dendrodendritic synapse release both excitatory and inhibitory neurotransmitters (Famiglietti 1970; Lagier et al. 2007; Shanks & Powell 1981; HIRATA 1964). Classical model for dendrodendritic synapse study is the connection between olfactory bulb mitral and granule cells dendrites. Depolarized mitral cell releases glutamate onto the dendrites of the granule cell. Activated granule cell then discharges GABA from the dendritic connection site, inhibiting activated mitral cells together with unstimulated mitral cells coupled to the granule cell in question (Rall et al. 1966; Rall & Shepherd 1968). GABA release in the mitral cell does not require depolarization at the level of AP and can happen through local dendritic depolarization (Egger et al. 2003). Dendritic GABA exocytosis, as in axons, depends on intracellular Ca^{2+} levels. Vesicle fusion is coupled to Ca^{2+} and slow Ca^{2+} chelator EGTA does not impact GABA release (Isaacson 2001).

The neurotransmitter dopamine was found in multiple types of dendritic organelles: large dense core vesicles, small synaptic-like vesicles and tubular structures (Kennedy & Ehlers 2011). Controversial mechanisms for dopamine release regulation were proposed. One hypothesis suggests that dopamine is released through reversal of the dopamine transporter (Falkenburger et al. 2001) and does not rely on vesicular fusion. On the other hand, Clostridial neurotoxins successfully block dopamine emission (Fortin et al. 2006), while dopamine transporter inhibitors does not, confirming vesicular character of the dopamine release. Dendritic dopamine exocytosis has a different Ca^{2+}-sensitivity from axonal one, dendritic form being sustained with lower levels of extracellular Ca^{2+}, indicating that different Ca^{2+} sensors should be involved in this type of release. Immunocytochemical studies suggest that dendritic dopamine release in substantia nigra dopaminergic neurons differs from classical SV machinery and probably depends on unconventional SNARE complex formed by VAMP2, SNAP-25 and syntaxin 3 SNARE proteins (Rice & Patel 2015).

Dendrites also perform retrograde signalling to presynaptic terminals, like growth factor or neurotrophins with brain derived neurotrophic factor (BDNF) among others. BDNF is principally released from axon terminals, but now it is known that BDNF can be released from dendritic compartments in activity-dependent manner (Altar et al. 1997). Neurons expressing BDNF fused with GFP have a punctate pattern all over dendritic arborisation. Upon membrane depolarization the BDNF-GFP puncta gradually disappear, implying vesicular BDNF secretion (Hartmann et al. 2001). Axonal BDNF is considered prevalently located in dense core vesicles; nevertheless, the source of dendritic BDNF and the identity of its harbouring organelles are still not well defined. Recent study demonstrates that exogenous BDNF, endocytosed mostly at the presynapse, can subsequently be released in synaptotagmin6 and complexin-dependent manner (Wong et al. 2015). Both axonal and dendritic BDNF releases are negatively regulated by synaptotagmin-4, a synaptotagmin family protein that lacks Ca^{2+} -binding domain and thus can bind to SNARE complex, but prevents the fusion step (Dean et al. 2009).

Another remarkable form of dendritic exocytosis is transcytosis, which stands for exocytosis of the presynaptic proteins harbouring organelles in the dendritic compartments. Presynaptic proteins like synaptophysin or VAMP2 are initially exocytosed to the dendritic PM with subsequent endocytosis and transport to axon (Sampo et al. 2003; Wisco et al. 2003). Transcytosis is probably an efficient way to use proteins that are required on both post- and presynaptic compartment. VAMP2 – driven exocytosis, for example, is involved in postsynaptic modifications during plasticity (Jurado et al. 2013). This latter phenomenon has been the subject of intense study. Given the functional importance and wealth of data on the implication of postsynaptic membrane trafficking on synaptic transmission and plasticity I will devote the following chapter to this phenomenon.

2.3.3 Postsynaptic trafficking during synaptic transmission and plasticity

Patch-clamp recording of post-synaptic currents allows the tight control through the recording glass electrode of the postsynaptic intracellular compartment. With this approach, the infusion of active proteolytic fragment of BoNT-B or TeNT, which selectively cleave VAMP2, as well as VAMP1 and 3, but not other VAMPs (Mallard et al. 2002), prevents the expression of LTP (Lledo 1998; Lu et al. 2001).

Moreover, this treatment also provokes the gradual decrease of the postsynaptic current, or EPSC (Lüscher et al. 1999). However it has been written (but not formally shown) that TeNT dialysis into the recording pipette was without effect on mEPSCs amplitude or frequency (Lu et al. 2001) , at odds with an effect on TeNT on basal synaptic transmission. Conversely, blocking endocytosis mediated by dynamin specifically in the postsynaptic cell induces a gradual increase in EPSC amplitude and blocks LTD (Lüscher et al. 1999; Morishita et al. 2005). Moreover, interfering with recycling endosome function with dominant negative Rab proteins (Rab11a) blocks LTP (Park et al. 2004; Brown et al. 2007). These data are consistent with a model where postsynaptic receptors are not stably anchored in the postsynaptic density but are constantly internalized and recycled in the postsynaptic cell (Figure 17).

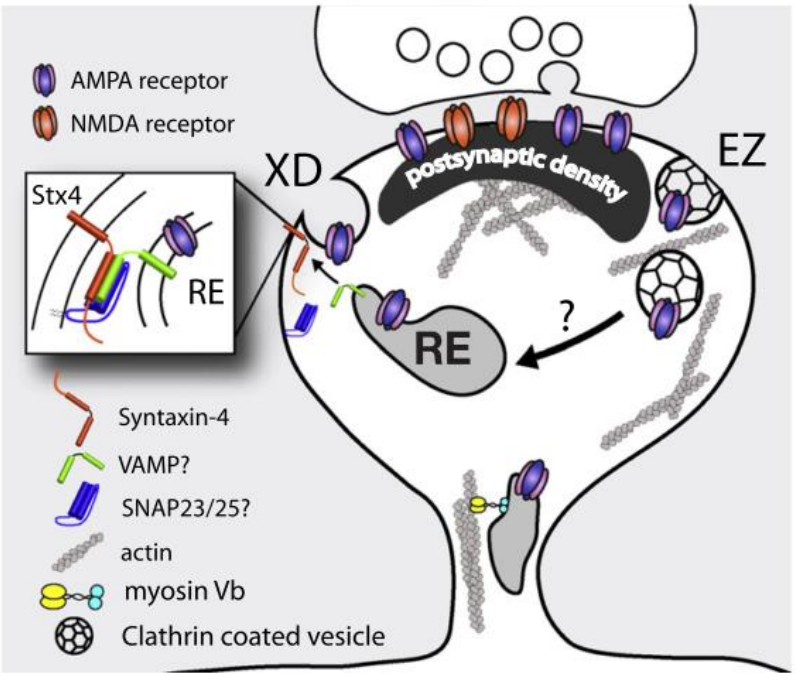

Figure 17 Postsynaptic AMPAR trafficking underlying synaptic plasticity
Recycling cargo fuses with the spine membrane at the exocytotic domain (XD) containing Stx4. Clathrin-mediated endocytosis occurs at the endocytic zone (EZ). Illustration from (Kennedy & Ehlers 2011)

In this model, the behaviour of recycling endosomes (REs) plays a central role in the trafficking of postsynaptic receptors and its modulation during synaptic plasticity. Imaging of the transferrin receptor (TfR), a classical marker of recycling endosomes, with GFP fusion constructs has confirmed that these organelles are transported from the dendritic shaft to spines following an LTP protocol in culture (Park et al. 2006). This transport is calcium dependent and is due to the binding of Rab11FIP2 to the actin motor Myosin Vb (Wang et al. 2008). Consistent with this data,

acute inhibition of MyosinVb prevents LTP (Wang et al. 2008). Moreover, preventing RE from entering the spine with chemical dimerization of a Myosin6 construct provoked a gradual decrease of EPSC amplitude (Esteves da Silva et al. 2015) suggesting that part of the recycling of AMPA receptors occurs within the spine. However, the same treatment did not prevent the spine enlargement following LTP induction, suggesting that the structural plasticity of spines concomitant to LTP is not directly linked to RE transport to spines (Esteves da Silva et al. 2015).

In addition to RE transport, exocytosis of RE can be visualized with a pH sensitive mutant of GFP, superecliptic pHluorin (SEP; Miesenbock et al. 1998). Indeed the SEP tag on the extracellular (when on the PM) or luminal (when in an intracellular organelle) side of membrane proteins will report the rapid change in pH following exocytosis (see Chapter 2 in Materials and methods). Fluorescence imaging of neurons transfected with such constructs allows the detection of individual exocytosis events (Yudowski et al. 2006; Yudowski et al. 2007; Park et al. 2006; Lin et al. 2009; Kennedy et al. 2010; Jullié et al. 2014). The frequency of events detected with the AMPA subunit GluA1 tagged with SEP increases with chemical LTP (Yudowski et al. 2007; Lin et al. 2009). Finally GluA1-SEP contained inside TfR—positive endosomes are inserted to the PM in postsynaptic spines (Kennedy et al. 2010; Patterson et al. 2010).

AMPARs and postsynaptic membrane delivery during LTP is mediated by SNARE proteins (Kennedy et al. 2010; Lledo et al. 1998; Lu et al. 2001). Moreover, recent evidence suggests that SNARE machinery mediating activity-dependent AMPAR exocytosis is different from SNAREs involved in constitutive AMPA cycling necessary for maintaining basal synaptic strength (Jurado et al. 2013), see Table 1. KD experiments in cultured neurons and acute slices demonstrated that it was specifically syntaxin3 (but not syntaxin4, as previously proposed by Kennedy et al. 2010), that was responsible for AMPAR exocytosis during LTP. Moreover, unlike syntaxin4, syntaxin3 binds to complexin that was previously reported to mediate LTP-related AMPAR delivery (Ahmad, J. S. Polepalli, et al. 2012). Besides syntaxin3, KD strategy identified t-SNARE SNAP47 as a part of SNARE machinery mediating regulated postsynaptic exocytosis (Jurado et al. 2013). SNAP-25 KD is not involved in activity-dependent exocytosis, but also indirectly affects LTP expression because of SNAP-25 involvement in NMDAR cycling (Lau et al. 2010; Jurado et al. 2013). As suggested by the study

using intracellular loading of the BoNT-B cleaving VAMP2 (Lledo et al. 1998; Schiavo et al. 1992), this VAMP isoform is the critical R-SNARE for AMPA receptor exocytosis during LTP. Experiments with neuronal cultures from VAMP2 KO mice confirm the inability of LTP induction in the absence of VAMP2, as well as impaired constitutive AMPAR cycling (Jurado et al. 2013). However, these results should be interpreted with caution, due to inevitable impairment of presynaptic function in VAMP2 KO neurons. This data can be summarized in the following Table 1; it suggests that different population of intracellular organelles, recycling endosomes, participate in constitutive and regulated exocytosis.

SNARE type	**Constitutive exocytosis**	**Regulated exocytosis**
t-SNARE	Syntaxin4 (?)	Syntaxin3
v-SNARE	VAMP2	VAMP2
SNAP-like	SNAP-25, SNAP-23	SNAP-47

Table 1 SNARE proteins involved in postsynaptic exocytosis.
So far identified SNARE proteins involved in constitutive exocytosis necessary for basal membrane composition maintenance and regulated or activity-induced exocytosis.

~

With this introduction, I tried to illustrate the diversity of the known neuronal forms of exocytosis and their importance for neuronal activity. Indeed, exocytosis is a fundamental cellular function that in neurons became a core part of neuron specific processes such as neurotransmitter release, morphological development and compartmentalization, receptor delivery and plasticity. The most intensively studied form of neuronal exocytosis is the one directly related to information transmission – the presynaptic neurotransmitter release. Studies of the presynaptic transmission have considerably enriched our knowledge about the universal fusion machinery, the SNARE protein complex. Recent advances in presynaptic exocytosis research show that vesicles are equipped with very diverse SNARE machinery and this diversity is directly related to the variety of exocytosis functions. Postsynaptic exocytosis, although attracting less attention, exists in multiple forms and mediates diverse physiological processes. However, the molecular machinery mediating somatodendritic forms of secretion is unclear. I have concentrated my work on investigating fusion proteins involved in postsynaptic REs exocytosis that is important for basal neuronal transmission maintenance and plasticity, a process, directly related to learning.

~

Objectives

The primary objective of the presented work is to identify **v-SNARE proteins mediating RE exocytosis in neuronal postsynaptic compartments**. Despite the functional diversity of RE exocytosis, current scientific knowledge has identified only one v-SNARE (VAMP2) involved in postsynaptic exocytosis. First, I wanted to test the implication the other v-SNAREs expressed in neurons, VAMP4 and VAMP7, in REs-exocytosis and especially its less studied form – the constitutive recycling. Second, after identifying potential v-SNARE candidates, I aimed at identifying their functional relevance.

To determine v-SNARE proteins potentially regulating somatodendritic secretion, I used different downregulation strategies and examined the effect they produce **directly on constitutive REs exocytosis**. Foremost, I applied genetically expressed agents that downregulate endogenous levels of the proteins of interest and observed exocytosis frequency changes with the high resolution and temporal precision of the live fluorescence microscopy. This strategy has identified VAMP4 as a major player of dendritic constitutive RE exocytosis.

After observing effects with genetic tools, I used the strategy of the **acute block of exocytosis** to confirm the obtained results. While technically more complex, acute block allows v-SNARE inactivation without the side effects of the chronic downregulation and grants a real-time manipulation with the cell recycling.

To verify **functional implication** of the found SNARE candidates I conducted experiments on two biological models: cultured hippocampal neurons and organotypic hippocampal slices. In cultures, I applied chronic protein downregulation and verified basal neuronal transmission in form of mEPSCs that relies on constitutive AMPARs cycling. In hippocampal slices, that have a better-conserved circuitry, I conducted LTP induction after genetic v-SNARE downregulation in postsynaptic neurons, as a functional read-out of regulated postsynaptic exocytosis.

Together these experiments should indicate proteins that drive postsynaptic RE cycling and determine its functional variety.

Materials and methods

1 Culture of hippocampal neurons

There are numerous ways to detect exocytosis in cells. One can monitor the exocytotic activity by measuring the increase in membrane capacitance due to the PM surface increase (Huynh et al. 2007; Cocucci et al. 2008). Minute changes in membrane capacitance is measured with the help of whole-cell patch-clamp recordings. However, in neurons, the precise measure of the membrane capacitance is technically complicated due to the morphological complexity of the neuronal PM and its non-linear properties.

Live antibody staining can also be used to estimate the amount of exocytosis or recycling (Kennedy et al. 2010; Park et al. 2004; Passafaro et al. 2001). Cells are transfected with receptors tagged with an extracellular epitope (HA). Between the tag and the receptor, in the amino-terminal portion of the receptor, there is a specific protease cleavage site. Transfected cells are incubated with the protease, and left to recover for specific time intervals. Surface fluorescence of the cells serves afterwards as an indicator of the exocytotic activity. This approach is useful to estimate the rate of exocytosis, but it does not tell much on the organelle's fusion dynamics.

In the current work I was aiming to study the dynamics and the distribution of the RE fusion events with high temporal and spatial resolution, that is why we relied on microscopy technique with the use of the pH-sensitive GFP mutant for imaging of the vesicular fusion events. Our microscopy technique of choice was Spinning-Disk confocal microscopy, which gives us the needed

temporal and spatial resolutions. In this chapter, I will discuss the details of the imaging experiments realization.

1.1 Banker protocol for neuronal cell culture

For studying the precise dynamics of exocytosis and distribution in postsynaptic compartments, the use of hippocampal primary neuronal culture is the most convenient choice. Low-density cultures allows relatively easy imaging of isolated neurons and facilitate the study of protein's subcellular distribution and trafficking with detail. It can be argued that cultures do not offer the best physiological condition for neuronal development. Nevertheless, neuronal cultures provide the unique environment for microscopy techniques.

We used hippocampal primary cultures obtained via so-called Banker protocol. Pyramidal neurons make the majority of the hippocampal population. In culture, they grow well-developed dendrites and connect with each other into a network of glutamatergic and GABAergic synapses. In the Banker protocol, dissociated hippocampal neurons grow on the underside of the coated glass coverslips. These coverslips are suspended by wax dots above an astroglial monolayer grown on the bottom of the culture dish for two weeks before seeding the neurons. Glial cells provide necessary trophic support for the growing neurons. By culturing neurons and glia cells on different supports in the same culture dish, we can obtain sparse neurons having good survival level with very little glia contamination. Such neurons are easier to image as they grow their processes in one plane, without intertwining with glial cells. The scheme for Banker culture dishes is provided on the Figure 18.

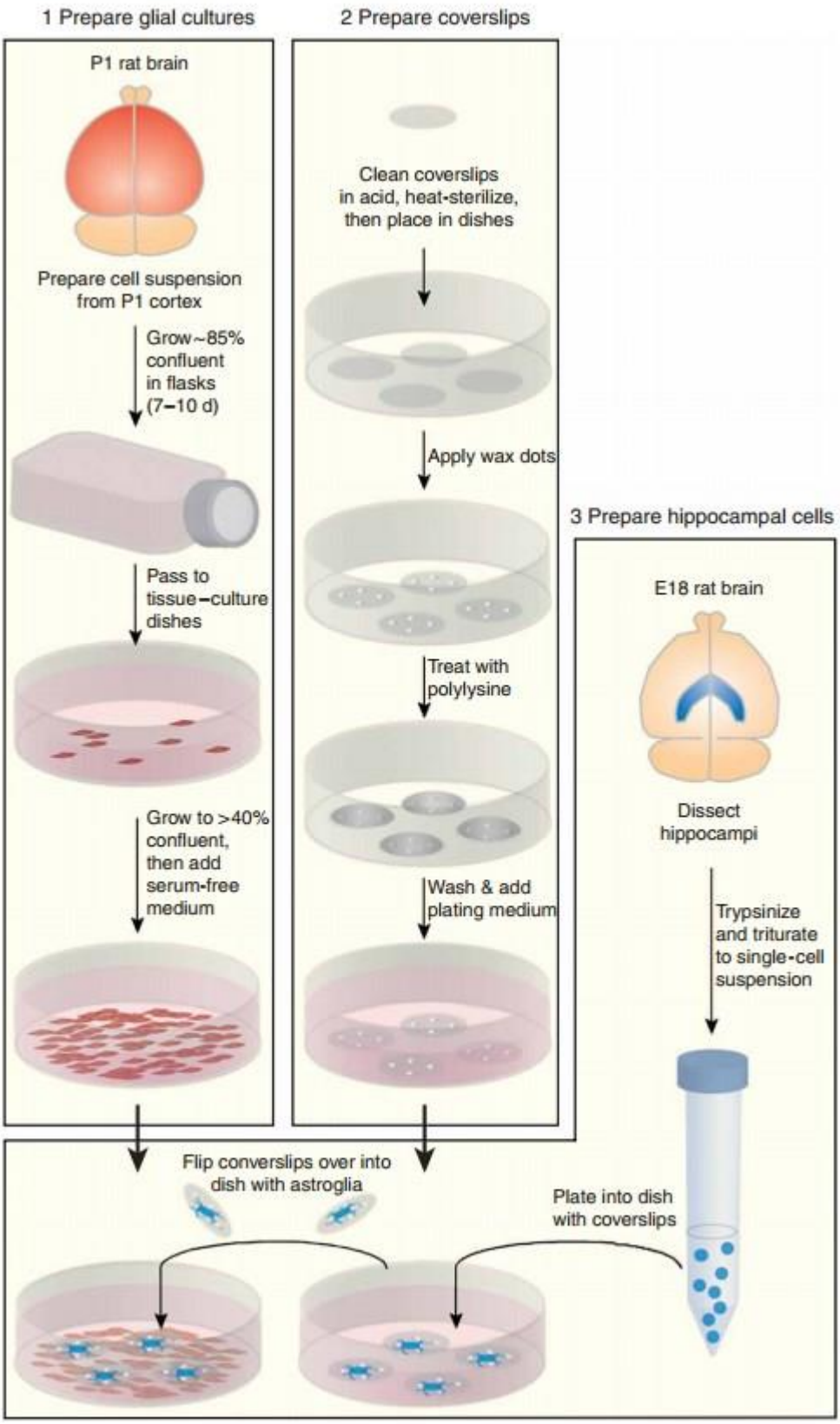

Figure 18 Preparing hippocampal neurons flowchart
The flowchart from Kaech & Banker, 2006 illustrates the three-partial protocol for cultured hippocampal neurons preparation.

The exact neuron culture protocol used in this work was the following:

Banker Culture protocol.

Dissociated hippocampal neurons from E18 Sprague-Dawley rat embryos of either sex were prepared as described in (Kaech & Banker 2006) at a density of 250,000 cells per 60-mm dish on poly-L-lysine pre-coated 1.5H coverslips (Marienfeld, cat. No. 117 580). Neurons cultures were maintained in Neurobasal medium supplemented with 2mM L-glutamine and 1X NeuroCult SM1 Neuronal supplement (STEMCELL technologies). After 3-4 days in culture, 5 µM Cytosine arabinoside (Ara-C) was added to the culture medium.

Astrocytes feeder layers were prepared from the same embryos, plated between 20,000 to 40,000 cells per 60-mm dish (according to the batch of horse serum used) and cultured in MEM (Fisher Scientific, cat. No. 21090-022) containing 4.5g/l Glucose, 2mM L-glutamine and 10% horse serum (Invitrogen) for 14 days.

I have also used neurons cultured without a feeder layer. For this configuration, cells were plated at a density of 200-600 x 10^3 cells per 60-mm dish containing coverslips. Cells were plated in supplemented Neurobasal medium containing 10% horse serum. 48h later, medium was replaced by pre-equilibrated maintenance medium to remove horse serum, and 5µM Ara-C was added between 6-8 days in vitro (DIV), depending on the glial cells proliferation.

1.2 Effecten transfection

1.2.1 Transfection protocol

Numerous tools for gene delivery into primary cell cultures are already available. We chose commercial Effectene transfection reagent (Qiagen). Effectene is a nonliposomal lipid for DNA transfection. It can be applied in both cell lines as well as primary cells and has low cytotoxicity.

For the transfection of the cultured neurons, we followed manufacturer's protocol. We used 1-3µg of total DNA for one culture dish transfection. First, DNA was mixed with Enhancer that condenses DNA molecules and a buffer that provides optimal salt conditions for efficient DNA condensation. Effectene reagent that coats DNA molecules with cationic lipids was added subsequently.

The mixture was incubated for 5-10 minutes in order to let the DNA-Effectene complexes form and added directly to the culture medium where the neurons were afterwards transferred for 45 minutes incubation. During the incubation, cationic lipids allow the DNA molecules penetrate into the cells.

Young neurons are easier to transfect due to better viability. Neurons were transfected at 7-11 DIV to avoid secondary effects due to the long DNA overexpression before the experiment. Small hairpin RNA plasmids were expressed for at least 4 days before the experiment in order to get an efficient downregulation. In most cases, we could obtain up to 10-15% of transfection efficiency.

1.2.2 Plasmid constructs

VAMP4-GFP, VAMP7-SEP, TeNT WT and TeNT E234Q constructs were kindly provided by Thierry Galli (Institut Jacques Monod, Paris, France) and TfR-SEP construct by C. Merrifield (Laboratory of Enzymology and Structural Biochemistry, Gif-sur-Yvette, France). VAMP2-SEP construct was kindly made available by Jürgen Klingauf (Institute of Medical Physics and Biophysics, Münster, Germany).

VAMP4-SEP construct was generated from VAMP4-GFP. VAMP4 cDNA was amplified by PCR with the following primers: VAMP4 forward, GAATTCGC-CACCATGCCTCCCAAGTTTAAGCGCCACC; VAMP4 reverse GGATCCGAAGTAC-GGTATTTCATGAC. DNA amplification products were subcloned into TfR-SEP plasmid by insertion of BamHI/EcoRI restriction sites.

We generated and tested three different versions of short hairpin RNA for VAMP4 knockdown. shVamp4-(1) targets the 3'UTR and has the following sequences: shVAMP4-1 forward, ATCCCCCTATCTTTATTTAACAACATTCAA-GAGATGTTGTTAAATAAAGATAGTTTTTC; shVamp4-1 reverse, CGAGAAAA-ACTATCTTTATTTAACAACATCTCTTGAATGTTGTTAAATAAAGATAGGGG.
Sequence of the second tested functional shRNA (shVAMP4-(2) further in the text) is based on a published sequence (Gordon et al. 2010), shifted by one nucleotide. shVamp4-(2) forward: GATCCCCGGACCATCTGGACCAAGATTTCAAGAGAATC-TTGGTCCAGATGGTCCTTTTTC; shVAMP4-(2) reverse: TCGAGAAAAAGG-

ACCATCTGGACCAAGATTCTCTTGAAATCTTGGTCCAGATGGTCCGGG. A third shVamp4 construct did not lead to significant protein downregulation and was not used. Following hybridization using BgIII and Xhol sites, both strands of the shRNA sequences were introduced into the pSuper néo GFP vector or pSuper vector (Oligoengine, Seattle, USA). Plasmid scramble shRNA was provided by Oligoengine.

VAMP4 fused to an HA tag withdrawn from the protein by Fibronectin 3 (FN3) domain was generated from VAMP4-SEP. FN3 and HA cDNAs were amplified by PCR with the following primers: FN3 forward GTCGGATCCACCGGTCGGTAGTTCTCCGCGTGGTTCG; HA reverse GTCGCTAGCTCAGCCCACGCGTGGTGCATAGTC. DNA amplification products were subcloned into VAMP4-SEP plasmid by insertion of BamHI/NheI restriction sites.

2 Visualization of the single exocytosis events

In the course of this work, we were primarily interested in observing individual exocytosis events in living cells. Shortly after exocytosis, cargo diffuses rapidly into the plasma membrane. Therefore, the events can last less than a second (Jullié et al. 2014; Yudowski et al. 2006; Yudowski et al. 2007). Spinning disk confocal microscopy (SDCM) and total internal reflection microscopy (TIRFM) appeared to be adapted for our aim since they provide good signal-to-noise ratio when imaging the adherent membrane surface. Apart from live-cell imaging, we also used these microscope systems for imaging fixed and immunolabeled cells. I will further introduce both techniques and their use in live microscopy.

2.1 Microscopy techniques

2.1.1 Spinning disk confocal microscopy

Acquiring images of localized fluorophores in living cells on the millisecond timescale presents many challenges that can be overcome by Spinning Disk Confocal Microscopy. SD CM is a system that combines the advantages of the confocal microscopy with the addition of Nipkow disk system that allows fast scanning and real-time imaging of the intrinsic biological activity. Main scheme of the SD CM functioning is represented on the Figure 19.

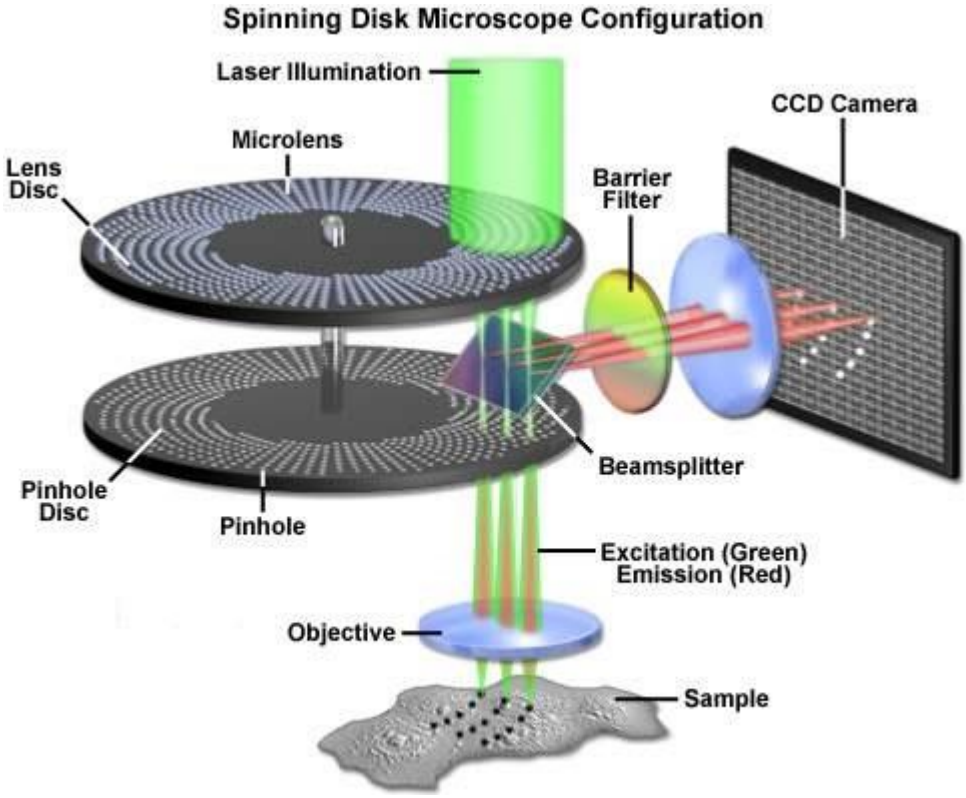

Figure 19: Spinning Disk Confocal Microscope configuration
Basic optical scheme of the SDC CM illumination and imaging in Yokogawa scanning units. Image from http://zeiss-campus.magnet.fsu.edu/

The principle of the SD CM is based on a Nipkow style scanning head. The head consist of two conjugated disks made of an opaque material and containing thousands of pinholes arranged in interleaved Archimedean spirals. The first disk, or Lens disk, contains microlenses that focus the illumination light. Illuminated pinholes are imaged on the specimen through the objective as diffraction limited spots. The emitted light is sent back through the Pinhole Disk that cuts the noise coming from the out-of-focus areas. It is then reflected by a Beamsplitter and filtered by the Barrier Filter before being imaged on the camera. The disk rotates and scans the entire specimen imaging multiple points in parallel in contrast to a classical confocal microscope that has to image one point after another in series. In this regards, the SD CM is significantly faster than a classical confocal microscope. Modern models of the SD can rotate with the maximum speed of 10,000 rotations per minute while scanning 12 frames during each 360° giving the theoretical frame rate of 2000 frames per seconds. However, in practice, the acquisition speed is limited by the camera exposure and integration time become limiting factors in image acquisition rates.

In the current work, we have used an inverted Leica DMI6000 Microscope (Leica Microsystems, Wetzlar, Germany) equipped with a CSU22 Yokogawa Confocal Scanner Unit (Yokogawa Electric Corporation, Tokyo, Japan) in combination with the Leica HCX PL APO CS 63X oil immersion objective and QuantEM 512 SC EMCCD camera (Photometrics, Tucson, USA). The objective has numerical aperture of 1.40 and a magnification of 63 that in combination with a camera pixel size of 16 μm gives the lateral resolution of 0.230 μm. Cells were illuminated by diode lasers of 473 nm, 532 nm and 635 nm wavelengths. The system has a barrier filter and an emission Barrier Filters Wheel that rotates fast enough to allow a multicolour imaging in Timelapses with 1Hz frequency. The imaging system is controlled by MetaMorph software (Molecular Devices, Sunnyvale, USA). The microscope is contained inside of temperature control system by Life Imaging Services (Basel, Switzerland) also known as "The Cube & The Box". The system controls precisely the temperature inside of its Box, keeping the sample at physiological temperature and eliminating focus instabilities caused by temperature changes.

2.1.2 Total Internal Reflection Fluorescence Microscopy

Total internal reflection (TIRF) microscopes are specifically designed for imaging the thin layer of the specimen, adjacent to the coverslip surface. They are based on the physical phenomenon of the total internal reflection that occurs when a wave, propagating from one media to another one with a lower refractive index (n), has the incident angle larger than a particular critical angle. Critical angle is found by Snell-Descartes's law:

$$n_1 \sin \Theta_i = n_2 \sin \Theta_t$$

The angle of incidence Θ_i (see Figure 20) reaches critical value Θ_c when the angle of refraction is equal to 90°. Knowing this we can easily calculate the critical angle, necessary for TIR:

$$\Theta_c = \arcsin(\frac{n_2}{n_1})$$

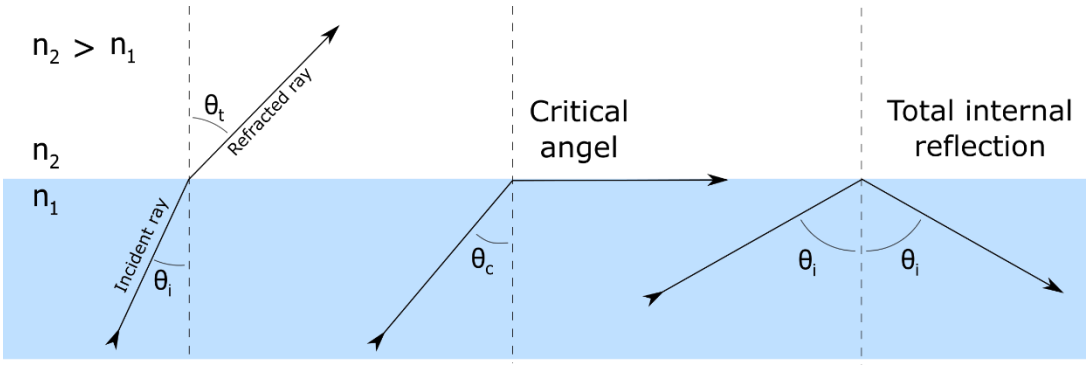

Figure 20: Refraction of the light and the TIR
When a ray strikes the interface between two media with an incident angle superior to the critical angle, it is totally reflected back internally. Such phenomena can happen only when the wave goes from the media with higher refractive index n_2 to the media with the lower refractive index n_1

One of the most important side effects of the TIR is the generation of the evanescent wave in the second media. It occurs due to the generation of a highly restricted electromagnetic field in the lower-index media by the reflected wave. The generated field is identical in frequency with the incident light and its intensity decays exponentially with distance from the surface.

In TIRF microscopes, the specimen cells containing fluorescent molecules are adherent to a glass coverslip. The refractive indices of the cells (~1.38) is smaller than the refractive index of the glass (~1.52) and that provides necessary conditions for the TIR within the coverslip. By illuminating the cell with the excitation laser beam under the angle greater than the critical angle, one can obtain the TIR of the laser illumination and the generation of the evanescent field, penetrating into the cell. The generated field has enough energy to excite fluorophores in approximately the first 100 nm from the media interface. Thus, we excite the fluorescent molecules only immediately adjacent to the glass surface. The generated fluorescence is collected by the microscope and imaged on the camera or observed through the eyepieces.

We have carried out part of our imaging experiments on the inversed Olympus IX71 microscope (Olympus, Japan) with oil immersion objective Olympus Apochromat N 60x that has a numerical aperture of 1.49 and 1.6x magnifying lens. Cells were illuminated with a 473 nm laser (Cobolt, Solna, Sweden). Such numerical aperture of the objective allows imaging in the TIRF mode. The images were acquired with the QuantEM 512SC camera

(Photometrics, Tucson, USA) piloted by the MetaVue software (Molecular Devices, Sunnyvale, USA).

2.1.3 Imaging experiment conditions

In our live imaging experiments, we used one of the standard HEPES (4-(2-hydroxyethyl)-1-piperazineethanesulfonic acid) -buffered saline extracellular solution (ESC) containing the following (in mM): 120 NaCl, 2 KCl, 2 MgCl2, 2 CaCl2, 5 D-(+)-Glucose, 10 HEPES. Solution's pH and osmolarity were adjusted to 7.4 and 265-275 mOsm respectively. For exocytosis detection, the acquisition was done in time-lapse videos of 1 Hz frequency and 100ms exposure time. Recorded time-lapse videos of living cells are stored in .stk format.

For imaging fixed and immunostained cells, images were taken in so-called z-stacks, when a picture was acquired every 0.2µm from the bottom to the top of the cell. The exposure and laser intensity were adjusted for each fluorophore individually and were kept constant during a given imaging experiment.

2.2 Superecliptic pHluorin for exocytosis tracking

Visualisation of the proteins exocytosis in live cells was achieved with the help of pH-sensitive fluorescent protein superecliptic pHluorin (SEP). SEP is the GFP (Tsien 1998; Yang et al. 1996) mutant with enhanced brightness and pH-sensitivity. The first version of pHluorin was obtained by directed mutagenesis of the key amino acids within the central fluorophore (Miesenbock et al. 1998). Mutations aimed the facilitation of the GFP conformation switch between protonated and deprotonated state, as GFP conformation defines its excitation wavelength. They also targeted coupling changes in bulk pH to changes in the chromophore's electrostatic environment, since the H^+ transfer is involved in fluorescence generation (Ashby et al. 2004). One of the obtained mutants was ecliptic pHluorin. The protein gradually loses its fluorescence as pH turns more acidic. At pH values lower than 6.0, pHluorin becomes not excitable, or eclipses, under 475 nm excitation wave, Figure 21A (Miesenbock et al. 1998). Superecliptic pHluorin (SEP) has two additional mutations (Sankaranarayanan et al. 2000), that render it approximately nine times more fluorescent then the original ecliptic version (Ashby et al. 2004).

The experimental paradigm for exocytosis imaging relies on the fact that SEP is not fluorescent at the acidic pH levels inside of the secretory vesicles, but visible when exposed to the physiological pH levels of the extracellular media. In most cases, SEP is fused to a luminal C-tail of a transmembrane protein of interest that faces the inside of the vesicle and becomes extracellular after exocytosis. As the result, SEP-tagged protein is almost not visible when trafficked in the intracellular compartments and becomes 20 times more fluorescent after exocytosis due to the rapid pH increase (Figure 21 B, C), (Sankaranarayanan et al. 2000). Fluorescence bursts allow detection of individual exocytosis events (Kennedy & Ehlers 2011; Balaji & Ryan 2007; Zhu et al. 2009; Woolfrey et al. 2015; Yudowski et al. 2006).

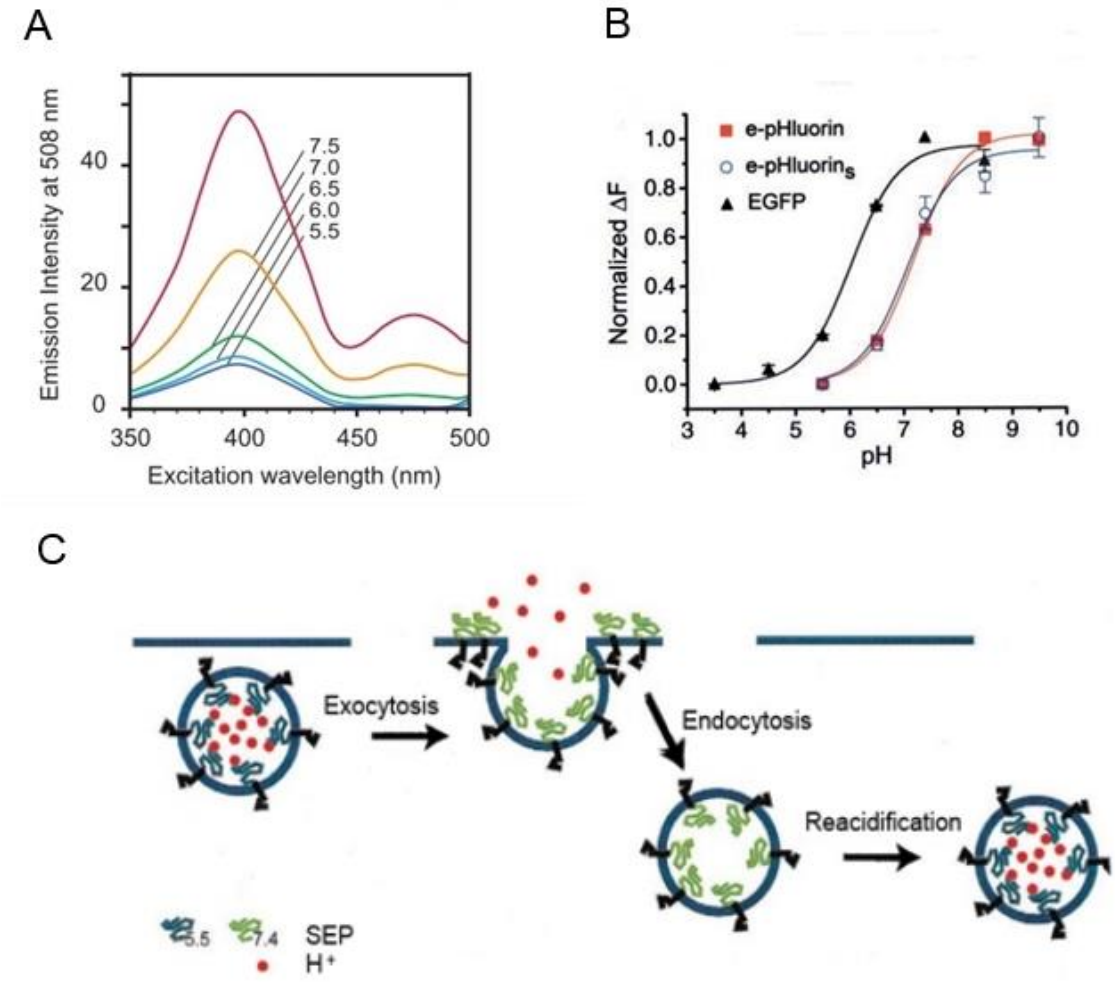

Figure 21: pHuorin emission pH-dependence.
A, pHluorin fluorescence excitation spectra, the excitation peak at 475nm vanishes at pH lower than 6.0 (Miesenbock et al. 1998). **B**, The average normalized change in fluorescence (ΔF) as a function of pH for ecliptic pHluorin, superecliptic pHluorin and EGFP. C, pHluorin proton-dependent fluorescence quench relieved under exocytosis (Sankaranarayanan et al. 2000).

2.3 Imaging data treatment

2.3.1 Exocytosis detection and quantification

For exocytosis events detection and exocytosis dynamics analysis we used Matlab script files (MathWorks, Natick, USA) written by David Perrais and complemented or adjusted for individual purposes by Damien Jullié, Morgane Rosendale or myself. Detection method is described in details previously (Jullié et al. 2014).

When a fluorescence burst, or exocytosis, appears on the movie, the intensity value registered on the corresponding group of pixels raises. The detection routine consists first of calculating for each movie frame the difference between the intensity value of every pixel at the moment n and their intensity at the previous moment n-1, plus a constant C to avoid negative values: $I_{diff} = I_n - I_{n-1} + C$. I_{diff} calculation allows us to attenuate background noise due to the membrane fluorescence, which remains mainly constant, and enhance the signal visibility. I_{diff} value is then attributed to the corresponding pixel on the reconstructed differential image. Differential images are reassembled as frames in a time-lapse movie where only pixels showing fluorescence burst are seen as bright (Figure 22 A). User manually chooses a threshold (Thr), which determines the minimal intensity raise during exocytosis event. All fluorescence raises that are above this threshold and more than two pixels in size (0.4 μm) will be considered as exocytosis event in automatic detection.

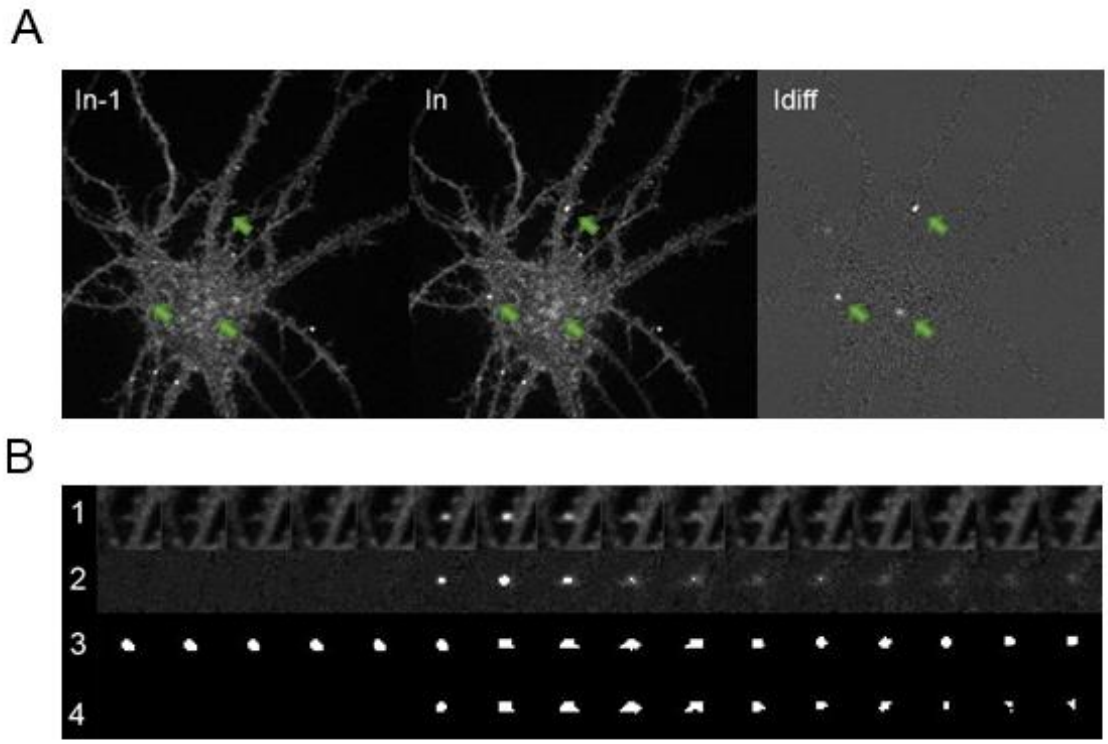

Figure 22 Exocytosis detection in Matlab.
A, Enhancing exocytosis visibility by creating differential image $I_{diff} = I_n - I_{n-1} + C$. B, Tracking and quantifying fluorescence burst during exocytosis event, 1Hz time-lapse. 1: raw data of 5 images before and 10 images after the exocytosis event. 2: raw data time-lapse minus the average of the first five images before the event. 3: binary image showing in white ROI pixels where exocytosis fluorescence before and after the event is quantified. 4: binary image showing in white pixels with intensity value that remains above the threshold.

After the first selection of all objects on the difference movie that were more fluorescent then the threshold, part of them is discriminated in order to partially get rid of the false-positive events. An object that is less than five pixels close to another object detected on the previous image will be excluded. In our experience, it is very unlikely that two consecutive exocytosis events on the somatodendritic compartment will happen one after another on the same area. Generally, in that case, the detected event corresponds to a long tubular object's contraction. If the detected object has dark area on less than 5 pixels distance around it, with the intensity value of two constants minus the detection threshold ($2C - Thr$), the event will be excluded as it corresponds to bright clusters fluorescence fluctuation.

On a small area of 41 pixel around the centroid of the detected objet (Figure 22, B), average of the first five images before the exocytosis event is

subtracted from the raw time apse video (Figure 22, B-2). Obtained time-lapse has excellent signal-to-noise ratio and serves as complementary tool for manual browse of all detected events in order to get rid of most false positives that were not rejected by the automatic criteria.

Detected exocytosis events are further characterized to get exocytosis fluorescence curves, event frequency and spatial distribution. Fluorescence quantification also takes place on the area of 41 pixels around the detected object (see Figure 22 B). The region of interest (ROI) is determined as the region with the pixel values more than 7 standard deviations (SDs). The SD of pixel's intensity values is determined on the first five background-subtracted images before exocytosis. If multiple objects are found, the closest to the image center is taken. In case if no object is found, the ROI is defined as a circle of 2.2 pixels (380 nm) radius, centred on the centroid of the originally detected object. The final ROI is the reunion of all pixels above 7 SDs and the 2.2 pixel radius circle. The surrounding region (SR) is the 2 pixels-wide zone around the determined ROI. The procedure of ROI and SR identification is repeated for all quantified images after exocytosis. For the images before the event, the ROI and SR defined at the moment of the exocytosis are applied.

For each exocytosis event, the quantification routine computes differential fluorescence value $F_{R-S} = F_{ROI} - F_{SR}$.

F_{ROI} and F_{SR} represent average fluorescence of the original raw images in the ROI and SR respectively. For F_{SR} calculation, we exclude 20% of the lowest and highest pixel values to attenuate background fluctuations that can be due to out-of-the cell dark areas or bright clusters presence. F_{R-S} values are normalized by subtracting the average of the first ten values before exocytosis and dividing by the values in the moment of exocytosis. Events are then classified as "burst", in case if their F_{R-S} is more than 50% for less than 2 seconds, or, otherwise, as "display".

For the exocytosis frequency per image estimation, we built an exocytosis cumulative frequency curve, which is linear, and estimated its slope that is equal to the number of exocytosis events per frame. The found frequency was

normalized by the cell's surface found by the application of simple threshold for bright pixels on the raw image.

3 Immunocytochemistry on cultured neurons

Immunocytochemistry techniques were used whenever it was necessary to estimate the level of expression or localisation of the protein of interest. Besides localisation experiments and downregulation tests, we applied this imaging tool in order to estimate the AMPA receptor's surface expression levels after chemical LTP treatment.

Immunocytochemistry protocol

Neurons were first fixed in room temperature 4% paraformaldehyde solution containing 4% sucrose for 10 minutes. For permeabilization before staining, cells were subsequently incubated in 0.1% Triton X-100. After fixation or fixation and permeabilization, cells were incubated for 30 min in 1% bovine serum albumin (BSA) in phosphate-buffered saline (PBS) blocking solution in order to prevent non-specific binding of the antibodies. Primary antibodies were applied in 1:1000 dilution in PBS-BSA1%, except for anti-GluA1 (polyclonal, Agrobio) which was diluted in 1:100. Secondary antibodies were applied in 1:200 dilution in PBS-BSA1%. Cell were incubated with primary and subsequently secondary antibodies at room temperature for 1 hour. Incubations were separated by multiple PBS washes. For surface receptors staining in cLTP experiments (see cLTP protocol chapter) live cells were first incubated with primary antibody diluted in culture media at 37°C for 5 min before fixation in PFA followed by the same steps as in basic protocol.

After staining coverslips were washed in PBS and distilled water and mounted on microscope slides in Mowiol mounting medium (Merck Millipore, USA). Imaging was performed on SD CM in z-stacks, for the details on the microscope and imaging see 2.1.1.

List of the primary antibodies:

Anti-VAMP2 and anti-VAMP4 were both rabbit polyclonal antibodies from Synaptic System (Gottingen, Germany).

Anti-GluA1 was rabbit polyclonal antibody against extracellular GluA1 epitope (271-285 AA), custom made for the institute by Agro-Bio (La Ferté Saint-Aubin, France).

Anti-HA-tag primary antibody was monoclonal rat antibody from Roche (Boulogne-Billancourt, France)

List of the secondary antibodies:

Anti-Rabbit IgG secondary antibody was goat antibody conjugated to Alexa 647 fluorophore from Thermo Fisher SCIENTIFIC (Waltham, MA USA).

Anti-Rat IgG Secondary antibody was goat antibody conjugated to Alexa 647 fluorophore from Thermo Fisher SCIENTIFIC (Waltham, MA USA).

4 Chemical long-term potentiation induction

The induction of the long-term potentiation of the synapses in neuronal culture without direct electrical stimulation in most of the times is done by chemical long-term potentiation protocol or cLTP (Lu et al. 2001; Jurado et al. 2013; Park et al. 2004; Kennedy & Ehlers 2011). In our experiments we first rinsed cells for 10 min in Mg free ECS containing in mM : 120 NaCl, 2 CaCl2 , 5 KCl, 10 HEPES, 5 Glucose, 0.001 tetrodotoxin (TTX, a sodium channels blocker), 0.01 strychnine (glycine receptors antagonist), 0.03 picrotoxin ($GABA_A$ receptors chloride channel blocker), equilibrated at pH7.4. Cells were afterwards treated with 300µM Glycine in Mg free ECS at RT for 3min, incubated without Glycine at 37°C for 20 minutes, live-stained with the primary anti GluA1 antibody and fixed. After fixation cell staining was continued following basic immunocytochemistry protocol, see 3 Immunocytochemistry on cultured neurons.

Incubation without magnesium relieves magnesium block of NMDA receptors. Upon glycine application, activated NMDA receptors allow Ca^{2+} entry into the spines during stimulation of the synapse with spontaneous miniature excitatory postsynaptic currents (Lu et al. 2001; Huganir & Nicoll 2013). Such stimulation launches protein interaction cascades that lead to long-term enhancing of the synaptic transmission. LTP of these synapses is accompanied by a rapid insertion of native AMPA receptors which is estimated by ICC surface staining protocol.

5 Organotypic hippocampal slices culture

In order to test SNARE protein candidates identified with the imaging and ICC techniques we also used organotypic hippocampal slices, a model that allows studying neuronal functionality in partially conserved network.

5.1 Organotypic slices preparation

Organotypic slices were prepared from Sprague-Dawley rats at postnatal days 4-6 by the membrane interface technique following indications from (Stoppini et al. 1991). The protocol steps are:

Before the dissection

1. Prepare membrane inserts (Merck Millipore, Billerica, MA USA) by putting them into a 6-well plate containing 1ml of filtered culture medium, which was minimum essential medium (MEM) supplemented with 15 % heat-inactivated horse serum, 0.25 mM ascorbic acid, 3 mM L-glutamine, 1 mM $CaCl_2$, 1 mM $MgSO_4$, 25 mM HEPES and 5 g/L D-Glucose.
2. Cut the confetti for slice support and manipulation (Merck Millipore, Billerica, MA USA) and put them on the wet inserts.
3. Place the plate into 37°C 5% CO2 incubator for at least 1h and up to 1 day before the dissection.

On the dissection day

4. Under sterile conditions, quickly decapitate the animal and place the extracted brain into previously refrigerated Gey's balanced salt solution.
5. Dissect out the hippocampi.
6. Cut 350 μm coronal slices using a tissue chopper (McIlwain).
7. Refrigerate slices in the dissection solution for 30 min.
8. Place slices on prepared confetti on membrane inserts.
9. Incubate slices at 34°C 5% CO2 incubator.
10. Change culture medium 24 hours after dissection and every 2-3 days from thereafter.

CA1 pyramidal neurons were processed for single cell electroporation (see below) after 3-4 days and up to 1 week in culture. Electrophysiological recordings were performed on electroporated neurons after 14-16 days in culture.

5.2 Single cell electroporation

Single cell electroporation is a powerful technique that allows targeting of individual cells in animals or in tissue (Weaver & Chizmadzhev 1996; Olofsson et al. 2003). For the electroporation of CA1 pyramidal neurons, we used a modified patch pipette filled with plasmid DNA diluted in intracellular solution and containing an electrode inside (Haas et al. 2001).

Single cell electroporation protocol

In stock before electroporation:

- Intracellular solution, in mM: 125 CsCH3SO3, 1 ethylene glycol-bis(β-aminoethyl ether)-N,N,N',N'-tetraacetic acid (EGTA), 0.1 CaCl2, 4MgCl2, 10 Hepes, 3 Na-L-Ascorbat, 4 Na_xATP, 0.4 Na_xGTP, 5 Na2phosphocreatine, adjusted to pH 7.2 and 305-315 mOsm/l, sterile filtered and stored in the fridge at -80°C.
- Extracellular solution, in mM: 145 NaCl, 2 KCl, 2 MgCl2, 2 CaCl2, 10 Hepes, and 10 D-glucose, adjusted to pH 7.4 and 315-325 mOsmol/l.

On the day of the electroporation

1. Dilute plasmid DNA (mixture) to 333 ng/µl with TE buffer, and then dilute 1/10 in intracellular solution. Centrifuge at top speed for 10-20 minutes to pellet any precipitate that could clog pipettes
2. Clean the microscope chamber with 75 % ethanol and allow to dry.
3. Pull 7-8 MOhm pipettes from borosilicate glass capillaries (GC 120F-10, Harvard Apparatus, US).
4. Back fill pipettes with DNA containing intracellular solution.
5. Transfer the slice in extracellular solution to the setup.

6. Place the pipette with positive pressure inside close to the soma of a neuron. Release the pressure to form a loose seal and within 1-2 sec apply a stimulus train of 50 pulses at 100 Hz, -12 V amplitude and 0.5 ms pulse width.
7. Gently remove the pipette from the cell body and proceed to the next cell. One pipettes is usable for up to 10 attempts of electroporation.
8. Maintain organotypic slice in chamber for no more than 30 minutes.

For positioning the pipette we used normal holder for patch-clamping with the filament connected to the external stimulator and the second stimulator's electrode being submerged in the extracellular solution of the chamber. The tubing connectivity of the holder allowed to put pressure into the pipette.

The success rate of the single cell electroporation is very variable and depends on many parameters as slice's health, manipulator's agility, etc. Usually, for ten electroporation attempts on slice one can obtain from 0 to 5-6 electroporated and survived neurons, expressing the construct (Figure 23).

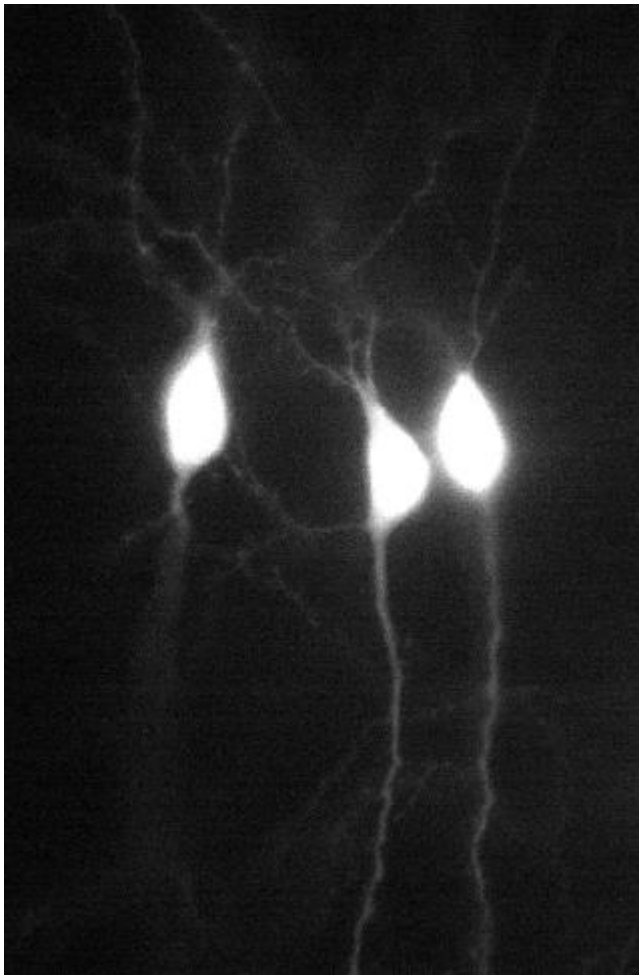

Figure 23 GFP-electroporated CA1 pyramidal neurons.
Image shows an example of fluorescent neurons in CA1 layer of a hippocampus organotypic slice, expressing GFP after SCE procedure.

For the electroporation we used the following constructs: shVamp4-SEP, shScramble-GFP, TeNT WT, TeNT E234Q. For constructs sequences, see section 1.2.2 Plasmid constructs in Materials and methods.

5.3 Electrophysiology in slices and pairing LTP protocol

LTP can be induced artificially by slow presynaptic stimulation of 1-2Hz, coupled with postsynaptic depolarization imposed by current injection through microelectrode or by voltage clamp (Bortolotto et al. 2011; Chen et al. 1999). Artificial depolarization in this pairing protocol relieves the Mg^{2+} block of NMDA channels. Open NMDA channels during presynaptic stimulation allow Ca^{2+} entry that triggers synaptic strengthening.

In the current work, pairing LTP induction was performed on cultured organotypic slices at 12-16 days after dissection and 8-10 days after electroporation (see 5.1 and 5.2). On the experiment day, CA3 region of slice was surgically cut and slice was transferred to the upright Leica DM5000 microscope (Leica Microsystems, Wetzlar, Germany). Slice was perfused with artificial cerebral spinal fluid (aCSF), containing in mM: 125 NaCl, 25 $NaHCO_3$, 2.5 KCl, 4 $CaCl_2$,4 $MgSO_4$, 10 D-glucose,1 Na-pyruvate, 0.005 picrotoxin, 0.001 2-chloroadenosine, 0.001 CGP-52432 and 10^{-6} CNQX. Solution's pH and osmolarity were adjusted to 7.4 and 320 - 325 mOsm respectively. During the experiment, aCSF was maintained at ~30°C by an in-line solution heater (WPI, US).

Patch-pipette and electrode positioning was visually guided with the help of 20X water immersion objective coupled with one of three installed lenses (0.6X; 1.5X; 4X) and infrared illumination adjusted to obtain differential interference contrast. Image was observed with Cool Snap HQ camera (Photometrics, Tuscon, US). For synaptic current evocation, bipolar glass stimulation electrode filled with aCSF was placed in the dendrite region to stimulate Schaffer collaterals. Whole-cell voltage clamp recordings were performed with patch-pipettes (4-6 Mohm when filled with usual intracellular solution) pulled from borosilicate glass capillaries (GC150F-10, Harvard Apparatus, US) and filled with Cs^+- based intracellular solution (see 5.2).

Stimulation control, analogue signal filtering and digitization was performed with EPC-10 USB amplifier controlled by Patchmaster software (HEKA Elektronik). Data was registered directly on the hard drive of the computer workstation operating under Windows XP (Microsoft). After obtaining a gigaohm seal, cells were voltage-clamped at -60mV and maintained in cell-attached configuration for 3min prior to opening. After breaking in the cell, the stimulation amplitude and polarity were adjusted to obtain excitatory postsynaptic current (EPSCs) with ~60pA amplitude. The pairing protocol recording always started no longer than 2 minutes after opening the cell and consisted of: 1) 10 stimulations at 0.05 Hz to obtain a baseline, 2) 100 stimulation pulses at 1Hz paired with depolarization of the cell, 3) 40min of 0.05Hz stimulation to record EPSCs after LTP stimulation. Short baseline was chosen to prevent washout before the induction of the LTP. At the beginning of

each EPSC recording, series resistance was monitored by measuring the peak current in response to 5mV, 100 msec depolarizing pulse. The amplitude of the EPSC was measured as difference between the average of data points just before the stimulus and around the peak of the response. All synaptic responses were normalized to the average of the baseline EPSCs.

6 Electrophysiological essays on dissociated cultured neurons

6.1 Basal transmission assay.

We examined basal transmission in cultured hippocampal neurons after chronic block of our vSNAREs of interest by measuring their spontaneous miniature excitatory postsynaptic currents (mEPSCs). Such measure implicitly reflects AMPARs-containing REs cycling.

Cultured hippocampal neurons were transfected with GFP, shVAMP4(1) + GFP, shVAMP4(1)+VAMP4-SEP or TeNT light chain+ GFP. Plasmid constructs are provided in 1.2.2 section of Materials and methods. At at 14-16 DIV, neurons were transferred to the lundin chamber of the inversed Olympus IX71 microscope (Olympus, Japan) described in Materials and methods section 2.1.2. Cells were maintained in the same ESC as for the imaging experiments, containing in mM: 120 NaCl, 2 KCl, 2 MgCl2, 2 CaCl2, 5 D-(+)-Glucose, 10 HEPES, 0.001 TTX (sodium channel blocker), 0.03 picrotoxin. Solution's pH and osmolarity were adjusted to 7.4 and 265-275 mOsm respectively. During the experiment, the ECS temperature was maintained at ~35°C by an in-line solution heater (WPI, US).

Transfected neurons were identified by GFP fluorescence signal under 473 nm laser illumination. Whole cell patch clamp recordings were performed with patch-pipettes (4-5 Mohm when filled with intracellular solution) pulled from borosilicate glass capillaries (Harvard Apparatus, US) and filled with K^+- based intracellular solution containing in mM: 110 KCH_3SO_3, 2 KCl, 1 EGTA, 0.1 CaCl2, 10 HEPES, 4 Mg_xATP, 0.4 Na_xGTP, 5 Na_2phosphocreatine. pH and osmolarity were adjusted to 7.2 and 260-265 mOsm.

EPC-10 USB amplifier controlled by Patchmaster software (HEKA Elektronik) were used to perform stimulation control, as well as analogue signal filtering and digitization. After establishing a gigaohm seal, cells membrane potential was voltage-clamped at -60mV. Spontaneous postsynaptic activity was registered for at least 3 min for each neuron.

mEPSCs frequency and amplitude were estimated upon the analysis of at least 100 seconds of the recording. Data analysis was performed with Matlab script written by Andrew Penn. The script detects spontaneous synaptic currents with the deconvolution-based method (Pernía-Andrade et al. 2012).

6.2 Acute block of the exocytosis machinery

After conducting experiments with the chronic downregulation of our candidate vSNARE proteins, we undertook a series of experiments where we tried to block acutely RE exocytosis by loading neurons with different SNARE inactivating agents through patch-pipette. RE exocytosis frequency before and after blockers dilution was estimated with the help of live imaging methods as described in Chapter 2 of Materials and methods. Such kind of acute block allows us to avoid possible specificity problems of the shRNAs and eventual compensatory mechanisms influences that could probably arise from a lasting downregulation.

Cultured hippocampal neurons transfected with TfR-SEP were placed at 14-16 DIV to the inversed Olympus IX71 microscope (Olympus, Japan) described in 2.1.2, where they were maintained in heated at ~35°C imaging ECS (in mM: 120 NaCl, 2 KCl, 2 MgCl2, 2 CaCl2, 5 D-(+)-Glucose, 10 HEPES, 0.001 TTX, 0.03 picrotoxin; pH 7.4 and osmolarity adjusted to 270-275 mOsm). Cells were patched with borosilicate glass pipettes (4-5 Mohm when filled with intracellular solution) containing various SNARE inhibitors diluted in the standard intracellular solution (in mM: 110 KCH_3SO_3, 2 KCl, 1 EGTA, 0.1 CaCl2, 10 HEPES, 4 Mg_xATP, 0.4 Na_xGTP, 5 Na_2phosphocreatine; pH 7.2 and osmolarity adjusted 260-265 mOsm).

SNARE inhibitors and their dilutions are represented on the Table 2. We loaded patch-pipettes with TeNT light chain to cleave VAMP2 (Pellizzari et al. 1999). VAMP4 block was realised by loading of the antiVAMP4 rabbit polyclonal

antibody from Synaptic System, directed against VAMP4. By fixing on the VAMP4 N-terminal domain, antibody obstructs VAMP4 from

Protein	Inhibitor	Concentration
VAMP2	TeNT	0.5 µM
SNAP25	BoNT C1	0.5 µM
VAMP4	αVAMP4	~0.04 µM

Table 2 SNARE inhibitors applied for the acute exocytosis block

Results

1 Observation of candidate v-SNAREs exocytosis

Study of the potential v-SNAREs involved in postsynaptic RE exocytosis started with the work of Damien Jullié, a former PhD student who has defended his thesis of the University of Bordeaux in October 2012. He has performed imaging experiments have initiated the current project and gave the basis for further investigations. As published in the previous work under David Perrais supervision, tubular recycling endosomes labelled with TfR-SEP undergo exocytosis in the somatodendritic compartment at high frequencies (Jullié et al. 2014). Our first motivation was to understand and identify the molecular machinery behind these phenomena.

We were interested in characterizing the proteins directly involved in RE exocytosis. We chose to characterize dendritic R-SNAREs as these proteins are relatively well described in vitro. Moreover, and contrarily to plasma membrane or cytosolic proteins, R-SNAREs are transmembrane proteins found on the vesicular membrane. Therefore tagging R-SNAREs in their luminal domain with SEP allows direct assessment of their involvement in exocytosis. Among the 7 VAMP protein isoforms that potentially can be involved in exocytosis, only VAMP2, VAMP4 and VAMP7 are expressed in hippocampal neurons and were the main candidates in our study.

VAMP2/synaptobrevin-2, together with it closely related isoform VAMP1, is the principal VAMP protein mediating rapid synchronous SV release (Deák et al. 2006; Südhof 2004). VAMP2 is the substrate of TeNT and BoNT-B endopeptidases, with its cleavage leading to a complete block of synaptic transmission (Pellizzari et al. 1999). VAMP2 is present in both pre- and post-

synaptic compartments, but its distribution is highly polarized, with considerably higher quantity in the axon (Sampo et al. 2003). VAMP2 trafficking passes though somatodendritic PM, where it undergoes exocytosis before being targeted to the presynaptic compartment (Sampo et al. 2003). In addition, LTP depends on AMPA receptor-containing REs exocytosis in the somatodendritic regions, and it has long been known to be blocked by TeNT and BoNT-B, indicating involvement of VAMP2 in this process (Lüscher et al. 1999; Lin et al. 2009; Lu et al. 2001). Recently, VAMP2 implication in LTP-dependent exocytosis and AMPA receptors insertion to the PM was demonstrated directly on VAMP2 KO neurons (Jurado et al. 2013). However, evidence for VAMP2 implication in constitutive AMPA exocytosis is still controversial, see (Lüscher et al. 1999; Lu et al. 2001)., There is experimental evidence, implying VAMP2 role in cultured neurons development. VAMP2 is necessary for axonal formation in neurons cultured on polylysine but not laminin substrate (Gupton & Gertler 2010), it is also associated with exocytosis required for axonal steering (Tojima et al. 2007; Tojima et al. 2011) and was shown to be implicated in axonal repulsion. These results are still disputable, as previous studies demonstrate that chronic TeNT treatment of the cultured hippocampal neurons does not alter neurite outgrowth or general neuronal morphology (Harms & Craig 2005; Grosse et al. 1999) and VAMP2 KO does not exhibit significant developmental defects in the brain (Susanne Schoch et al. 2001). Comparably, despite the severe synaptic transmission deficit in VAMP2 KO mice, its brain structure develops normally (Susanne; Schoch et al. 2001)

VAMP4 and VAMP7/TI-VAMP are both insensitive to clostridial toxins (Proux-Gillardeaux, Rudge, et al. 2005; Mallard et al. 2002). VAMP7 mediates lysosome exocytosis (Arantes & Andrews 2006; Chaineau et al. 2009), as well as synaptic vesicle exocytosis associated with the spontaneous transmission (Bal et al. 2013; Hua et al. 2011). Moreover, VAMP7 was reported to be implicated in neurite outgrowth (Martinez-Arca et al. 2001). On the other hand, VAMP4 is especially enriched in *trans*-Golgi compartments where it plays an important role in retrograde trafficking from endosomes to Golgi (Mallard et al. 2002). Additionally, VAMP4 is found on early endosomes, and it participates in homotypic fusion of these organelles (Brandhorst et al. 2006). VAMP4 is also implicated in exotic processes like regulated exocytosis of enlargeosomes, small

vesicles undergoing exocytosis in embryonic and postnatal neurons (Cocucci et al. 2008). Finally, VAMP4 was reported to be participate as R-SNARE in asynchronous SV release in the hippocampal neurons (Raingo et al. 2012).

We expressed in cultured hippocampal neurons candidate VAMP proteins fused with SEP, monitored single exocytosis events in somatodendritic regions (Yudowski et al. 2006; Kennedy et al. 2010; Lin et al. 2009) and characterized their exocytotic behaviour in order to identify potential R-SNARE for constitutive RE exocytosis. We found that in basal conditions the frequency of VAMP2 exocytosis events is low in comparison to those of VAMP4 and transferrin receptor (TfR), a known RE-marker. Moreover, the normal rates of TfR exocytosis are reduced after VAMP4, but not VAMP2 downregulation.

2 Exocytosis activity of VAMP2, VAMP4 and VAMP7 in somatodendritic regions

First, we expressed candidate VAMP proteins VAMP2, VAMP4 and VAMP7 all fused with SEP in cultured hippocampal neurons at 7 DIV. Neurons were afterwards imaged at 13-15 DIV. VAMP2-SEP was strongly polarized to axons and had relatively weak signal in somatodendritic compartments (Figure 24 A). VAMP4 and VAMP7 were more uniformly distributed on the cell surface. Single exocytosis events were observed as local bursts of fluorescence that were automatically detected with our custom Matlab routine and sorted manually in subsequent data treatment. InVAMP2-SEP transfected neurons, we could detect exocytosis events in the soma, dendrites and axon. Somatodendritic exocytosis events detected during 3 min are shown with asterisks (Figure 24 A, left panel). For VAMP4-SEP axon could not be distinguished unambiguously, however, exocytosis events were detected abundantly in soma and dendrites (Figure 24 A, right panel). In neurons expressing VAMP7-SEP, we could not detect any exocytosis events (not shown).

After automated detection of exocytosis events and manual sorting, we compared average exocytosis frequency of VAMP2-SEP and VAMP4SEP proteins to that of the TfR-SEP, a marker for RE. Exocytosis events were detected with a similarly high frequency for TfR-SEP and VAMP4-SEP (Figure 24 B: 0.037 ± 0.004 and 0.05 ± 0.015 ev·µm^{-2}·min^{-1}, respectively). VAMP2-SEP exhibited exocytosis frequencies significantly lower than TfR-SEP (Figure 24 B: 0.006 ± 0.0015 ev·µm^{-2}·min^{-1}, P-value in unpaired t-test less than 0.0001). These observations suggest that VAMP4 and TfR could be targeted to the same organelles and report their exocytosis. On the other hand, in basal conditions, VAMP2 undergoes exocytosis in somatodendritic regions with rates that are too low to account for the exocytosis of all TfR-SEP containing organelles.

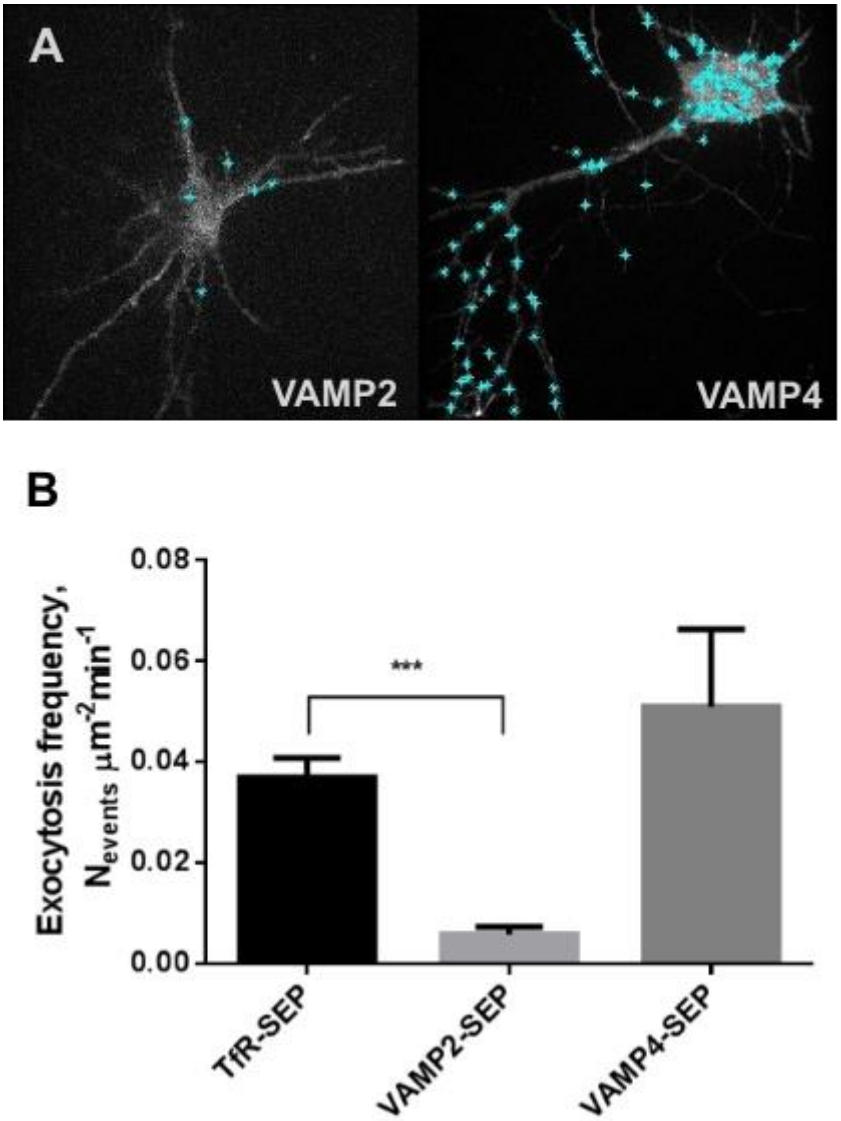

Figure 24 Exocytosis frequency of VAMP proteins in somatodendritic compartments

A, Panel shows somatodendritic exocytosis events (cyan asterisks) of VAMP2-SEP (on the left) or VAMP4-SEP (on the right) proteins, detected during 3 min of imaging. **B**, Frequency of exocytosis events for TfR-SEP (n = 14 cells), VAMP2-SEP (8 cells) and VAMP4-SEP(n = 11 cells) proteins. *** - P-value in unpaired t-test less than 0.0001.

3 Subcellular localization of endogenous VAMP2, VAMP4

The next step in our study was to determine the subcellular localization of VAMP4 and VAMP2 proteins with regards to RE. It was already shown by Damien Jullié (Figure 25, unpublished data), in hippocampal neurons expressing VAMP2-SEP or VAMP4-SEP together with TfR-mCherry, that exocytosis events detected as bursts of SEP fluorescence are often colocalized with TfR-mCherry clusters. As it can be seen on the examples shown at the Figure 25, TfR-mCherry cluster is seen before the moment of exocytosis event detection.

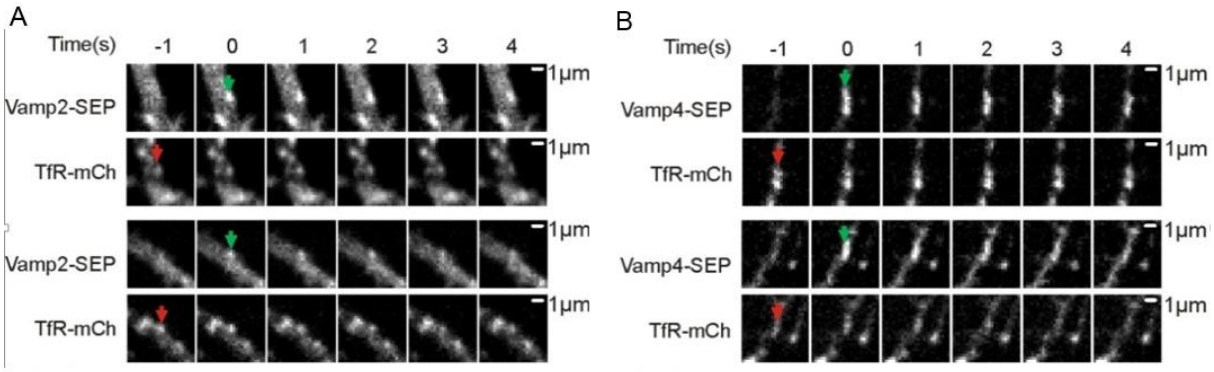

Figure 25 VAMP2 and VAMP4 clusters colocalization with transferrin receptor exocytosis sites
Examples of exocytosis events recorded in neurons (14-16 DIV) transfected with VAMP2-SEP and TfR-mCherry (**A**) or VAMP4-SEP and TfR-mCherry (**B**). In many cases, exocytosis events of VAMP2 and VAMP4 proteins were colocalized with TfR-mCherry clusters. Green arrows indicate exocytosis sites and red arrows indicate TfR-SEP clusters

In order to investigate subcellular localization of endogenous VAMP2 and VAMP4 proteins, we performed immunocytochemical labelling in cultured neurons (14-16 DIV). Neurons were fixed, permeabilized, stained for candidate vSNAREs and imaged with confocal microscope. For VAMP2, labelling analysis revealed strong enrichment in presynaptic boutons (Figure 26 A), as expected from previous studies of its subcellular distribution (Sampo et al. 2003) and from its presynaptic role in SV exocytosis in neurons. Weak labelling was also observed in soma and dendrites, but no clear structure could be discerned.

In agreement with VAMP4 role in retrograde trafficking to *trans*-Golgi compartments, endogenous VAMP4 staining is highly enriched in perinuclear regions corresponding to the TGN. Punctate and tubular structures were also

observed in endogenous VAMP4 staining of the dendritic compartments (Figure 26 B), which goes in agreement with published study of VAMP4 presence in dendrites (Raingo et al. 2012). However, the signal-to noise ratio of the fluorescent signal from endogenous VAMP4 labelling in dendrites is too low to conclude about its precise location or colocalization with other proteins. The same staining pattern was observed for overexpressed VAMP4 fused with HA-tag in immunocytochemical experiments labelling HA-tag (Figure 30,).

In order to investigate the subcellular localization of VAMP4 with better precision we performed observations with electron microscopy technique. Electron microscopy experiments were conducted by Jennifer Petersen. Cells were fixed, permeabilized and incubated with primary antibodies against endogenous TfR or VAMP4. Afterwards, a silver intensification technique on gold conjugated secondary antibodies was applied in order to reveal protein localisation at the ultrastructural level. As expected, silver intensified immunogold labelling revealed TfR presence in tubular endosomal-like structures (Figure 26 C, filled arrows) and sometimes at the PM surface as well as in the clathrin coated pits (Figure 26 C, empty arrows). VAMP4 immunogold staining showed VAMP4 abundant presence in tubular compartments around the nucleus that probably correspond to TGN structures (Figure 26Da, N stands for nucleus). Moreover, VAMP4-labelling immunogold particles were also observed in dendritic vesicular and tubular structures (Figure 26 Db, filled arrows), probably endosomal, as well as in close apposition to the PM (Figure 26Db, empty arrows). These results suggest that VAMP4 is present in endosomal compartments and is probably found on the REs undergoing exocytosis.

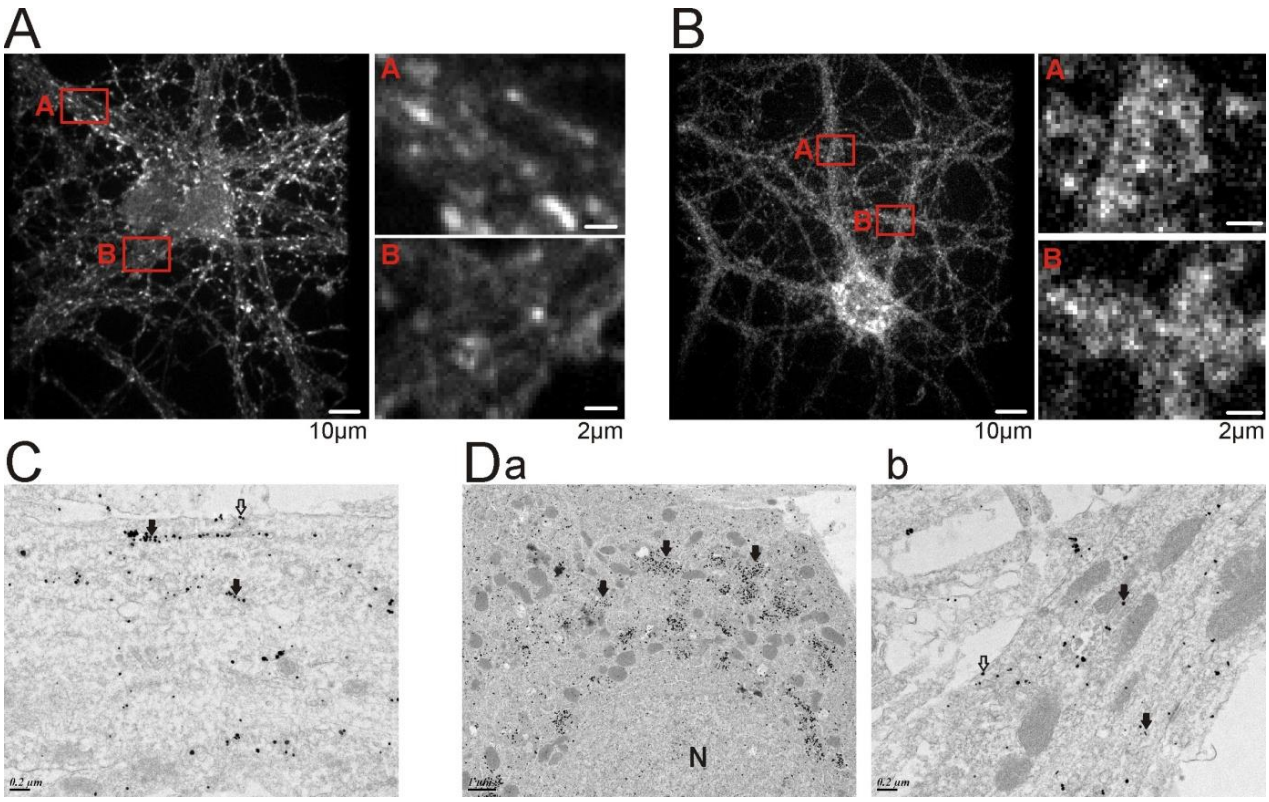

Figure 26 Endogenous VAMP2 and VAMP4 distribution in hippocampal neurons.
A, Immunocytochemical staining of cultured hippocampal neurons for endogenous VAMP2. Bright clusters likely represent presynaptic boutons. **B**, Immunocytochemical staining of endogenous VAMP4. VAMP4 is particularly enriched in Golgi apparatus, but also shows punctate localisation in dendrites as shown in enlarged regions of interest A and B. **C**, Silver intensified immunogold labelling of endogenous TfR reveals TfR presence in tubular endosomal structures (filled arrow), and at the PM, sometimes in clathrin coated pits (open arrow). **D**, Silver intensified immunogold labelling of endogenous VAMP4. Staining is enriched in the TGN compartments (filled arrows) close to the nucleus (N). On an enhanced view of a part of dendrite (b), VAMP4 is also found in endosomal-like compartments (filled arrows) and close to the membrane (open arrow)

4 Knock down of VAMP4 reduces exocytosis frequency of recycling endosomes

To investigate functional implication of the three v-SNARE candidates for RE exocytosis regulation, we applied different ways to downregulate their levels or interfere with their function and examine the consequences on the constitutive exocytosis. VAMP2 can be cleaved by TeNT (Pellizzari et al. 1999). TeNT protease activity is mediated by the light chain and its expression in cells is sufficient to successfully cleave VAMP1-3 (Proux-Gillardeaux, Rudge, et al. 2005). The N-terminal domain of VAMP7, also called longin domain, inhibits VAMP7 association with t-SNARE SNAP25 (Martinez-Arca, Alberts, Zahraoui, et al. 2000). Overexpression of soluble longin domain has dominant negative effect on SNARE complex formation and exocytosis. There is currently no molecular tool such as a specific protease or a dominant negative mutant to interfere with VAMP4 function. Therefore we adopted a strategy of VAMP4 down-regulation by specific shRNA vectors, which was successful in reducing VAMP4 function in neurons in previous studies (Raingo et al. 2012; Nicholson-Fish et al. 2015).

In neurons, coexpressing TfR-SEP together with VAMP7 longin domain did not affect the frequency of TfR-SEP exocytosis events (Figure 28, last columns). This result is consistent with the absence of VAMP7-SEP spontaneous somatodendritic exocytosis events observed earlier. Similarly, we expressed TeNT light chain or, as a control, its inactive mutant TeNT-LC E234Q with TfR-SEP. The TeNT expression did not significantly affect the frequency of TfR-SEP exocytosis (Figure 28, middle columns). The latter observation suggest that the majority of the observed TfR-SEP constitutive exocytosis events are not mediated by VAMP2 nor VAMP7.

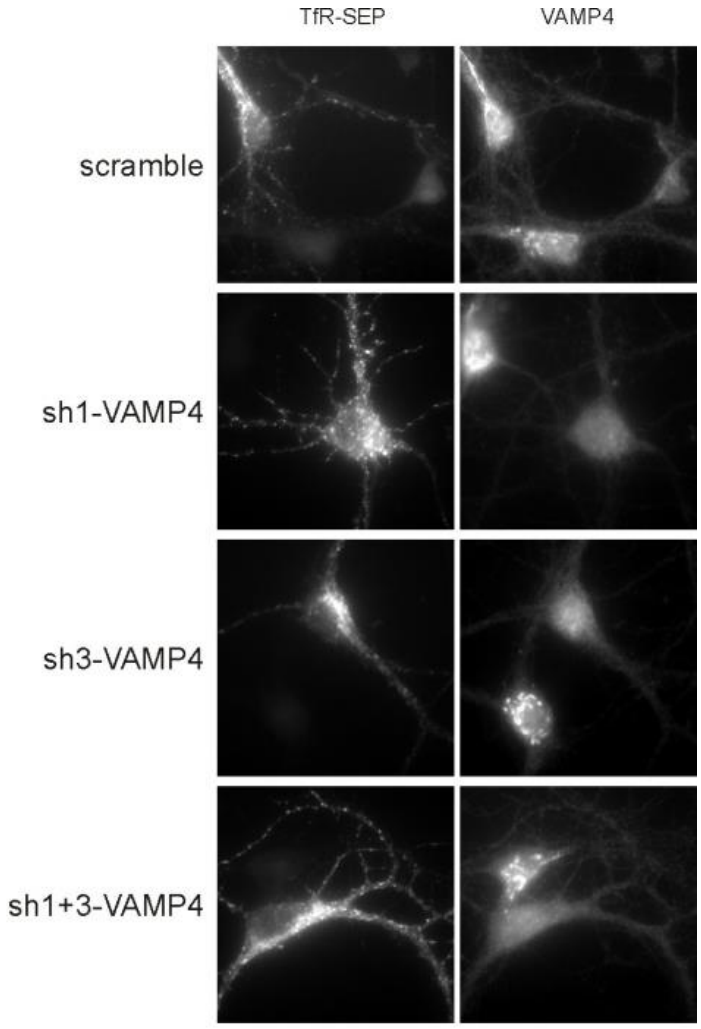

Figure 27 Downregulation of VAMP4 levels after transfection with shRNA
Neurons co-transfected with TfR-SEP and shRNA against VAMP4 (1, 2 or both). Immunolabeling of endogenous VAMP4 (right column) shows decrease in VAMP4 protein level in transfected neurons, detected by SEP signal coming from TfR-SEP (left column).

For VAMP4 downregulation, we have selected two shRNAs. ShVAMP4(1) targeted the 3' untranslated region (3'UTR) of VAMP4 RNA and shVAMP4(2) targeted the translated VAMP4 mRNA. Immunofluorescence analysis demonstrated strong decrease in endogenous VAMP4 levels after 4 days of each shRNA expression as compared to transfection with shScramble (see Figure 27). Live imaging of cultured neurons (14 DIV) cotransfected with shRNA against VAMP4 (shVAMP4 (1), shVAMP4 (2) or both) and TfR-SEP, revealed significant reduction in exocytosis frequency for TfR (Figure 28, shScramble – 0.06 ± 0.01 ev·µm^{-2}·min^{-1}, shVamp4(1) – 0.03 ± 0.004 ev·µm^{-2}·min^{-1}; shVAMP4(2) - 0.02 ± 0.003 ev·µm^{-2}·min^{-1}; shVAMP4(1+2) - 0.03 ± 0.005 ev·µm^{-2}·min^{-1}). This data indicates that efficient TfR recycling depends on VAMP4.

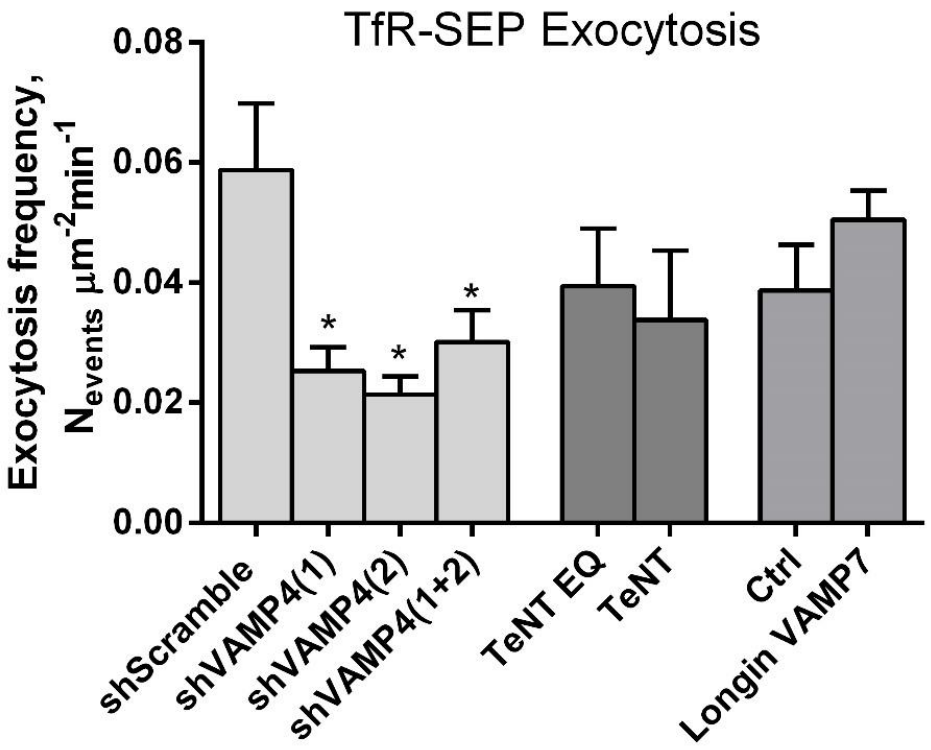

Figure 28 TfR-exocytosis rates after downregulation of VAMP proteins level. Graph demonstrates TfR-SEP exocytosis rates in neurons cotransfected with TfR-SEP and shRNAs against VAMP4 (shVAMP4 (1), shVAMP4 (2) or both) for VAMP4 downregulation; TfR-SEP and TeNT light chain for VAMP2 cleavage or its inactive form TeNT E234Q (TeNT EQ on the graph) as a control; TfR-SEP and VAMP7 dominant negative longin domain. Only shVAMP4 transfection resulted in significant alteration of TfR-SEP exocytosis. Mean exocytosis frequency values: shScramble – 0.06 ± 0.01 ev·µm^{-2}·min^{-1}, n = 15 cells; shVamp4(1) – 0.03 ± 0.004 ev·µm^{-2}·min^{-1}, n= 9 cells; shVAMP4(2) - 0.02 ± 0.003 ev·µm^{-2}·min^{-1}, n = 10 cells; shVAMP4(1+2) - 0.03 ± 0.005 ev·µm^{-2}·min^{-1}, n= 18 cells; TeNT EQ – 0.04 ±0.01 ev·µm^{-2}·min^{-1}, n = 6 cells; TeNT – 0.03 ± 0.01 ev·µm^{-2}·min^{-1}; n = 10 cells; Ctrl – 0.04 ± 0.007 ev·µm^{-2}·min^{-1}, n = 9 cells; VAMP7 longin domain 0.05 ± 0.004 0.01 ev·µm^{-2}·min^{-1}. Error bars represent standard error of mean. * - P-value in unpaired t-test less than 0.05.

KD experiments raise concerns about specificity of the shRNA action, so a number of controls should be performed in order to make sure that the observed phenotype is actually due to our protein of interest downregulation. ShRNA specificity could be tested in different ways. First, the observed phenotype should be reproduced by multiple independent shRNAs: in our case, two unrelated shRNAs had the same phenotype. The second control can be expression of shRNA resistant WT protein to test whether it rescues the shRNA-generated phenotype, with the condition that WT rescue protein overexpression does not produce a phenotype itself.

To conduct rescue experiments we generated several VAMP4 constructs fused with HA tag on their luminal C-terminal tail in order to be able to verify

their expression in neurons by immunofluorescence (construct sequences are described in 1.2.2 section of Materials and Methods). VAMP4-HA constructs were either shRNA-resistant (i.e. with codon substitutions), to rescue phenotypes in neurons expressing both shVAMP4 (1) and shVAMP4(2); or the usual WT translated VAMP4 sequence without (3'UTR) that would be able to rescue phenotype in neurons expressing shVAMP(1). In the first version of the constructs, HA tag was fused directly to VAMP4 C- terminal. However, we could not detect HA-tag with antiHA immunolabeling in fixed and permeabilized neurons expressing these versions of VAMP4-HA despite positive anti HA staining control (data not shown). We presumed that HA tag was probably not accessible to the antibody because of its obstruction in completely folded VAMP4 protein. To solve this problem we generated several VAMP4-HA constructs with different linkers in between the VAMP4 protein and the HA tag in order to withdraw the HA tag further from the protein. We could only detect a specific HA staining when using a Fibronectin 3 domain (FN3) as a linker between VAMP4 and HA. (Figure 30). This means that HA tag close position to VAMP4 C-terminal tail restricted antibody access.

Anti-HA staining in VAMP4-FN3-HA expressing neurons showed the same VAMP4 distribution as immunolabeling against endogenous protein (Figure 30). Immunofluorescence analysis revealed strong signal in perinuclear regions similar to TGN structures. The signal from dendrites had signal-to-noise ratio too low to conclude about VAMP4-FN3-HA ultrastructural localisation.

As VAMP4-FN3-HA protein was not shRNA resistant, we could perform the rescue experiment only for shVAMP4(1), which is targeted against 3'UTR of VAMP4 mRNA. I first assessed shVAMP4(1) efficiency in downregulation of endogenous VAMP4 levels. Cultured hippocampal neurons (14DIV), coexpressing TfR-SEP with shVAMP4(1) or control shScramble for four days were fixed and immunolabeled with antiVAMP4 primary antibody and fluorescently tagged secondary antibody. Neurons, transfected with shVAMP4(1) were ~50% less fluorescent than control group. This observation indicates that even if the level of endogenous VAMP4 is decreased, the efficiency of our shRNA stays limited, but with a measurable effect of RE exocytosis.

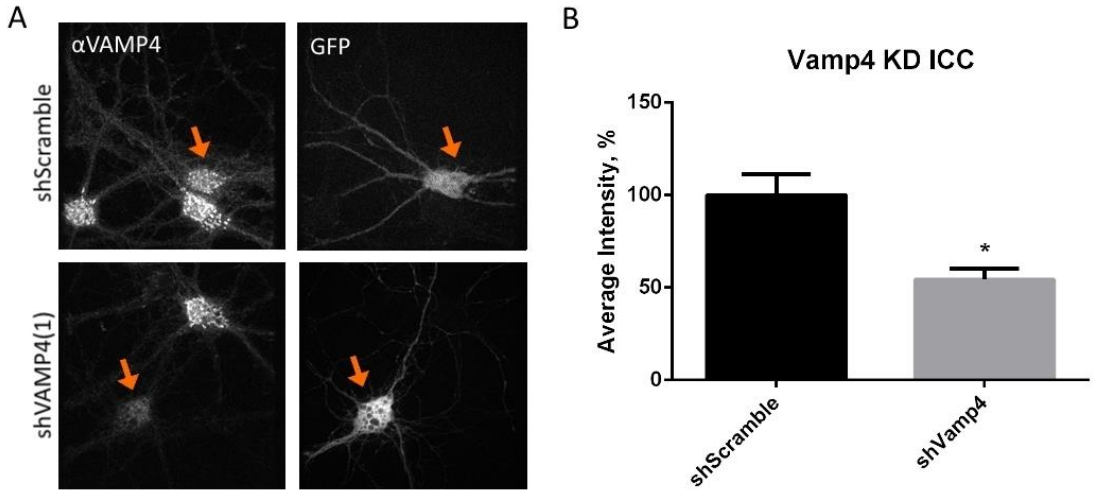

Figure 29 Decrease in VAMP4 levels after transfection with shRNA
Immunofluorescence analysis of shVAMP4(1) efficiency in VAMP4 downregulation. **A**, Cultured hippocampal neurons were cotransfected with TfR-SEP and shVAMP4(1) or shScramble as a control and immunolabeled for VAMP4. **B**, Immunofluorescence quantification revealed ~50% downregulation in VAMP4 levels (normalized fluorescence: shScramble 100% ± 11.23%, n = 12 cells; shVAMP4(1) – 54.27 ± 5.94%, n = 17 cells). * - P-value in unpaired t-test less than 0.05.

Finally we conducted rescue live imaging experiment where we recorded TfR-SEP exocytosis events in neurons cotransfected with shVAMP4(1), only VAMP4-FN3-HA or both. VAMP4-FN3-HA overexpression alone did not have any compelling effect on RE exocytosis (Figure 31, mean TfR-SEP exocytosis frequency: shScramble +TfR-SEP – 0.042 ±0.006 01 ev·μm^{-2}·min^{-1}; VAMP4-FN3-HA +TfR-SEP – 0.035 ± 0.005 01 ev·μm^{-2}·min^{-1}). However, VAMP4-FN3-HA coexpression together with shVAMP4(1) rescued the rates of TfR-SEP exocytosis (Figure 31, mean TfR-SEP exocytosis frequency: TfR-SEP and shVAMP4(1) – 0.02 ± 0.03 01 ev·μm^{-2}·min^{-1}; TfR-SEP, shVAMP4(1) and VAMP4-FN3-HA – 0.032 ± 0.009 ev·μm^{-2}·min^{-1}). Such results indicate that the observed phenotype in shRNA transfected neurons is due specifically to reduced VAMP4 levels.

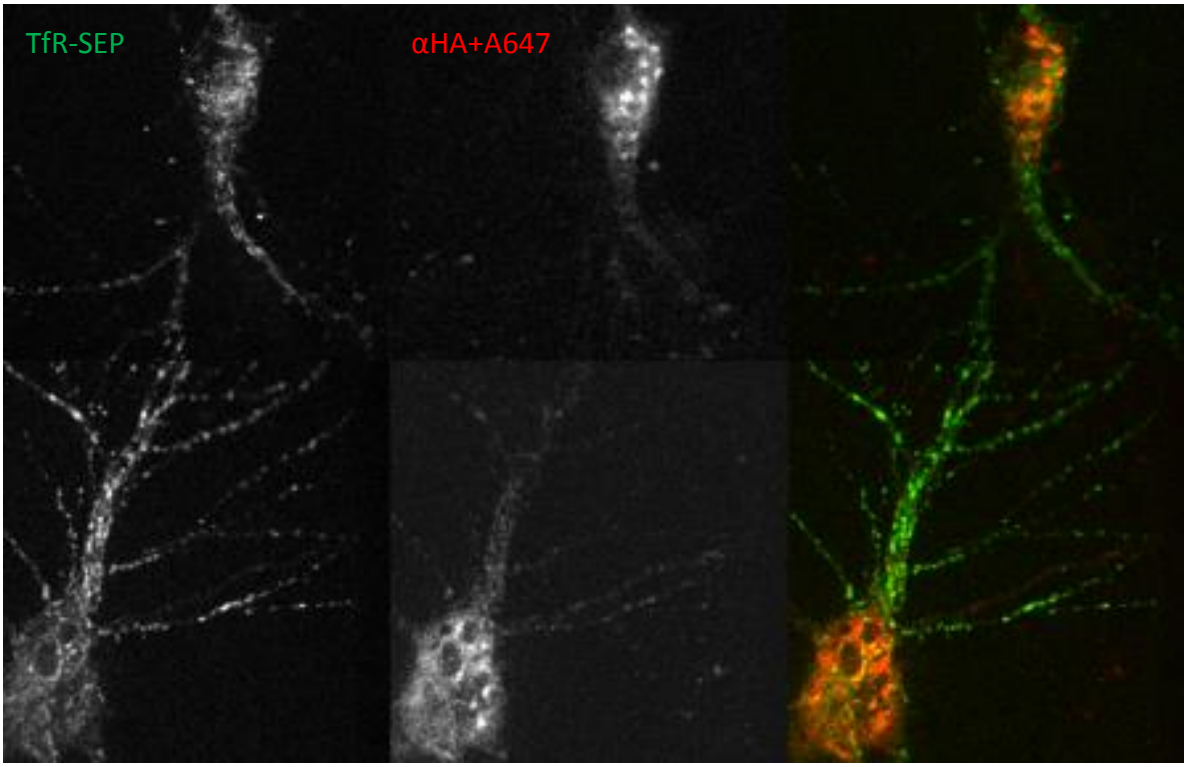

Figure 30 Distribution of the overexpressed VAMP4-FN3-HA and its colocalization with TfR-SEP
Figure demonstrates immunocytochemical staining of HA-tag (middle column) in permeabilized cultured hippocampal neurons, overexpressing VAMP4-FN3-HA and TfR-SEP (left column). Labelling of the VAMP4-FN3-HA in permeabilized neurons shows that intracellular distribution of the overexpressed VAMP4-FN-HA in hippocampal neurons varies a lot. Most of the time, the staining is enriched is TGN structures with weak signal in dendrites. Signal-to-noise ratio of the immunofluorescent signal from dendrites is too low to examine the colocalization (right column).

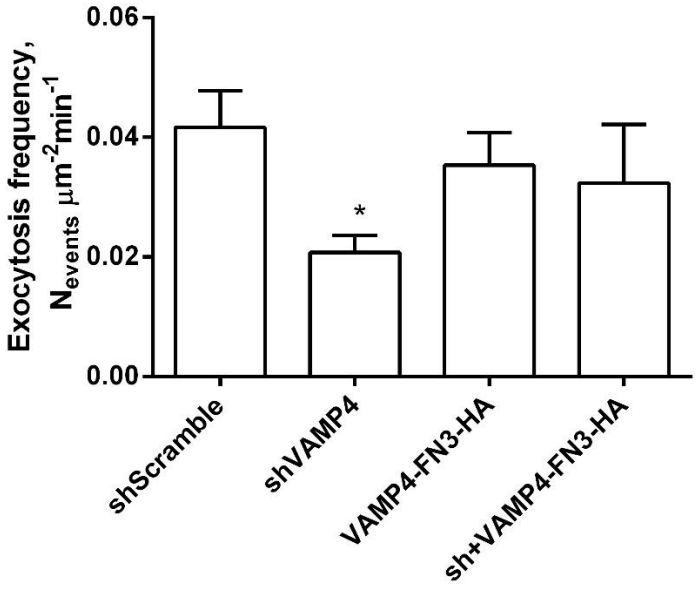

Figure 31 Rescue of the TfR-SEP exocytosis frequency in shVAMP4 neurons
Frequency of TfR-SEP exocytosis in neurons coexpressing TfR-SEP and shScramble – 0.042 ±0.006 01 ev·µm^{-2}·min^{-1}, n = 33 cells; TfR-SEP and shVAMP4(1) – 0.02 ± 0.03 01 ev·µm^{-2}·min^{-1}, n = 23 cells; TfR-SEP and VAMP4-FN3-HA – 0.035 ± 0.005 ev·µm^{-2}·min^{-1}, n = 7 cells; TfR-SEP, shVAMP4(1) and VAMP4-FN3-HA – 0.032 ± 0.009 ev·µm^{-2}·min^{-1}, n = 9 cells. * - P-value in unpaired t-test less than 0.05.

5 VAMP4 or VAMP2 downregulation does not affect basal transmission in cultured neurons.

Our previous findings suggest that at least a sub-population of organelles, undergoing exocytosis in the postsynaptic domain, has VAMP4 as their R-SNARE for fusion with the plasma membrane. Further, I wanted to test the involvement of VAMP4 and VAMP2 in the constitutive recycling of AMPA receptors, which is important for basal transmission maintenance or synaptic strengthening during LTP (Lüscher et al. 1999).

First, I examined the effect of VAMP4 knockdown and VAMP2 cleavage on spontaneous miniature excitatory postsynaptic currents (mEPSCs), see Figure 32. Cultured hippocampal neurons were transfected with shRNA against VAMP4 or TeNT light chain and GFP. As this experiment did not include live imaging, I used VAMP4 fused with SEP as a rescue construct in VAMP4 KD neurons. TeNT light chain expression did not affect mEPSCs frequency (GFP - 4.79 ± 0.98 Hz, n = 8; TeNT + GFP - 4.4 ± 0.76 Hz, n = 7) or amplitude (GFP – 16.4 ± 2.6 pA; TeNT + GFP – 15.6 ± 1.1 pA). This confirms previous findings about VAMP2 role in basal transmission maintenance explored with TeNT infusion or in VAMP2 KO neurons (Schoch et al. 2001; Petrini et al. 2009). Downregulation of VAMP4 slightly decreased mEPSCs frequency (shVAMP4 + GFP - 3.2 ± 0.5, n = 12), but the effect was not statistically significant (P = 0.1, unpaired t test). Moreover, VAMP4 KD did not alter the amplitude of the mEPSCs (shVAMP4 + GFP - 15 ± 1.1 pA). Overexpression of VAMP4-SEP with shRNA slightly increased mEPSCs frequency (shVAMP4 + VAMP4-SEP - 5.9 ± 1.27 Hz, n = 14) and amplitude (shVAMP4+VAMP4-SEP – 22.5 ± 3.2), but again the differences were not statistically significant.

This study suggests that reduction of RE exocytosis by VAMP4 KD does not affect synaptic AMPA receptors. On the other hand, such experiment is not sufficient to conclude on VAMP2 or VAMP4-dependent AMPA receptor cycling as chronic protein block can evoke compensatory mechanisms.

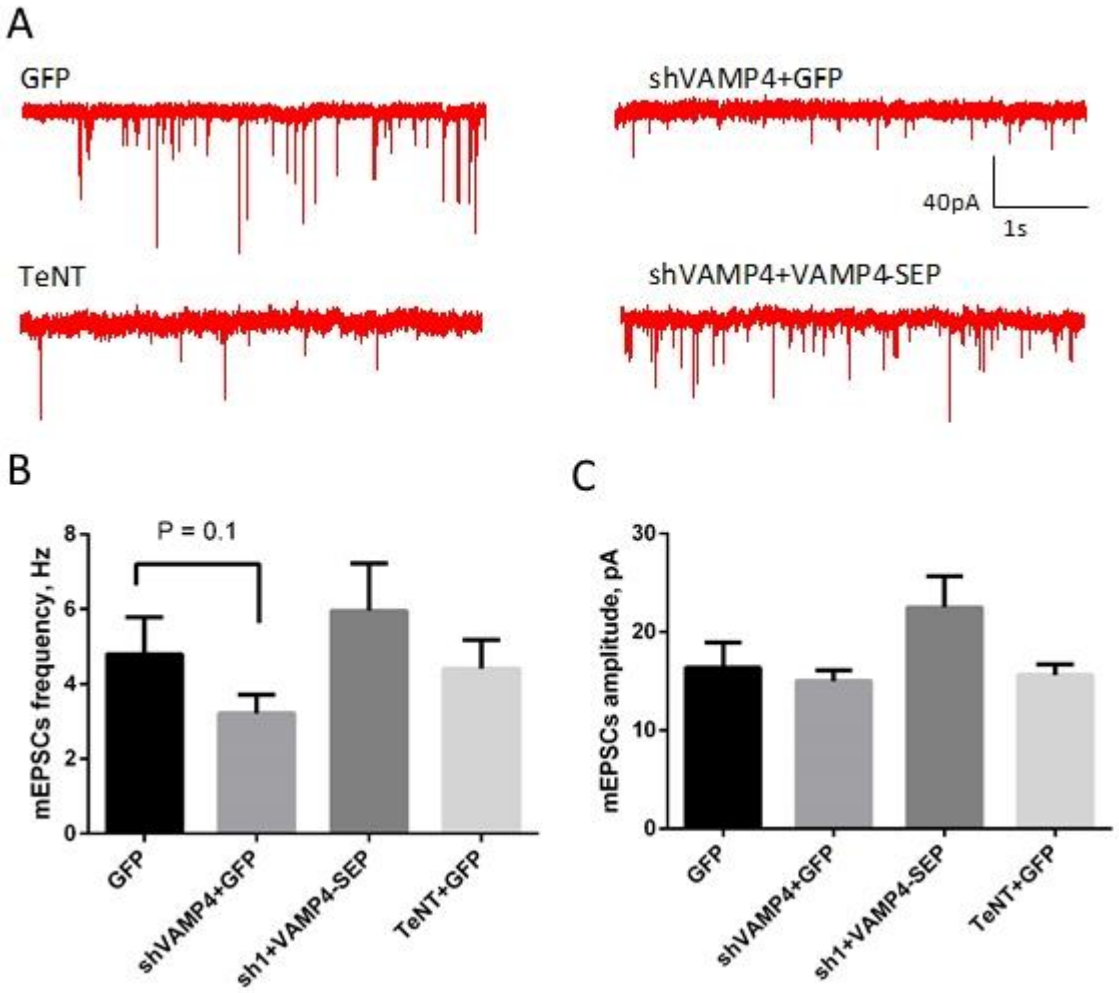

Figure 32 Basal transmission in VAMP4 KD neurons

A, Example traces of miniature excitatory postsynaptic currents (mEPSCs) in cultured hippocampal neurons expressing only GFP, shRNA for VAMP4 together with GFP, shRNA for VAMP4 and VAMP4 fused with SEP, or TeNT with GFP. **B**, Graph represents mean values of the mEPSCs frequencies. **C**, Mean values of the mEPSCs amplitudes are shown. Error bars represent SEM. Number of cells in each condition: GFP (8 cells), shVAMP4 + GFP (12 cells), shVAMP4+ VAMP4-SEP (13 cells), TeNT with GFP (7). Number of independent experiments: 11. P-value was calculated for unpaired t-test.

6 The endeavor cLTP in cultured hippocampal neurons

At excitatory synapses in the mammalian brain, trafficking of AMPA receptors can be regulated in order to induce plastic changes in synaptic strength. In this way, AMPA receptors are endocytosed and their number at the postsynapse is decreased during LTD, while NMDA-triggered LTP provokes exocytosis in AMPA receptors and an increase in the synaptic receptor number (Bredt & Nicoll 2003; Collingridge et al. 2004; Malinow & Malenka 2002; Newpher & Ehlers 2008; Shepherd & Huganir 2007). Previous studies advocate that SNAREs are implicated in activity-dependent AMPA receptor delivery to the PM during LTP (Kennedy et al. 2010; Lledo et al. 1998; Lu et al. 2001). So far only VAMP2 was identified as vSNARE implicated in regulated AMPA exocytosis after LTP induction (Jurado et al. 2013). In order to determine possible functional implication of VAMP4 in activity-regulated RE exocytosis we decided to examine its involvement LTP-triggered AMPA receptor insertion to the PM.

One of the classic approaches to study LTP in neuronal culture is the cLTP protocol (Park et al. 2006; Ahmad, J. S. Polepalli, et al. 2012; Passafaro et al. 2001; Kennedy et al. 2010). cLTP protocol implies activation of NMDA receptors by bath application of the coagonist glycine in a Mg^{2+} -free medium from 3 to 5 minutes. In order to suppress all activity except excitatory spontaneous transmission, neuronal saline solution also contains sodium channel blocker TTX, glycine receptors antagonist strychnine and $GABA_A$ receptors chloride channel blocker picrotoxin. In the course of glycine application, activated NMDA receptors allow maximum Ca^{2+} influx during miniature spontaneous excitatory transmission. Such Ca^{2+} influx triggers intracellular LTP cascades resulting ultimately in increased number of synaptic AMPA receptors and intensified transmission. LTP action can be evaluated by measuring the intensity of surface staining of the AMPA receptor subunits.

We attempted to develop cLTP assay in our laboratory. The final goal of such test would be evaluation of candidate vSNAREs implication in activity-regulated AMPA exocytosis during LTP. We developed two different approaches in order to test the protocol. In the first procedure cultured hippocampal neurons

transfected with Homer1C-GFP were incubated for 10 minutes in Mg^{2+} free solution and consequently stimulated with glycine application. Afterwards, they were incubated back in at 37°C for various time (see Table 3), then fixed and stained for surface GluA1 subunit of AMPA receptors (Figure 33 A). However, after multiple attempts (number of independent experiments N = 12), we have never obtained a significant increase in surface AMPARs. In our experiments, the typical augmentation of surface AMPARs staining intensity was about 10-20% (Figure 33 B), unlike published increases of 50-100 % (Jaafari et al. 2012; Ahmad et al. 2012), too small to be considered a reliable marker of LTP.

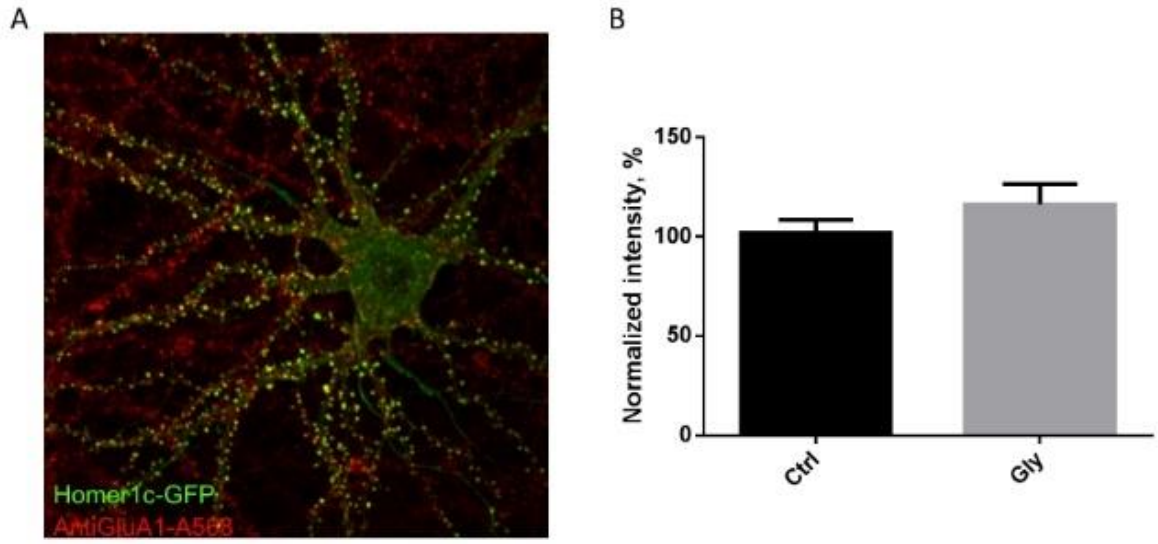

Figure 33 antiGluA1 staining in Gly-treated neurons
A, Panel shows superimposed image of Homer1C-GFP transfected neuron (green) and antiGluA1 immunofluorescent staining (red). **B**, Graph shows average antiGluA1 staining fluorescence intensity quantified in ROI defined by bright areas in Homer1c-GFP signal that likely correspond to spines for cLTP stimulated neurons (Gly) or control group. Average intensity: Ctrl – 100 ± 6.15%, n = 9 cells; Gly – 116.2 ± 10.24%, n = 5 cells.

To determine the key factors that could influence final experimental output we have varied different experimental parameters provided in Table 3, but it did not influence obtained results.

PARAMETER	VALUES
Culture density	300, 400, 600 · 10^3 cells per dish
Incubation time after glycine application	10, 15, 20 minutes
Surface AMPARs quantification	Average intensity in spines, defined with homer1c-GFP fluorescence, average intensity in AMPAR-enriched pixels

Table 3 Different experimental parameters used in cLTP protocol
Table provide different parameters that were varied during cLTP protocol adjustment.

Finally, in regards of unfruitful attempts to obtain LTP in cell culture we proceeded to functional vSNARE study in cultured organotypic slices.

7 VAMP4 and VAMP2 downregulation affects LTP in cultured hippocampal slices

We chose organotypic slices as a model for postsynaptic vSNARE involvement in LTP investigation, since it is biologically more faithful for studying memory-related phenomena and gives more reproducible results in experiments with LTP induction. In organotypic slices neuronal innate network structure is preserved, and at the same time they allow chronic treatments such as cell transfection with relative ease.

Individual CA1 neurons were transfected 4 days before recording with single cell electroporation. I have electroporated typically 10 cells per slice with plasmids coding for soluble GFP and either shVAMP4(1) or TeNT, or their respective controls (shScramble or TeNT E234Q) to downregulate VAMP4 or VAMP2. The details of the technical implementation are provided in Materials and Methods part.

LTP was induced in synapses between CA3 and CA1 neurons of the hippocampal slices after 14-16 DIV (Figure 34). I have recorded CA1 pyramidal neuronal excitatory postsynaptic currents with patch-clamp in voltage-clamp mode. EPSCs were evoked every 20 s of the recording by stimulation of the Schaffer collateral fibers emerging from CA3 with stimulation electrode. After breaking into the cell and adjusting electrical stimulation to obtain a stable postsynaptic response, 10 baseline currents were recorded. Short baseline recording time was chosen to avoid a “wash-out” effect. Immediately after baseline stimulation, LTP was induced with so-called “pairing protocol”. It consists of stimulating presynaptic fibers with a 1Hz stimulation train of 100 pulses while simultaneously holding postsynaptic membrane potential at 0V by current injection via the recording electrode. For the details on the pairing protocol see 5.3 chapter in Materials and methods.

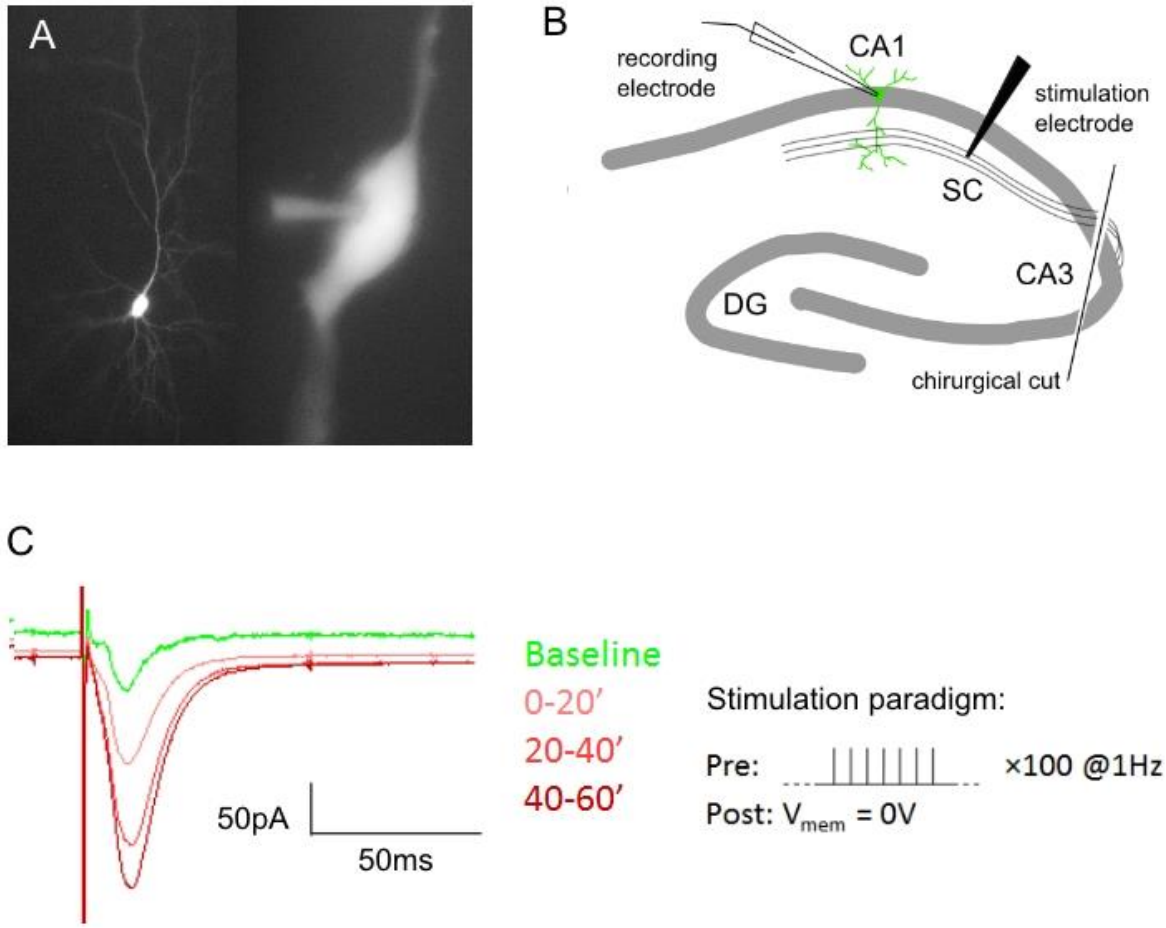

Figure 34 Pairing LTP on electroporated CA1 pyramidal neurons
A, Left panel illustrates an electroporated CA1 pyramidal neuron in hippocampal slice expressing GFP; right panel shows a zoom in a soma of an electroporated neuron with an electrode in whole cell configuration. **B**, Schematic representation of the LTP induction experiment. Electroporated neuron is patched in voltage-clump configuration. Stimulation electrode passes current through schaffer-collateral fibers coming from CA3. **C**, Average excitatory postsynaptic currents (EPSC) for first 3 min of baseline recordings (green), or for different time intervals after LTP stimulation (grades of res). LTP stimulation consist of 100 pulses of 1Hz frequency coupled with imposed postsynaptic membrane depolarization.

The data obtained is represented on 4 different graphs of the Figure 35, where each datapoint represents an average of 5 consecutive EPSCs. Red arrows mark the timing of the LTP protocol. The control condition with neurons electroporated with shScramble had good potentiation to around 200 % of initial amplitude (Figure 35A, n = 4). It should be noted that the level of potentiation was not very stable and dropped around 30' of recording after stimulation before going back up. This can be attributed to the inherent variability of LTP and should average out with more recordings. Consistent with published literature (Jurado et al. 2013), in neurons expressing TeNT, LTP was abolished (Figure 35C, n = 4). Mutant TeNT EQ did not supress potentiation in recorded neurons,

however in our data we observe a certain delay in potentiation onset (Figure 35D, n = 5). Finally, the potentiation could not be elicited in VAMP4 KD neurons (Figure 35B, n = 6).

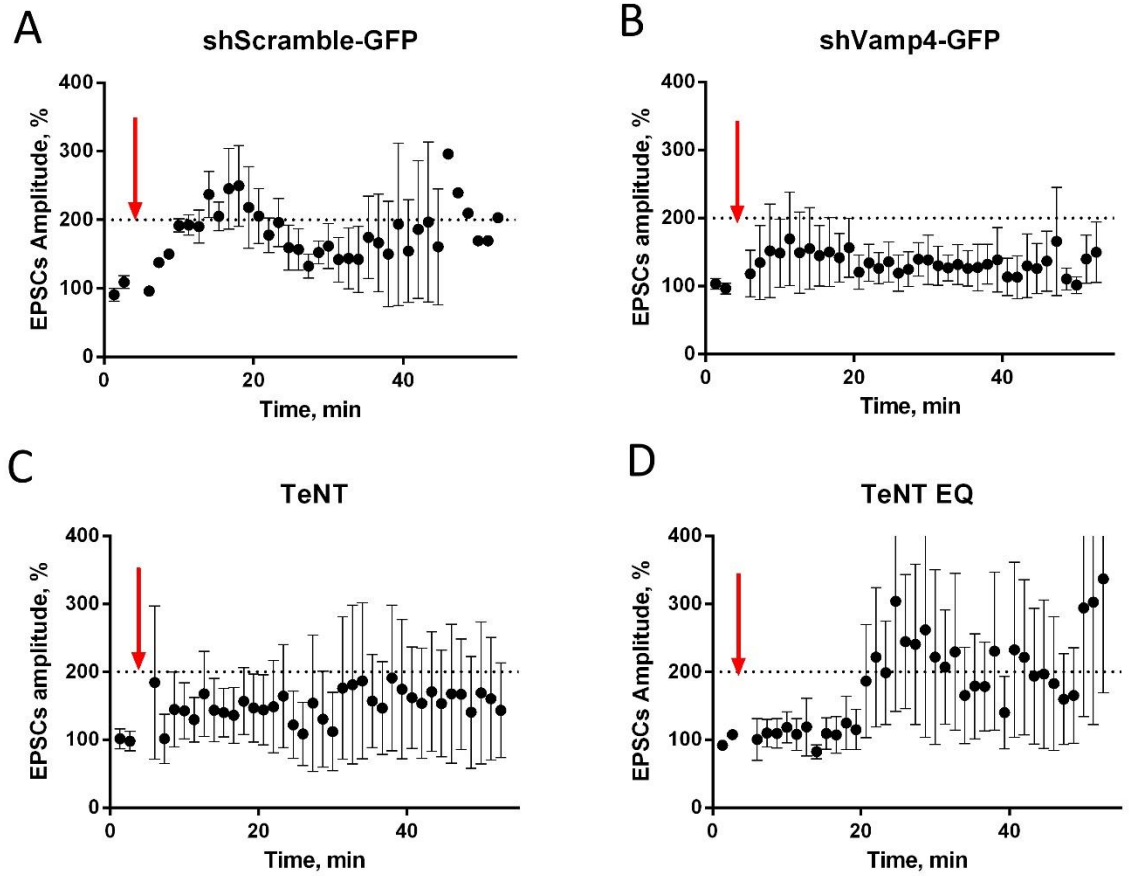

Figure 35 EPSCs LTP is affected by VAMP2 orVAMP4 downregulation
Graphs show normalized EPSC recorded before and after LTP stimlation in CA1 pyramidal neurons electroporated with (**A**) shScramble-GFP, n= 4 cells; (**B**) shVAMP4-GFP, n = 6 cells; (**C**) TeNT light chain, n = 4 cells; (**D**) TeNT E234Q (TeNT inactive form), n = 5 cells. Timepoints on the graph represent average values of five consecutive EPCSs, red arrows indicate pairing LTP stimulation, error bars sho S.E.M.

LTP recording in slices after VAMP4 and VAMP2 downregulation advocate that postsynaptic receptor trafficking involved in LTP expression depends on both SNARE proteins. However, we are well aware that a recue experiments should be performed before fully concluding on the obtained results.

8 Acute block of the RE exocytosis.

The chronic block, for four days, of the SNARE activity is susceptible to side effects and can possibly induce compensatory mechanism. To avoid these issues and confirm the specificity of the results obtained with the KD strategy we decided to acutely block the candidate SNAREs and directly assess the effect on the postsynaptic TfR-positive REs exocytosis.

To acutely interfere with the SNARE functioning we used patch-clamp pipette filled with intracellular solution containing different blocking agents. After breaking into the cell and installing the whole-cell configuration, blocking agents diffuse into the neuron and interact with their targets. Loading cells with proteolytic chains of the clostridial toxins has already been applied to acutely block postsynaptic exocytosis and examine the effect on mEPSCs (Lüscher et al. 1999). In the same manner, we loaded neurons with TeNT light chain, which cleaves VAMP2 (Schiavo et al. 1992; Pellizzari et al. 1999), to acutely block VAMP2-dependent exocytosis. It is possible to interfere with VAMP4 association into the SNARE complex by microinjecting an antibody directed against VAMP4 (Cocucci et al. 2008). By interacting with VAMP4 N-terminal domain, the antibody would prevent VAMP4 interaction with its partners on the target membrane. We used similar approach and loaded neurons with an antibody against VAMP4 through the patch pipette. As a positive control, we used intracellular solution containing BoNT-C1 light chain that is known to cleave postsynaptic t-SNARE SNAP-25 and syntaxin1 (Pellizzari et al. 1999).

Before the experiment, cultured neurons were transfected with TfR-SEP. Cells were imaged for TfR-SEP exocytosis in cell attach mode, while cell membrane is still intact and forms a tight seal with the patch-pipette (Figure 36 B). After opening the membrane, neurons were imaged during 0-2, 5-7 and 10-12 min of the intracellular solution dilution. Imaging time was chosen as an accommodation between time, potentially sufficient for blockers diffusion (Lledo et al. 1998; Lüscher et al. 1999), and cell viability monitored by the stability of the leak current. Measured exocytosis frequency was normalized, with 100% defined by exocytosis rates of the intact cells.

After 10 minutes of normal intracellular solution diffusion neurons manifested a slight decrease in observed exocytosis frequency (Figure 36 C: Vehicle – 74.01 ±14.08%, n = 6 cells), which was probably due to the 'wash-out' effect of the patch-clamping. BoNT-C1 loading caused a strong decrease in TfR-SEP exocytosis (Figure 36 C: BoNT-C1 – 20.66, n = 1 cell), however we cannot judge the statistical significance of the observed effect, as with BoNT-C1 containing intracellular solution we've succeeded to patch only one cell. TeNT or antiVAMP4 dilution into the neurons did not provoke a stronger effect on exocytosis decline than with usual intracellular solution introduction (Figure 36 C: TeNT – 63.09 ± 28.21%, n = 5 cells; antiVAMP4 – 73.26 ± 2.7%, n = 2 cells).

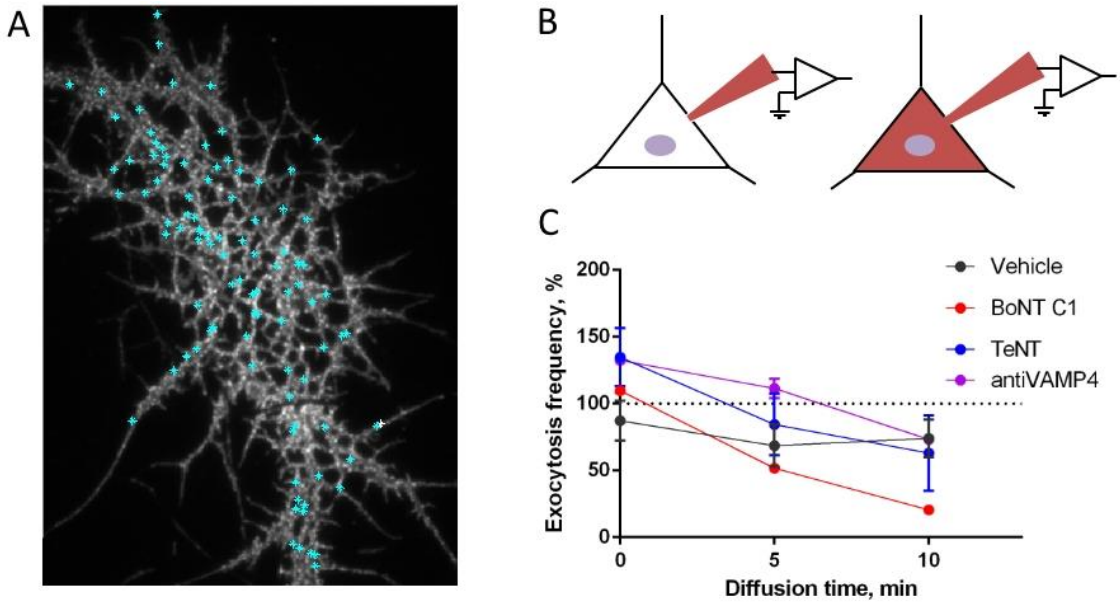

Figure 36 Acute block of the dendritic RE exocytosis

A, Cultured hippocampal neurons (14DIV) transfected with TfR-SEP. Image from time-lapse movie, recorded after breaking into the cell pith-patch pipette containing, in this example, usual intracellular solution Cyan asterisks show detected exocytosis events detected over the course of two minutes. **B**, Sematic representation of the exocytosis blocking agents loading inside neurons. Patch-pipette filled with the intracellular solution containing toxins or antibodies interfering with SNARE machinery is first attached to the cell body (left panel). After entering the whole-cell configuration, exocytosis blockers diffuse into the cell (right panel). **C**, exocytosis frequency estimated on 0-2, 5-7 and 10-12 minutes of blockers dilution, normalized to the frequency registered in cell-attached mode (100%, dotted horizontal line). Normalized exocytosis frequency values after 10 min of loading: Vehicle – 74.01 ±14.08%, n = 6 cells; BoNT-C1 – 20.66, n = 1 cell; TeNT – 63.09 ± 28.21%, n = 5 cells; antiVAMP4 – 73.26 ± 2.7%, n = 2 cells. Number of independent experiments, N = 11. Unpaired t-test showed no statistical differences between exocytosis frequency decrease after 10 minutes of Vehicle or TeNT, or antiVAMP4 dilution.

The absence of a significant effect of the antibody loading is difficult to interpret, as we cannot be sure if this is due to the fact that RE-exocytosis

independency from VAMP4 or technical problems, like the diffusion of the antibody within dendrites. One could suggest introducing to the patch-pipette of a small fluorescent tags like Alexa flourophores in order to follow the time-course of the intracellular solution diffusion into the cell. However, Alexa diffusion dynamics won't tell us much about the antibody diffusion, as they vary considerably in size (Alexa fluor molecular weight ~1000, antibody molecular mass ~ 150,000).

Loading neurons with clostridial toxins light chain (50kDa) produces an effect after 10 min contact with the intracellular solution (Lüscher et al. 1999; Lu et al. 2001). We did not observe a significant decrease in TfR-SEP exocytosis after 10 min TeNT light chain diffusion into the cells. The effectiveness of this batch of TeNT was confirmed in my laboratory, as it blocked LTP in acute hippocampal slice preparation (Andrew Penn, personal communication). This goes in-line with our previous results obtained on neurons genetically expressing TeNT light chain (section 4 of the Results), and argues for a minor involvement of VAMP2 in constitutive RE exocytosis.

Discussion

The involvement of the SNARE proteins in postsynaptic exocytosis

The study presented in this work was motivated by the necessity to understand the mechanisms regulating postsynaptic forms of neuronal exocytosis, a fundamental process that underlies neuronal membrane composition, transmission and synaptic plasticity. Postsynaptic REs exocytosis is at least involved in supporting basal transmission and synaptic potentiation through constitutive and regulated AMPARs delivery to the PM (Lüscher et al. 1999; Kennedy et al. 2010; Park et al. 2004). The constitutive recycling is observed in hippocampal neurons with classical RE marker TfR fused to SEP occurs with high frequency and exhibits various dynamics (Jullié et al. 2014). We hypothesized that, apart from the already identified postsynaptic v-SNARE VAMP2 (Jurado et al. 2013), involved in LTP, there should be other proteins involved in RE exocytosis. The evidence on VAMP2 action in constitutive AMPARs recycling is controversial: some studies have found an effect of BoNT-B, which cleaves VAMP2, on EPSCs (Lüscher et al. 1999) but others claim that BoNT-B or TeNT do not have an effect on EPSC amplitude (Lledo et al. 1998; Lu et al. 2001). In addition, spontaneous postsynaptic excitatory currents are unaffected in neuronal cultures from VAMP2 KO mice (Susanne; Schoch et al. 2001). Moreover, in the example of extensively studied presynaptic exocytosis, it now becomes clear that SV release is mediated not only by the classical v-SNARE VAMP2, but also by VAMP4, VAMP7 and Vti1A (Crawford & Kavalali 2015; Hua et al. 2011) which play a specific role in different types of SVs release. Therefore,

diverse SNARE machinery may be one of the ways for neurons to regulate tightly and locally presynaptic secretion. We thus investigated the role of the v-SNARE proteins by live cell fluorescence microscopy and electrophysiology to figure out the molecular mechanisms underlying the diversity or RE exocytosis in neuronal dendrites.

Observation of VAMP-SEP exocytosis in hippocampal neurons

We started investigation of the postsynaptic vSNAREs by identifying potential candidates for exocytic fusion in hippocampal neurons. Among the seven VAMP proteins isoforms only VAMP2, VAMP4 and VAMP7 are expressed in hippocampal neurons. These three candidate VAMP proteins are implicated in various types of exocytosis in neurons and other cell types. In presynaptic SV exocytosis evoked synchronous, asynchronous and spontaneous neurotransmitter release are mediated by VAMP2, VAMP4 and VAMP7 respectively (Deák et al. 2004; Bal et al. 2013; Raingo et al. 2012). We genetically expressed in cultured hippocampal our candidate v-SNAREs or endosomal marker TfR fused with SEP and imaged them with a spinning disk confocal microscope in order to identify if they underwent exocytosis in somatodendritic regions. By observing VAMP proteins behaviour in unstimulated conditions, we found that VAMP2 and VAMP4 were constitutively recycled though PM in somatodendritic regions. VAMP2-containing organelles underwent exocytosis significantly less often than TfR-SEP positive endosomes. Therefore, it is not likely that VAMP2 mediates for the totality of TfR-SEP exocytosis events. On the other hand, VAMP4 constitutive exocytosis rates were comparable to those of the TfR, suggesting that VAMP4 could potentially mediate postsynaptic REs exocytosis. Previous studies have detected VAMP7 somatodendritic exocytosis events in very young neuronal cultures (0-3DIV) (Burgo et al. 2012; Gupton & Gertler 2010). Nonetheless, we did not record any postsynaptic VAMP7-SEP exocytosis in older preparations (14-16 DIV). Consequently, it is not likely that VAMP7 plays a significant role in constitutive RE fusion with the somatodendritic PM in mature neurons.

These results raise multiple questions. If VAMP4 and VAMP2 mediate exocytosis at the postsynaptic compartments of the hippocampal neurons, what proteins would account for their partners in SNARE complex formation? To form a functional SNARE complex, R-SNAREs VAMPs require Q_a SNARE syntaxin and SNAP-25 related protein (Q_{bc}- SNARE). As of today, we know that SNAP-25, SNAP-23, SNAP-47, syntaxin4 and syntaxin3 are present on the postsynaptic membrane where they have physiological implications. Syntaxin4 and syntaxin3 were suggested to be involved in regulated AMPARs trafficking to the postsynaptic membrane, however evidence for a role of syntaxin4 is controversial (Kennedy et al. 2010; Jurado et al. 2013). It would be possible to extend the described imaging technique for dual-colour imaging of VAMP4-SEP and VAMP2-SEP recycling together with the postsynaptic syntaxins fused at their TM C-terminal domain to an HA-tag fluorescently stained with an antiHA IgG fused to a fluorophore (Kennedy et al. 2010). This would allow the analysis of the spatial VAMPs exocytosis distribution comparatively to a surface syntaxin3 or 4 enrichment sites.

Both SNAP-23 and SNAP-25 were proposed to specifically regulate NMDARs traffic to synapses (Lau et al. 2010; Lan et al. 2001; Suh et al. 2010; Washbourne 2004). SNAP-47 is potential VAMP2 partner in mediating activity-dependent exocytosis during LTP (Jurado et al. 2013). It is more complicated to conduct imaging experiments with SNAP t-SNAREs, as they lack TM domain, convenient for fusion with a tag without interfering with the proteins function and for specific labelling of the plasma membrane pool of t-SNAREs.

Downregulation of the postsynaptic SNAREs

After identifying two v-SNAREs undergoing exocytosis in dendritic compartments, we tested their involvement in constitutive RE exocytosis. Chronic VAMP2 inactivation by genetic expression of its endopeptidase TeNT light chain (Pellizzari et al. 1999) did not lead to significant changes in frequency of TfR-positive exocytosis events, consistent with the fact that VAMP2 does not mediate the majority of the endosomal fusion events in basal conditions. Furthermore, VAMP4 downregulation through gene expression silencing with shRNAs resulted in significant reduction of the TfR-SEP constitutive exocytosis

that could be restored by a rescue construct expression. Such outcome points at VAMP4 as a v-SNARE for an important fraction of postsynaptic RE exocytosis and leaves us wonder about which kind of cargo VAMP4-mediated exocytosis would transport and what is the functional significance of this recycling.

Chronic downregulation strategies, like TeNT and shVAMP4 transfection, are often subjects to compensatory mechanisms. In addition, the strategy raises concerns about its specificity. Furthermore, long-term VAMP4 downregulation can produce up-stream effects, taking into account its role in retrograde EE to TGN traffic (Steegmaier et al. 1999; Mallard et al. 2002). To overcome the mentioned limitations, we proceeded to the acute block of VAMP2 and VAMP4 proteins by dilution of the TeNT and anti-VAMP4 IgG though the patch pipette while simultaneously imaging constitutive REs exocytosis. Once again, during TeNT infusion into the cells, there was no significant rundown in observed exocytosis, confirming our previous results. Unfortunately, technical complexity of the experiment have not allowed us to gather enough data to judge the statistical significance of the obtained effect after antiVAMP4 loading (for antiVAMP4 IgG n = 2 cells). Nevertheless, in both cells, the decrease in constitutive exocytosis was about 25%, which is comparable to the control cells loaded with normal intracellular solution. Once again, a number of controls should be performed to make sure that antibody diffusion in the time course of the experiment really inhibits VAMP4.

Consequences on synaptic transmission and plasticity

We applied the chronic downregulation strategies to explore the functional consequences of the long-term VAMPs block, notably on the basal excitatory transmission and synaptic potentiation. TeNT light chain transfection did not influence basal mEPSCs frequency or amplitude, that confirms results described in (Lledo et al. 1998) but contradicts described role in constitutive AMPARs recycling (Jurado et al. 2013). VAMP4 KD also did not influence measured mEPSCs frequency and amplitude. It may indicate that VAMP4-mediated postsynaptic exocytosis events are not involved in AMPARs supply for basal transmission maintenance. In addition, as ICC quantification showed only 50%

decrease of VAMP4 fluorescence in KD cells, it is possible that the generated shRNA was not sufficient to block fully VAMP4-mediated fusion. In this regards, it would be preferential to attempt VAMP4 downregulation with CRISPR/Cas9, a newly emerged system of selective gene inactivation (Incontro et al. 2014). Absence of effect on mEPSCs may also mean that VAMP4 mediated constitutive exocytosis bring other cargo than AMPARs.

To test directly the involvement of different VAMPs in postsynaptic exocytosis necessary for synaptic potentiation, we wanted to develop a robust protocol in cultured neurons. A classic method for LTP induction in culture is the so-called cLTP protocol. It is based on the short (3-5 min) exposure of neurons to glycine (100 μM) in a Mg^{2+}-free solution in presence of TTX, picrotoxin and strychnine (Park et al. 2006; Ahmad, J. S. Polepalli, et al. 2012; Passafaro et al. 2001; Kennedy et al. 2010). cLTP protocol would provide us with the possibility of real-time imaging of the exocytosis events during synaptic potentiation. During the course of my thesis work, I undertook many attempts to reproduce such cLTP protocol that would stably generate an increase in synaptic AMPARs levels in the cultured hippocampal neurons. Nonetheless, in my hands, the published protocol has never given a raise in synaptic surface AMPRs staining of more than 10-20%. This increase was not stable from one experiment to another and, additionally, it was far less than published increase of 50-100% (Ahmad et al. 2012; Jurado et al. 2013). Within the time framework of the presented project, I varied multiple parameters that could potentially influence cLTP robustness (see Table 1), but it did not affect the protocol's outcome. The instability of the obtained results may be due to the high sensitivity of the cultured neurons excitability to external factors like feeding media and temperature instabilities. To judge if the obtained 10-20% in synaptic surface AMPARs staining reflects real potentiation, a simultaneous electrophysiological measurements of the mEPSCs should be performed.

To overcome this inability to generate robust cLTP in dissociated cultures, I developed the preparation of organotypic hippocampal slices which display robust LTP in published work (Brachet et al. 2015) as well as in neighbour research teams in my laboratory. We performed the same downregulation strategy in this preparation in order explore the implication VAMPs in regulated

exocytosis for LTP expression. LTP was stimulated in synapses between CA3 and CA1 neurons of the hippocampal slices. Downregulation constructs were expressed in postsynaptic CA1 pyramidal neurons by the means of single cell electroporation to introduce plasmid only to the postsynaptic neurons and assure more physiological level of expression than in case of viral infection. As expected from previous explorations (Jurado et al. 2013; Park et al. 2004), TeNT expression impaired proper LTP. Yet, in the few VAMP4 KD neurons that we were able to record, shVAMP4 was able to abolish proper LTP manifestation. To conclude finally on this result, a rescue experiment should be performed. However, if this experimental tendency were confirmed, that would mean that VAMP4-driven exocytosis of endosomes would bring some LTP-associated cargo to the PM. alternatively, it could be an outcome of some up-stream effects in the endosomal trafficking, due to the chronic VAMP4 KD.

Conclusion

Thanks to an interdisciplinary approach combining techniques of cellular biology, videomicrosopy, immunocytochemistry with confocal and electron microscopy, biochemistry and image analysis, it was possible to study the role of vesicular SNARE proteins involved in somatodendritic REs exocytosis. I have examined VAMP proteins implication by directly observing the effect of chronic and acute downregulation of the candidate v-SNAREs on the somatodendritic REs exocytosis. I have also examined the functional implication of the two proteins, by assessing their involvement in basal neuronal transmission and plasticity.

The results obtained confirm the heterogeneity of the REs population undergoing constitutive exocytosis in neuronal postsynaptic compartments. According to our observations, VAMP2 regulates activity-dependent AMPARs delivery in the time of LTP expression, but not the constitutive AMPARs or RE exocytosis. VAMP4 undergoes postsynaptic exocytosis in neurons and potentially mediates a part of REs population fusion with the PM.

References

Advani, R.J. et al., 1998. Seven novel mammalian SNARE proteins localize to distinct membrane compartments. *Journal of Biological Chemistry*, 273(17), pp.10317–10324.

Advani, R.J. et al., 1999. VAMP-7 Mediates Vesicular Transport from Endosomes to Lysosomes. *The Journal of Cell Biology*, 146(4), pp.765–775.

Ahmad, M., Polepalli, J., et al., 2012. Postsynaptic Complexin Controls AMPA Receptor Exocytosis during LTP. *Neuron*, 73(2), pp.260–267.

Ahmad, M., Polepalli, J.S., et al., 2012. Postsynaptic complexin controls AMPA receptor exocytosis during LTP. *Neuron*, 73(2), pp.260–7.

Altar, C.A. et al., 1997. Anterograde transport of brain-derived neurotrophic factor and its role in the brain. *Nature*, 389(6653), pp.856–860.

Antonin, W. et al., 2002. Crystal structure of the endosomal SNARE complex reveals common structural principles of all SNAREs. *Nature Structural Biology*, 9(2), pp.107–111.

Arantes, R.M.E. & Andrews, N.W., 2006. A role for synaptotagmin VII-regulated exocytosis of lysosomes in neurite outgrowth from primary sympathetic neurons. *The Journal of Neuroscience*, 26(17), pp.4630–7.

Araque, A. et al., 1999. Tripartite synapses: glia, the unacknowledged partner. *Trends in Neurosciences*, 22(5), pp.208–215.

Araque, A. & Navarrete, M., 2010. Glial cells in neuronal network function. *Philosophical Transactions of the Royal Society B*, 365(1551), pp.2375–2381.

Ashby, M.C., Ibaraki, K. & Henley, J.M., 2004. It's green outside: Tracking cell surface proteins with pH-sensitive GFP. *Trends in Neurosciences*, 27(5), pp.257–261.

Atluri, P.P. & Regehr, W.G., 1998. Delayed release of neurotransmitter from cerebellar granule cells. *The Journal of Neuroscience*, 18(20), pp.8214–27.

Auld, D.S. & Robitaille, R., 2003. Glial Cells and Neurotransmission: An Inclusive View of Synaptic Function. *Neuron*, 40(2), pp.389–400.

Azevedo, F.A.C. et al., 2009. Equal numbers of neuronal and nonneuronal cells make the human brain an isometrically scaled-up primate brain. *The Journal of Comparative Neurology*, 513(5), pp.532–41.

Bacaj, T. et al., 2013. Synaptotagmin-1 and synaptotagmin-7 trigger synchronous and asynchronous phases of neurotransmitter release. *Neuron*, 80(4), pp.947–59.

Baker, R.W. & Hughson, F.M., 2016. Chaperoning SNARE assembly and disassembly. *Nature reviews. Molecular Cell Biology*.

Bal, M. et al., 2013. Reelin mobilizes a VAMP7-dependent synaptic vesicle pool and selectively augments spontaneous neurotransmission. *Neuron*, 80(4), pp.934–46.

Balaji, J. & Ryan, T. a, 2007. Single-vesicle imaging reveals that synaptic vesicle exocytosis and endocytosis are coupled by a single stochastic mode. *Proceedings of the National Academy of Sciences of the United States of America*, 104(51), pp.20576–81.

Bandeira, F., Lent, R. & Herculano-Houzel, S., 2009. Changing numbers of neuronal and

non-neuronal cells underlie postnatal brain growth in the rat. *Proceedings of the National Academy of Sciences of the United States of America*, 106(33), pp.14108–13.

Baumert, M. et al., 1989. Synaptobrevin: an integral membrane protein of 18,000 daltons present in small synaptic vesicles of rat brain. *The EMBO Journal*, 8(2), pp.379–84.

Bekkers, J.M. & Clements, J.D., 1999. Quantal amplitude and quantal variance of strontium-induced asynchronous EPSCs in rat dentate granule neurons. *The Journal of Physiology*, 516 (Pt 1, pp.227–248.

Blasi, J., Chapman, E.R., Link, E., et al., 1993. Botulinum neurotoxin A selectively cleaves the synaptic protein SNAP-25. *Nature*, 365(6442), pp.160–3.

Blasi, J., Chapman, E.R., Yamasaki, S., et al., 1993. Botulinum neurotoxin C1 blocks neurotransmitter release by means of cleaving HPC-1/syntaxin. *The EMBO journal*, 12(12), pp.4821–8.

Bliss, T. V & Collingridge, G.L., 1993. A synaptic model of memory: long-term potentiation in the hippocampus. *Nature*, 361(6407), pp.31–39.

Block, M.R. et al., 1988. Purification of an N-ethylmaleimide-sensitive protein catalyzing vesicular transport. *Proceedings of the National Academy of Sciences of the United States of America*, 85(21), pp.7852–6.

Bortolotto, Z. a. et al., 2011. Synaptic plasticity in the hippocampal slice preparation. *Current Protocols in Neuroscience*, (January), pp.1–26.

Bosch, M. & Hayashi, Y., 2012. Structural plasticity of dendritic spines. *Current Opinion in Neurobiology*, 22(3), pp.383–388.

Brachet, A. et al., 2015. LTP-triggered cholesterol redistribution activates Cdc42 and drives AMPA receptor synaptic delivery. *Journal of Cell Biology*, 208(6), pp.791–806.

Brandhorst, D. et al., 2006. Homotypic fusion of early endosomes: SNAREs do not determine fusion specificity. *Proceedings of the National Academy of Sciences of the United States of America*, 103(8), pp.2701–6.

Bredt, D.S. & Nicoll, R.A., 2003. AMPA Receptor Trafficking at Excitatory Synapses. *Neuron*, 40(2), pp.361–379.

Brown, T.C. et al., 2007. Functional compartmentalization of endosomal trafficking for the synaptic delivery of AMPA receptors during long-term potentiation. *The Journal of neuroscience : the official journal of the Society for Neuroscience*, 27(48), pp.13311–13315.

Brunger, A.T. et al., 1998. Crystal structure of a SNARE complex involved in synaptic exocytosis at 2.4 Å resolution. *Nature*, 395(6700), pp.347–353.

Brunger, A.T. et al., 1999. Folding intermediates of SNARE complex assembly. *Nature Structural Biology*, 6(2), pp.117–123.

Burgo, A. et al., 2012. A Molecular Network for the Transport of the TI-VAMP/VAMP7 Vesicles from Cell Center to Periphery. *Developmental Cell*, 23(1), pp.166–180.

Calloway, N. et al., 2015. The active-zone protein Munc13 controls the use-dependence of presynaptic voltage-gated calcium channels. *eLife*, 4.

Castillo, P.E., 2012. Presynaptic LTP and LTD of Excitatory and Inhibitory Synapses.

Cold Spring Harbor Perspectives in Biology, 4(2), pp.a005728–a005728.

Chaineau, M., Danglot, L. & Galli, T., 2009. Multiple roles of the vesicular-SNARE TI-VAMP in post-Golgi and endosomal trafficking. *FEBS Letters*, 583(23), pp.3817–3826.

Chapman, E.R., 2002. Synaptotagmin: A Ca2+ sensor that triggers exocytosis? *Nature Reviews Molecular Cell Biology*, 3(7), pp.498–508.

Chen, C. & Regehr, W.G., 1999. Contributions of residual calcium to fast synaptic transmission. *The Journal of neuroscience : the official journal of the Society for Neuroscience*, 19(15), pp.6257–66.

Chen, H.X. et al., 1999. Requirements for LTP induction by pairing in hippocampal CA1 pyramidal cells. *Journal of neurophysiology*, 82(2), pp.526–32.

Chicka, M.C. et al., 2016. Role of Munc13-4 as a Ca2+-dependent tether during platelet secretion. *The Biochemical journal*, 473(5), pp.627–39.

Clary, D.O., Griff, I.C. & Rothman, J.E., 1990. SNAPs, a family of NSF attachment proteins involved in intracellular membrane fusion in animals and yeast. *Cell*, 61(4), pp.709–21.

Cocucci, E. et al., 2008. The regulated exocytosis of enlargeosomes is mediated by a SNARE machinery that includes VAMP4. *Journal of Cell Science*, 121(Pt 18), pp.2983–2991.

Collingridge, G.L., Isaac, J.T.R. & Wang, Y.T., 2004. Receptor trafficking and synaptic plasticity. *Nature Reviews Neuroscience*, 5(12), pp.952–962.

Cooney, J.R. et al., 2002. Endosomal compartments serve multiple hippocampal dendritic spines from a widespread rather than a local store of recycling membrane. *The Journal of Neuroscience*, 22(6), pp.2215–2224.

Crawford, D.C. & Kavalali, E.T., 2015. Molecular Underpinnings of Synaptic Vesicle Pool Heterogeneity. *Traffic (Copenhagen, Denmark)*.

Croft, W., Dobson, K.L. & Bellamy, T.C., 2015. Plasticity of Neuron-Glial Transmission: Equipping Glia for Long-Term Integration of Network Activity. *Neural Plasticity*, 2015, p.765792.

Cummings, D.D., Wilcox, K.S. & Dichter, M.A., 1996. Calcium-dependent paired-pulse facilitation of miniature EPSC frequency accompanies depression of EPSCs at hippocampal synapses in culture. *The Journal of Neuroscience*, 16(17), pp.5312–23.

Danglot, L. et al., 2012. Absence of TI-VAMP/Vamp7 Leads to Increased Anxiety in Mice. *Journal of Neuroscience*, 32(6), pp.1962–1968.

Daste, F., Galli, T. & Tareste, D., 2015. Structure and function of longin SNAREs. *Journal of cell science*, 128(23), pp.4263–4272.

Deák, F. et al., 2006. Structural determinants of synaptobrevin 2 function in synaptic vesicle fusion. *The Journal of neuroscience : the official journal of the Society for Neuroscience*, 26(25), pp.6668–76.

Deák, F. et al., 2004. Synaptobrevin is essential for fast synaptic-vesicle endocytosis. *Nature cell biology*, 6(11), pp.1102–1108.

Dean, C. et al., 2009. Synaptotagmin-IV modulates synaptic function and long-term potentiation by regulating BDNF release. *Nature neuroscience*, 12(6), pp.767–76.

Denker, A. & Rizzoli, S.O., 2010. Synaptic vesicle pools: An update. *Frontiers in*

Synaptic Neuroscience, 2(OCT), pp.1–12.

Dulubova, I. et al., 1999. A conformational switch in syntaxin during exocytosis: role of munc18. *The EMBO Journal*, 18(16), pp.4372–82.

Dulubova, I. et al., 2007. Munc18-1 binds directly to the neuronal SNARE complex. *Proceedings of the National Academy of Sciences of the United States of America*, 104(8), pp.2697–702.

Egger, V., Svoboda, K. & Mainen, Z.F., 2003. Mechanisms of lateral inhibition in the olfactory bulb: efficiency and modulation of spike-evoked calcium influx into granule cells. *The Journal of Neuroscience*, 23(20), pp.7551–8.

Ehlers, M.D. et al., 2000. Reinsertion or Degradation of AMPA Receptors Determined by Activity-Dependent Endocytic Sorting. *Neuron*, 28(2), pp.511–525.

Esteves da Silva, M. et al., 2015. Positioning of AMPA Receptor-Containing Endosomes Regulates Synapse Architecture. *Cell Reports*, 13, pp.933–943.

Falkenburger, B.H., Barstow, K.L. & Mintz, I.M., 2001. Dendrodendritic Inhibition Through Reversal of Dopamine Transport. *Science*, 293(5539).

Famiglietti, E. V., 1970. Dendro-dendritic synapses in the lateral geniculate nucleus of the cat. *Brain Research*, 20(2), pp.181–191.

Fasshauer, D. et al., 1998. Conserved structural features of the synaptic fusion complex: SNARE proteins reclassified as Q- and R-SNAREs. *Proceedings of the National Academy of Sciences of the United States of America*, 95(26), pp.15781–6.

Fasshauer, D. & Margittai, M., 2004. A Transient N-terminal Interaction of SNAP-25 and Syntaxin Nucleates SNARE Assembly. *Journal of Biological Chemistry*, 279(9), pp.7613–7621.

Fatt, P. & Katz, B., 1952. SPONTANEOUS SUBTHRESHOLD ACTIVITY AT MOTOR NERVE ENDINGS. *J. Physiol*, 117, pp.109–128.

Feng, D. et al., 2002. Subcellular distribution of 3 functional platelet SNARE proteins: human cellubrevin, SNAP-23, and syntaxin 2. *Blood*, 99(11), pp.4006–14.

Fernández-Chacón, R. et al., 2001. Synaptotagmin I functions as a calcium regulator of release probability. *Nature*, 410(6824), pp.41–49.

Fortin, G.D. et al., 2006. Basal somatodendritic dopamine release requires snare proteins. *Journal of Neurochemistry*, 96(6), pp.1740–1749.

Galli, T. et al., 1998. A Novel Tetanus Neurotoxin-insensitive Vesicle-associated Membrane Protein in SNARE Complexes of the Apical Plasma Membrane of Epithelial Cells. *Molecular Biology of the Cell*, 9(6), pp.1437–1448.

Galli, T. et al., 1994. Tetanus toxin-mediated cleavage of cellubrevin impairs exocytosis of transferrin receptor-containing vesicles in CHO cells. *The Journal of Cell Biology*, 125(5), pp.1015–24.

Ganley, I.G., Espinosa, E. & Pfeffer, S.R., 2008. A syntaxin 10–SNARE complex distinguishes two distinct transport routes from endosomes to the trans-Golgi in human cells. *The Journal of Cell Biology*, 180(1).

Geiger, J.R. & Jonas, P., 2000. Dynamic control of presynaptic Ca(2+) inflow by fast-inactivating K(+) channels in hippocampal mossy fiber boutons. *Neuron*, 28(3), pp.927–39.

Geppert, M. et al., 1994. Synaptotagmin I: a major Ca2+ sensor for transmitter release at

a central synapse. *Cell*, 79(4), pp.717–27.

Ghosh, D. et al., 2016. VAMP7 regulates constitutive membrane incorporation of the cold-activated channel TRPM8. *Nature communications*, 7, p.10489.

Gordon, D.E. et al., 2010. A Targeted siRNA Screen to Identify SNAREs Required for Constitutive Secretion in Mammalian Cells. *Traffic*, 11(9), pp.1191–1204.

Grosse, G. et al., 1999. SNAP-25 requirement for dendritic growth of hippocampal neurons. *Journal of Neuroscience Research*, 56(5), pp.539–546.

Gupton, S.L. & Gertler, F.B., 2010. Integrin signaling switches the cytoskeletal and exocytic machinery that drives neuritogenesis. *Developmental Cell*, 18(5), pp.725–736.

Haas, K. et al., 2001. Single-Cell Electroporation Neurotechnique for Gene Transfer In Vivo. *Neuron*, 29, pp.583–591.

Hanson, P.I. et al., 1997. Structure and Conformational Changes in NSF and Its Membrane Receptor Complexes Visualized by Quick-Freeze/Deep-Etch Electron Microscopy. *Cell*, 90(3), pp.523–535.

Harada, K., Kamiya, T. & Tsuboi, T., 2015. Gliotransmitter Release from Astrocytes: Functional, Developmental, and Pathological Implications in the Brain. *Frontiers in Neuroscience*, 9, p.499.

Harata, N. et al., 2001. Visualizing recycling synaptic vesicles in hippocampal neurons by FM 1-43 photoconversion. *Proceedings of the National Academy of Sciences of the United States of America*, 98(22), pp.12748–53.

Harms, K.J. & Craig, A.M., 2005. Synapse composition and organization following chronic activity blockade in cultured hippocampal neurons. *Journal of Comparative Neurology*, 490(1), pp.72–84.

Hartmann, M. et al., 2001. Synaptic secretion of BDNF after high-frequency stimulation of glutamatergic synapses. *The EMBO Journal*, 20(21), pp.5887–97.

Hasan, N., Corbin, D. & Hu, C., 2010. Fusogenic pairings of vesicle-associated membrane proteins (VAMPs) and plasma membrane t-SNAREs - VAMP5 as the exception. *PLoS ONE*, 5(12), pp.1–12.

Hata, Y., Slaughter, C.A. & Südhof, T.C., 1993. Synaptic vesicle fusion complex contains unc-18 homologue bound to syntaxin. *Nature*, 366(6453), pp.347–351.

HIRATA, Y., 1964. Some Observations on the Fine Structure of the Synapses in the Olfactory Bulb of the Mouse, with Particular Reference to the Atypical Synaptic Configurations. *Archivum Histologicum Japonicum*, 24(3), pp.293–302.

Hong, W., 2005. SNAREs and traffic. *Biochimica et Biophysica Acta - Molecular Cell Research*, 1744(2), pp.120–144.

Horton, A.C. et al., 2005. Polarized secretory trafficking directs cargo for asymmetric dendrite growth and morphogenesis. *Neuron*, 48(5), pp.757–771.

Horton, A.C. et al., 2005. Polarized secretory trafficking directs cargo for asymmetric dendrite growth and morphogenesis. *Neuron*, 48(5), pp.757–71.

Hua, Z. et al., 2011. v-SNARE Composition Distinguishes Synaptic Vesicle Pools. *Neuron*, 71(3), pp.474–487.

Huganir, R.L. & Nicoll, R. a, 2013. AMPARs and synaptic plasticity: the last 25 years. *Neuron*, 80(3), pp.704–17.

Huynh, K.K. et al., 2007. Fusion, fission, and secretion during phagocytosis. *Physiology (Bethesda, Md.)*, 22, pp.366–72.

Incontro, S. et al., 2014. Efficient, Complete Deletion of Synaptic Proteins using CRISPR. *Neuron*, 83(5), pp.1051–1057.

Isaac, J.T.R. et al., 1995. Evidence for silent synapses: Implications for the expression of LTP. *Neuron*, 15(2), pp.427–434.

Isaacson, J.S., 2001. Mechanisms governing dendritic gamma-aminobutyric acid (GABA) release in the rat olfactory bulb. *Proceedings of the National Academy of Sciences of the United States of America*, 98(1), pp.337–42.

Jaafari, N., Henley, J.M. & Hanley, J.G., 2012. PICK1 Mediates Transient Synaptic Expression of GluA2-Lacking AMPA Receptors during Glycine-Induced AMPA Receptor Trafficking. *Journal of Neuroscience*, 32(34), pp.11618–11630.

Jackman, S.L. et al., 2016. The calcium sensor synaptotagmin 7 is required for synaptic facilitation. *Nature*, 529(7584), pp.88–91.

Jahn, R., Lang, T. & Südhof, T.C., 2003. Membrane fusion. *Cell*, 112(3), pp.519–533.

Jahn, R. & Scheller, R.H., 2006. SNAREs — engines for membrane fusion. *Nature Reviews Molecular Cell Biology*, 7(9), pp.631–643.

Johnson, J.L. et al., 2016. Munc13-4 Is a Rab11-binding Protein That Regulates Rab11-positive Vesicle Trafficking and Docking at the Plasma Membrane. *The Journal of Biological Chemistry*, 291(7), pp.3423–38.

Jović, M. et al., 2014. Endosomal sorting of VAMP3 is regulated by PI4K2A. *Journal of cell science*, 127(Pt 17), pp.3745–56.

Jullié, D., Choquet, D. & Perrais, D., 2014. Recycling endosomes undergo rapid closure of a fusion pore on exocytosis in neuronal dendrites. *The Journal of Neuroscience*, 34(33), pp.11106–18.

Jurado, S. et al., 2013. LTP Requires a Unique Postsynaptic SNARE Fusion Machinery. *Neuron*, 77(3), pp.542–58.

Kaech, S. & Banker, G., 2006. Culturing hippocampal neurons. *Nature protocols*, 1, pp.2406–2415.

Kaeser, P.S. & Regehr, W.G., 2014. Molecular mechanisms for synchronous, asynchronous, and spontaneous neurotransmitter release. *Annual Review of Physiology*, 76, pp.333–63.

Katz, B., Miledi, R. & Miledi, B., 1967. A STUDY OF SYNAPTIC TRANSMISSION IN THE ABSENCE OF NERVE IMPULSES. *The Journal of Physiology*, 192, pp.407–436.

Kennedy, M.J. et al., 2010. Syntaxin-4 defines a domain for activity-dependent exocytosis in dendritic spines. *Cell*, 141(3), pp.524–35.

Kennedy, M.J. & Ehlers, M.D., 2011. Mechanisms and function of dendritic exocytosis. *Neuron*, 69(5), pp.856–75.

Kim, S.H. & Ryan, T. a, 2010. CDK5 serves as a major control point in neurotransmitter release. *Neuron*, 67(5), pp.797–809.

Van der Kloot, W. & Molgó, J., 1993. Facilitation and delayed release at about 0 degree C at the frog neuromuscular junction: effects of calcium chelators, calcium transport inhibitors, and okadaic acid. *Journal of Neurophysiology*, 69(3), pp.717–29.

Kopec, C.D. et al., 2006. Glutamate Receptor Exocytosis and Spine Enlargement during Chemically Induced Long-Term Potentiation. *Journal of Neuroscience*, 26(7).

Lagier, S. et al., 2007. GABAergic inhibition at dendrodendritic synapses tunes gamma oscillations in the olfactory bulb. *Proceedings of the National Academy of Sciences of the United States of America*, 104(17), pp.7259–64.

Lan, J.Y. et al., 2001. Protein kinase C modulates NMDA receptor trafficking and gating. *Nat Neurosci*, 4(4), pp.382–390.

Lau, C.G. et al., 2010. SNAP-25 is a target of protein kinase C phosphorylation critical to NMDA receptor trafficking. *The Journal of Neuroscience*, 30(1), pp.242–254.

Lin, D.-T. et al., 2009. Regulation of AMPA receptor extrasynaptic insertion by 4.1N, phosphorylation and palmitoylation. *Nature Neuroscience*, 12(7), pp.879–887.

Lin, R.C. et al., 1997. Structural Organization of the Synaptic Exocytosis Core Complex. *Neuron*, 19(5), pp.1087–1094.

Liu, Y., Sugiura, Y. & Lin, W., 2011. The role of synaptobrevin1/VAMP1 in Ca2+-triggered neurotransmitter release at the mouse neuromuscular junction. *The Journal of Physiology*, 589(Pt 7), pp.1603–1618.

Lledo, P., 1998. Postsynaptic Membrane Fusion and Long-Term Potentiation. *Science*, 279(5349), pp.399–403.

Lledo, P.M. et al., 1998. Postsynaptic membrane fusion and long-term potentiation. *Science (New York, N.Y.)*, 279(January), pp.399–403.

Llinás, R.R. & Heuser, J., 1977. Depolarization-release coupling systems in neurons. *Neurosciences Research Program bulletin*, 15(4), pp.555–687.

Lou, X. & Shin, Y.-K., 2016. SNARE zippering. *Bioscience Reports*, 36(3).

Lu, W. et al., 2001. Activation of Synaptic NMDA Receptors Induces Membrane Insertion of New AMPA Receptors and LTP in Cultured Hippocampal Neurons. *Neuron*, 29, pp.243–254.

Lüscher, C. et al., 1999. Role of AMPA Receptor Cycling in Synaptic Transmission and Plasticity. *Neuron*, 24(3), pp.649–658.

Lüscher, C. & Malenka, R.C., 2012. NMDA receptor-dependent long-term potentiation and long-term depression (LTP/LTD). *Cold Spring Harbor Perspectives in Biology*, 4(6), pp.1–16.

Malenka, R.C. et al., 2004. LTP and LTD. *Neuron*, 44(1), pp.5–21.

Malenka, R.C. et al., 1994. Synaptic plasticity in the hippocampus: LTP and LTD. *Cell*, 78(4), pp.535–538.

Malinow, R. & Malenka, R.C., 2002. AMPA R ECEPTOR T RAFFICKING AND S YNAPTIC P LASTICITY. *Annual Review of Neuroscience*, 25(1), pp.103–126.

Mallard, F. et al., 2002. Early/recycling endosomes-to-TGN transport involves two SNARE complexes and a Rab6 isoform. *Journal of Cell Biology*, 156(4), pp.653–664.

Marra, V. et al., 2012. A preferentially segregated recycling vesicle pool of limited size supports neurotransmission in native central synapses. *Neuron*, 76(3), pp.579–89.

Martinez-Arca, S. et al., 2001. A common exocytotic mechanism mediates axonal and dendritic outgrowth. *The Journal of Neuroscience*, 21(11), pp.3830–3838.

Martinez-Arca, S., Alberts, P., Zahraoui, A., et al., 2000. Role of tetanus neurotoxin insensitive vesicle-associated membrane protein (TI-VAMP) in vesicular transport mediating neurite outgrowth. *Journal of Cell Biology*, 149(4), pp.889–899.

Martinez-Arca, S., Alberts, P. & Galli, T., 2000. Clostridial neurotoxin-insensitive vesicular SNAREs in exocytosis and endocytosis. *Biology of the Cell*, 92, pp.1996–2000.

Maxfield, F.R. & McGraw, T.E., 2004. Endocytic recycling. *Nature Reviews Molecular Cell Biology*, 5(2), pp.121–132.

Maximov, A. & Südhof, T.C., 2005. Autonomous function of synaptotagmin 1 in triggering synchronous release independent of asynchronous release. *Neuron*, 48(4), pp.547–554.

Menna, E. et al., 2013. Eps8 controls dendritic spine density and synaptic plasticity through its actin-capping activity. *The EMBO Journal*, 32(12), pp.1730–44.

Miesenbock, G., De Angelis, D.A. & Rothman, J.E., 1998. Visualizing secretion and synaptic transmission with pH-sensitive green fluorescent proteins. *Nature*, 394(9).

Misura, K.M.S., Scheller, R.H. & Weis, W.I., 2000. Three-dimensional structure of the neuronal-Sec1–syntaxin 1a complex. *Nature*, 404(6776), pp.355–362.

Mohrmann, R., Dhara, M. & Bruns, D., 2015. Complexins: small but capable. *CMLS*, 72(22), pp.4221–35.

Nabavi, S. et al., 2014. Engineering a memory with LTD and LTP. *Nature*, 511(7509), pp.348–352.

Newpher, T.M. & Ehlers, M.D., 2008. Glutamate Receptor Dynamics in Dendritic Microdomains. *Neuron*, 58(4), pp.472–497.

Nicholson-Fish, J.C. et al., 2015. VAMP4 Is an Essential Cargo Molecule for Activity-Dependent Bulk Endocytosis. *Neuron*, 88(5), p.973.

Olofsson, J. et al., 2003. Single-cell electroporation. *Current Opinion in Biotechnology*, 14(1), pp.29–34.

Pang, Z.P. et al., 2006. A Gain-of-Function Mutation in Synaptotagmin-1 Reveals a Critical Role of Ca2+-Dependent Soluble N-Ethylmaleimide-Sensitive Factor Attachment Protein Receptor Complex Binding in Synaptic Exocytosis. *Journal of Neuroscience*, 26(48).

Park, M. et al., 2006. Plasticity-induced growth of dendritic spines by exocytic trafficking from recycling endosomes. *Neuron*, 52(5), pp.817–830.

Park, M. et al., 2004. Recycling endosomes supply AMPA receptors for LTP. *Science*, 305, pp.1972–1975.

Parpura, V. et al., 1994. Glutamate-mediated astrocyte-neuron signalling. *Nature*, 369(6483), pp.744–7.

Passafaro, M., Piëch, V. & Sheng, M., 2001. Subunit-specific temporal and spatial patterns of AMPA receptor exocytosis in hippocampal neurons. *Nature Neuroscience*, 4(9), pp.917–926.

Patterson, M.A., Szatmari, E.M. & Yasuda, R., 2010. AMPA receptors are exocytosed in stimulated spines and adjacent dendrites in a Ras-ERK-dependent manner during long-term potentiation. *Proceedings of the National Academy of Sciences of the United States of America*, 107(36), pp.15951–6.

Peden, A.A., Park, G.Y. & Scheller, R.H., 2001. The Di-leucine Motif of Vesicle-associated Membrane Protein 4 Is Required for Its Localization and AP-1 Binding. *Journal of Biological Chemistry*, 276(52), pp.49183–49187.

Pellizzari, R. et al., 1999. Tetanus and botulinum neurotoxins: mechanism of action and therapeutic uses. *Philosophical Transactions of the Royal Society of London. Series B, Biological sciences*, 354(1381), pp.259–268.

Perea, G. & Araque, A., 2010. GLIA modulates synaptic transmission. *Brain Research Reviews*, 63(1), pp.93–102.

Pernía-Andrade, A.J. et al., 2012. A deconvolution-based method with high sensitivity and temporal resolution for detection of spontaneous synaptic currents in vitro and in vivo. *Biophysical Journal*, 103(7), pp.1429–1439.

Petrini, E.M. et al., 2009. Endocytic trafficking and recycling maintain a pool of mobile surface AMPA receptors required for synaptic potentiation. *Neuron*, 63(1), pp.92–105.

Pocard, T. et al., 2007. Distinct v-SNAREs regulate direct and indirect apical delivery in polarized epithelial cells. *Journal of Cell Science*, 120, pp.3309–3320.

Proux-Gillardeaux, V., Gavard, J., et al., 2005. Tetanus neurotoxin-mediated cleavage of cellubrevin impairs epithelial cell migration and integrin-dependent cell adhesion. *Proceedings of the National Academy of Sciences of the United States of America*, 102(18), pp.6362–7.

Proux-Gillardeaux, V., Rudge, R. & Galli, T., 2005. The Tetanus Neurotoxin-Sensitive and Insensitive Routes to and from the Plasma Membrane: Fast and Slow Pathways? *Traffic*, 6(5), pp.366–373.

Raingo, J. et al., 2012. VAMP4 directs synaptic vesicles to a pool that selectively maintains asynchronous neurotransmission. *Nature Neuroscience*, 15(5), pp.738–745.

Rall, W. et al., 1966. Dendrodendritic synaptic pathway for inhibition in the olfactory bulb. *Experimental Neurology*, 14(1), pp.44–56.

Rall, W. & Shepherd, G.M., 1968. Theoretical reconstruction of field potentials and dendrodendritic synaptic interactions in olfactory bulb. *Journal of Neurophysiology*, 31(6), pp.884–915.

Ramirez, D.M.O. et al., 2014. Vti1a identifies a vesicle pool that preferentially recycles at rest and maintains spontaneous neurotransmission. *NIH*, 60(1), pp.51–52.

Raptis, A. et al., 2005. Distribution of synaptobrevin/VAMP 1 and 2 in rat brain. *Journal of Chemical Neuroanatomy*, 30(4), pp.201–211.

Reim, K. et al., 2001. Complexins Regulate a Late Step in Ca2+-Dependent Neurotransmitter Release. *Cell*, 104(1), pp.71–81.

Rice, M.E. & Patel, J.C., 2015. Somatodendritic dopamine release: recent mechanistic insights. *Philosophical Transactions of the Royal Society of London B: Biological Sciences*, 370(1672).

Rizzoli, S.O. & Betz, W.J., 2005. Synaptic vesicle pools. *Nature Reviews. Neuroscience*, 6(1), pp.57–69.

Rossetto, O. et al., 1996. VAMP/synaptobrevin isoforms 1 and 2 are widely and differentially expressed in nonneuronal tissues. *The Journal of Cell Biology*, 132(1–2), pp.167–79.

Sahlender, D.A., Savtchouk, I. & Volterra, A., 2014. What do we know about gliotransmitter release from astrocytes? *Philosophical transactions of the Royal Society of London. Series B, Biological sciences*, 369(1654), p.20130592.

Sampo, B. et al., 2003. Two distinct mechanisms target membrane proteins to the axonal surface. *Neuron*, 37(4), pp.611–624.

Sankaranarayanan, S. et al., 2000. The Use of pHluorins for Optical Measurements of Presynaptic Activity. *Biophysical Journal*, 79(4), pp.2199–2208.

Schiavo, G. et al., 1992. Tetanus and botulinum-B neurotoxins block neurotransmitter release by proteolytic cleavage of synaptobrevin. *Nature*, 359(6398), pp.832–835.

Schikorski, T. & Stevens, C.F., 2001. Morphological correlates of functionally defined synaptic vesicle populations. *Nature Neuroscience*, 4(4), pp.391–395.

Schikorski, T. & Stevens, C.F., 1997. Quantitative ultrastructural analysis of hippocampal excitatory synapses. *The Journal of Neuroscience*, 17(15), pp.5858–5867.

Schoch, S. et al., 2001. SNARE Function Analyzed in Synaptobrevin/VAMP Knockout Mice. *Science*, 294(5544), pp.1117–1122.

Schoch, S. et al., 2001. SNARE Function Analyzed in Synaptobrevin/VAMP Knockout Mice. *Science*, 294(5544).

Shanks, M.F. & Powell, T.P.S., 1981. An electron microscopic study of the termination of thalamocortical fibres in areas 3b, 1 and 2 of the somatic sensory cortex in the monkey. *Brain Research*, 218(1), pp.35–47.

Shen, J. et al., 2007. Selective Activation of Cognate SNAREpins by Sec1/Munc18 Proteins. *Cell*, 128(1), pp.183–195.

Shepherd, J.D. & Huganir, R.L., 2007. The cell biology of synaptic plasticity: AMPA receptor trafficking. *Annual Review of Cell and Developmental Biology*, 23, pp.613–643.

Shin, J. et al., 2014. Multiple conformations of a single SNAREpin between two nanodisc membranes reveal diverse pre-fusion states. *Biochemical Journal*, 459(1).

Shin, O.-H. et al., 2010. Munc13 C2B domain is an activity-dependent Ca2+ regulator of synaptic exocytosis. *Nature Structural & Molecular Biology*, 17(3), pp.280–8.

Siksou, L. et al., 2007. Three-Dimensional Architecture of Presynaptic Terminal Cytomatrix. *Journal of Neuroscience*, 27(26), pp.6868–6877.

Simons, M. & Raposo, G., 2009. Exosomes--vesicular carriers for intercellular communication. *Current Opinion in Cell Biology*, 21(4), pp.575–81.

Söllner, T. et al., 1993. SNAP receptors implicated in vesicle targeting and fusion. *Nature*, 362(6418), pp.318–324.

Spacek, J. & Harris, K.M., 1997. Three-dimensional organization of smooth endoplasmic reticulum in hippocampal CA1 dendrites and dendritic spines of the immature and mature rat. *The Journal of Neuroscience*, 17(1), pp.190–203.

Steegmaier, M. et al., 1999. Vesicle-associated Membrane Protein 4 is Implicated in Trans -Golgi Network Vesicle Trafficking. *Molecular Biology of the Cell*, 10(June), pp.1957–1972.

Stein, A. et al., 2009. Helical extension of the neuronal SNARE complex into the membrane. *Nature*, 460(7254), pp.525–528.

Stenmark, H., 2009. Rab GTPases as coordinators of vesicle traffic. *Nature reviews. Molecular Cell Biology*, 10(8), pp.513–25.

Stoppini, L., Buchs, P.-A. & Muller, D., 1991. A simple method for organotypic cultures of nervous tissue. *Journal of Neuroscience Methods*, 37, pp.173–182.

Südhof, T.C., 2013a. A molecular machine for neurotransmitter release: synaptotagmin and beyond. *Nature Medicine*, 19(10), pp.1227–1231.

Südhof, T.C., 2013b. A molecular machine for neurotransmitter release: synaptotagmin and beyond. *Nature Medicine*, 19(10), pp.1227–1231.

Südhof, T.C., 2013c. Neurotransmitter release: the last millisecond in the life of a synaptic vesicle. *Neuron*, 80(3), pp.675–90.

Südhof, T.C., 2004. THE SYNAPTIC VESICLE CYCLE. *Annual Review of Neuroscience*, 27(1), pp.509–547.

Südhof, T.C. et al., 2000. The Synaptic VesicleCycle Revisited. *Neuron*, 28(2), pp.317–320.

Südhof, T.C. & Rothman, J.E., 2009. Membrane fusion: grappling with SNARE and SM proteins. *Science*, 323(5913), pp.474–7.

Suh, Y.H. et al., 2010. A neuronal role for SNAP-23 in postsynaptic glutamate receptor trafficking. *Nat Neurosci*, 13(3), pp.338–343.

Takamori, S. et al., 2006. Molecular Anatomy of a Trafficking Organelle. *Cell*, 127(4), pp.831–846.

Tang, J. et al., 2006. A Complexin/Synaptotagmin 1 Switch Controls Fast Synaptic Vesicle Exocytosis. *Cell*, 126(6), pp.1175–1187.

Tao, H. et al., 2000. Selective presynaptic propagation of long-term potentiation in defined neural networks. *The Journal of Neuroscience*, 20(9), pp.3233–3243.

Tojima, T. et al., 2007. Attractive axon guidance involves asymmetric membrane transport and exocytosis in the growth cone. *Nature Neuroscience*, 10(1), pp.58–66.

Tojima, T. et al., 2011. Second messengers and membrane trafficking direct and organize growth cone steering. *Nature reviews. Neuroscience*, 12(4), pp.191–203.

Tran, T.H.T., Zeng, Q. & Hong, W., 2007. VAMP4 cycles from the cell surface to the trans-Golgi network via sorting and recycling endosomes. *Journal of Cell Science*, 120(Pt 6), pp.1028–1041.

Trimble, W.S., Cowan, D.M. & Scheller, R.H., 1988. VAMP-1: a synaptic vesicle-associated integral membrane protein. *Proceedings of the National Academy of Sciences of the United States of America*, 85(12), pp.4538–42.

Tsien, R.Y., 1998. THE GREEN FLUORESCENT PROTEIN. *Annu. Rev. Biochem*, 67, pp.509–44.

Ventura, R. & Harris, K.M., 1999. Three-dimensional relationships between hippocampal synapses and astrocytes. *The Journal of Neuroscience*, 19(16), pp.6897–906.

Verhage, M. et al., 2000. Synaptic Assembly of the Brain in the Absence of Neurotransmitter Secretion. *Science*, 287(5454).

Wang, C.-C. et al., 2004. A role of VAMP8/endobrevin in regulated exocytosis of pancreatic acinar cells. *Developmental Cell*, 7(3), pp.359–71.

Wang, C.-C. et al., 2007. VAMP8/endobrevin as a general vesicular SNARE for regulated exocytosis of the exocrine system. *Molecular Biology of the Cell*, 18(3), pp.1056–63.

Wang, Z. et al., 2008. Myosin Vb Mobilizes Recycling Endosomes and AMPA Receptors for Postsynaptic Plasticity. *Cell*, 135(3), pp.535–548.

Washbourne, P., 2004. Cycling of NMDA Receptors during Trafficking in Neurons before Synapse Formation. *Journal of Neuroscience*, 24(38), pp.8253–8264.

Watanabe, S. et al., 2013. Ultrafast endocytosis at mouse hippocampal synapses. *Nature*, 504(7479), pp.242–7.

Weaver, J.C. & Chizmadzhev, Y.A., 1996. Theory of electroporation: A review. *Bioelectrochemistry and Bioenergetics*, 41(2), pp.135–160.

Williams, D. & Pessin, J.E., 2008. Mapping of R-SNARE function at distinct intracellular GLUT4 trafficking steps in adipocytes. *Journal of Cell Biology*, 180(2), pp.375–387.

Wisco, D. et al., 2003. Uncovering multiple axonal targeting pathways in hippocampal neurons. *The Journal of Cell Biology*, 162(7).

Wong, S.H. et al., 1998. Endobrevin, a novel synaptobrevin/VAMP-like protein preferentially associated with the early endosome. *Molecular Biology of the Cell*, 9(6), pp.1549–63.

Wong, Y.-H. et al., 2015. Activity-dependent BDNF release via endocytic pathways is regulated by synaptotagmin-6 and complexin. *Proceedings of the National Academy of Sciences of the United States of America*, 112(32), pp.E4475-84.

Woolfrey, K.M., Sanderson, J.L. & Dell'Acqua, M.L., 2015. The Palmitoyl Acyltransferase DHHC2 Regulates Recycling Endosome Exocytosis and Synaptic Potentiation through Palmitoylation of AKAP79/150. *Journal of Neuroscience*, 35(2), pp.442–456.

Xu, J., Mashimo, T. & Südhof, T.C., 2007. Synaptotagmin-1, -2, and -9: Ca2+ Sensors for Fast Release that Specify Distinct Presynaptic Properties in Subsets of Neurons. *Neuron*, 54(4), pp.567–581.

Yang, T.T., Cheng, L. & Kain, S.R., 1996. Optimized codon usage and chromophore mutations provide enhanced sensitivity with the green fluorescent protein. *Nucleic Acids Research*, 24(22), pp.4592–4593.

Yudowski, G. a et al., 2007. Real-time imaging of discrete exocytic events mediating surface delivery of AMPA receptors. *The Journal of Neuroscience*, 27(41), pp.11112–21.

Yudowski, G. a, Puthenveedu, M. a & von Zastrow, M., 2006. Distinct modes of regulated receptor insertion to the somatodendritic plasma membrane. *Nature Neuroscience*, 9(5), pp.622–7.

Zeng, Q. et al., 2003. The cytoplasmic domain of Vamp4 and Vamp5 is responsible for their correct subcellular targeting: The N-terminal extension of Vamp4 contains a dominant autonomous targeting signal for the trans-Golgi network. *Journal of Biological Chemistry*, 278(25), pp.23046–23054.

Zhu, Y., Xu, J. & Heinemann, S.F., 2009. Two pathways of synaptic vesicle retrieval revealed by single-vesicle imaging. *Neuron*, 61(3), pp.397–411.

Zwilling, D. et al., 2007. Early endosomal SNAREs form a structurally conserved SNARE complex and fuse liposomes with multiple topologies. *The EMBO Journal*, 26(1), pp.9–18.

Annex : Résumé en français

L'implication des protéines SNARE dans l'exocytose postsynaptique

L'étude présentée dans ce travail a été motivée par la nécessité de comprendre les mécanismes régissant les formes de l'exocytose neuronale postsynaptiques, un processus fondamental qui est à la base de la composition de la membrane neuronale, la transmission et la plasticité synaptique. L'exocytose des ER postsynaptiques est au moins impliquée dans le soutien de la transmission basale et dans la potentialisation synaptique par la délivrance constitutive et régulée des récepteurs AMPA à la membrane plasmique (Lüscher et al., 1999). Le recyclage constitutif observé dans les neurones de l'hippocampe avec le marqueur classique des ER, le récepteur de la transferrine fusionné à la SEP, se produit à haute fréquence et présente diverses dynamiques (Jullié et al., 2014). Nous avons émis l'hypothèse que, à part le v-SNARE VAMP2 déjà identifié (Jurado et al., 2013) en tant qu'un acteur de la PLT, il devrait y avoir d'autres protéines v-SNARE impliquées dans l'exocytose des ER. La preuve de l'action de VAMP2 dans le recyclage constitutif des récepteurs AMPA est controversée: certaines études ont trouvé un effet de BoNT-B, qui clive VAMP2, sur les courants synaptique spontanés (Lüscher et al., 1999), mais d'autres affirment que BoNT-B ou TeNT n'ont pas d'effet sur l'amplitude des courants spontanés (Lledo et al., 1998, Lu et al., 2001). En outre, les courants excitateurs postsynaptiques spontanés ne sont pas affectés dans les cultures neuronales de souris VAMP2 KO (Schoch et al., 2001). De plus, dans l'exemple de l'exocytose présynaptique largement étudiée, il devient clair que la libération de vésicules synaptiques est assurée non seulement par le v-SNARE classique VAMP2, mais également par VAMP4, VAMP7 et Vti1A (Crawford & Kavalali 2015, Hua et al., 2011) qui jouent un rôle spécifique dans différents types de libération des vésicules synaptiques. Par conséquent, divers mécanismes SNARE neuronales peuvent être l'un des moyens de réguler étroitement et localement la sécrétion présynaptique. Nous avons étudié le rôle des protéines v-SNARE par microscopie à fluorescence des cellules vivantes et électrophysiologie pour déterminer les mécanismes

moléculaires sous-jacents à la diversité de l'exocytose des ER dans les dendrites neuronales.

Observation de l'exocytose de VAMP-SEP dans les neurones de l'hippocampe

Nous avons commencé l'étude des vSNARE postsynaptiques en identifiant les protéines candidates, potentiellement participant à la fusion membranaire lors de l'exocytose dans les neurones de l'hippocampe. Parmi les sept isoformes des protéines VAMP, seuls VAMP2, VAMP4 et VAMP7 sont exprimés dans les neurones de l'hippocampe. Ces trois protéines VAMP sont impliquées dans divers types d'exocytose dans les neurones et d'autres types cellulaires. Dans l'exocytose des vésicules synaptiques, la libération du neurotransmetteur synchrone et asynchrone évoquée ou la libération spontanée sont médiée par VAMP2, VAMP4 et VAMP7 respectivement (Deák et al., 2004 ; Raingo et al., 2012). Nous avons exprimé génétiquement les vSNARE candidates et le marqueur endosomal le TfR fusionné avec SEP dans les neurones d'hippocampe en culture. Les neurones étaient imagés avec un microscope confocal à disque rotatif afin d'identifier si les protéines surexprimées subissaient l'exocytose dans les régions somatodendritiques. En observant le comportement des protéines VAMP dans des conditions non stimulées, nous avons constaté que VAMP2 et VAMP4 étaient recyclés constitutivement par la membrane plasmique dans les régions somatodendritiques. Les organelles contenant VAMP2 subissaient l'exocytose significativement moins fréquemment que les organelles TfR-SEP positive. Par conséquent, il est peu probable que VAMP2 intervienne pour la totalité des événements d'exocytose du TfR-SEP. En revanche, les taux d'exocytose constitutifs de VAMP4 étaient comparables à ceux du TfR, ce qui suggère que le VAMP4 pourrait potentiellement être impliqué dans l'exocytose des ER postsynaptiques. Des études antérieures ont mis en évidence des événements d'exocytose somatodendritiques de VAMP7 dans les cultures neuronales très jeunes (0-3DIV) (Burgo et al., 2012; Gupton & Gertler 2010). Néanmoins, nous n'avons pas enregistré d'exocytose postsynaptique de VAMP7-SEP dans les préparations plus anciennes (14-16 DIV). Par conséquent, il n'est pas vraisemblable que VAMP7 joue un rôle significatif dans la fusion constitutive de

ER avec la membrane plasmique dans les régions somatodendritiques chez les neurones matures.

Ces résultats soulèvent de multiples questions. Si VAMP4 et VAMP2 sont impliquées dans l'exocytose dans les compartiments postsynaptiques des neurones de l'hippocampe, quelles protéines représenteraient leurs partenaires dans la formation du complexe SNARE? Pour former un complexe SNARE fonctionnel, les VAMPs (R-SNARE) requièrent une syntaxine (Qa-SNARE) et une protéine du type SNAP-25 (Qbc-SNARE). A ce jour, nous savons que SNAP-25, SNAP-23, SNAP-47, syntaxin4 et syntaxin3 sont présents sur la membrane postsynaptique où ils ont des implications physiologiques. Il a était suggéré que syntaxine4 et syntaxine3 étaient impliquées dans le trafic des récepteurs AMPAs régulé vers la membrane postsynaptique, mais les preuves d'un rôle de la syntaxine4 sont controversées (Kennedy et al., 2010; Jurado et al., 2013). Il serait possible d'étendre la technique d'imagerie décrite pour l'imagerie bicolore du recyclage de VAMP4-SEP et VAMP2-SEP conjointement avec les syntaxines postsynaptiques fusionnées à leur domaine C-terminal à un marqueur HA, visualisé à l'aide d'un un IgA antiHA fusionné avec un fluorophore (Kennedy et al., 2010). Ceci permettrait d'analyser la distribution spatiale de l'exocytose des VAMP par rapport aux sites d'enrichissement de syntaxine3 ou 4.

A la fois SNAP-23 et SNAP-25 ont étaient proposés de réguler spécifiquement le trafic des récepteur NMDA vers les synapses (Lau et al., 2010, Lan et al, 2001, Suh et al.). SNAP-47 est un partenaire potentiel de VAMP2 dans la médiation de l'exocytose dépendante de l'activité pendant la PLT (Jurado et al., 2013). Il est plus compliqué de mener des expériences d'imagerie avec les t-SNARE du type SNAP25, car ils manquent de domaine transmembranaire, pratique pour la fusion avec un marqueur sans interférer avec la fonction de la protéine.

L'étude d'inactivation des SNARE postsynaptiques

Après avoir identifié deux v-SNARE subissant l'exocytose dans les compartiments dendritiques, nous avons testé leur implication dans l'exocytose constitutive des ER. L'inactivation chronique de VAMP2 par expression génétique de la chaîne légère de l'endopeptidase TeNT (Pellizzari et al., 1999) n'a

pas entraîné de changements significatifs dans la fréquence des événements d'exocytose du TfR, ce qui est compatible avec le fait que VAMP2 n'est pas le médiateur de la majorité des événements de fusion lors de l'exocytose dans des conditions basales. De plus, la régulation négative de VAMP4 par l'expression des shRNAs a entraîné une réduction significative de l'exocytose constitutive de TfR-SEP qui pourrait être restaurée par l'expression d'une construction de récupération (rescue). Ces résultats indiquent que VAMP4 est un v-SNARE pour une fraction importante de l'exocytose post-synaptiqu. Il est néanmoins nécessaire de définir type de cargo peut être transporté par l'exocytose VAMP4 dépendant et quelle est l'importance fonctionnelle de ce recyclage.

Les stratégies de régulation négative chronique, comme la transfection de TeNT et de shVAMP4, sont souvent des sujets de mécanismes compensatoires. En outre, une telle stratégie suscite des inquiétudes quant à sa spécificité. La régulation négative à long terme de VAMP4 peut produire des effets en amont, notamment lié à son rôle dans le transfert rétrograde des endosomes précoces vers *trans*-Golgi (Steegmaier et al., 1999, Mallard et al., 2002). Pour surmonter les limitations mentionnées, on a procédé au bloc aigu des protéines VAMP2 et VAMP4 par dilution du TeNT et de l'IgG anti-VAMP4 dans les neurones en culture par la pipette patch tout en imageant simultanément l'exocytose des ER constitutives. Une fois encore, au cours de l'infusion de TeNT dans les cellules, il n'y a pas eu de diminution significative de l'exocytose observée, confirmant nos résultats précédents. Malheureusement, la complexité technique de l'expérience ne nous a pas permis de recueillir suffisamment de données pour juger de la signification statistique de l'effet obtenu après le chargement d'antiVAMP4 (le nombre de cellules chargé avec IgG antiVAMP4 n = 2). Néanmoins, dans les deux cellules, la diminution de l'exocytose constitutive était d'environ 25%, ce qui est comparable aux cellules témoins chargées avec une solution intracellulaire normale. Un certain nombre de contrôles doivent être effectués pour s'assurer que la diffusion d'anticorps dans le temps de l'expérience inhibe réellement VAMP4.

Conséquences sur la transmission synaptique et la plasticité

Nous avons appliqué les stratégies d'inactivation chroniques des vSNARE cnadidate pour explorer les conséquences fonctionnelles à long terme, notamment sur la transmission excitatrice basale et la potentialisation synaptique. La transfection de la chaîne légère de TeNT n'a pas influencé la fréquence ou l'amplitude basale des courants miniatures spontanées, ce qui confirme les résultats décrits dans (Lledo et al., 1998), mais contredit le rôle décrit dans le recyclage constitutif des récepteur AMPA (Jurado et al., 2013). L'expression de shVAMP4 n'a pas non plus influencé la fréquence et l'amplitude mesurées des courants miniatures spontanées. Il peut indiquer que les événements d'exocytose postsynaptiques VAMP4 dépendant ne sont pas impliqués dans la livraison des récepteurs AMPA pour l'entretien de la transmission basale. De plus, comme la quantification du marquage immunocytochimique montre seulement 50% de diminution de la fluorescence VAMP4 dans les cellules KD, il est possible que le shRNA généré ne soit pas suffisant pour bloquer complètement l'exocytose VAMP4 dépendant. A cet égard, il serait préférable de tenter une régulation négative de VAMP4 par une stratégie CRISPR / Cas9, un système d'inactivation génétique sélective récemment émergé (Incontro et al., 2014). L'absence d'effet sur les courants miniatures spontanés peut également signifier que l'exocytose constitutive médiée par VAMP4 apporte un autre cargo que les récepteur AMPA.

Pour tester directement l'implication de différents VAMP dans l'exocytose postsynaptique nécessaire à la potentialisation synaptique, nous avons voulu développer un protocole robuste dans les neurones cultivés. Une méthode classique pour l'induction de LTP en culture est le protocole dit de cLTP (PLT chimique). Il est basé sur l'exposition courte (3-5 min) des neurones à la glycine (100 μM) dans une solution libre de Mg^{2+} en présence de TTX, de picrotoxine et de strychnine (Park et al., 2006, Ahmad, et al. 2012 ; Passafaro et al., 2001, Kennedy et al., 2010). Le protocole cLTP nous donnerait la possibilité d'imagerie en temps réel des événements d'exocytose pendant la potentialisation synaptique. Au cours de mon travail de thèse, j'ai entrepris de nombreuses

tentatives pour reproduire un protocole cLTP qui générerais de manière stable une augmentation de niveau des récepteurs AMPA synaptiques dans les neurones d'hippocampe en culture. Néanmoins, dans mes expériences, le protocole publié n'a jamais donné une augmentation de l'intensité du marquage des récepteurs AMPA synaptiques à la surface de plus de 10-20%. Cette augmentation n'était pas stable d'une expérience à l'autre et, en outre, elle était bien inférieure à l'augmentation publiée de 50 à 100% (Ahmad, et al. 2012 ; Jurado et al., 2013). Dans le cadre temporel du projet présenté, j'ai varié plusieurs paramètres qui pouvaient influencer potentiellement la robustesse du protocole cLTP (voir le tableau 1), mais cela n'a pas affecté le résultat du protocole. L'instabilité des résultats obtenus peut être due à la grande sensibilité de l'excitabilité des neurones cultivés à des facteurs externes comme le milieux d'alimentation et les instabilités de température. Pour juger si augmentation de l'intensité du marquage des récepteurs AMPA synaptiques superficielles de 10-20% reflète une réelle potentialisation, il est nécessaire de mener des enregistremlent électrophysiologiques simultanées des courants synaptiques.

Pour surmonter cette incapacité à générer une robuste potentialisation dans des cultures dissociées, nous avons passé sur des expériences de potentialisation dans les tranches d'hippocampe organotypiques qui affichent des PLT robustes dans des travaux publiés (Brachet et al., 2015) ainsi que dans des équipes de recherche voisines de mon laboratoire. Nous avons réalisé la même stratégie de régulation négative chronique dans cette préparation afin d'explorer l'implication des VAMP dans l'exocytose régulée nécessaire pour l'expression de la PLT. La PLT a été stimulée dans les synapses entre les neurones des régions CA3 et CA1 des tranches hippocampiques. Les constructions de régulation négative ont été exprimées dans des neurones postsynaptiques pyramidaux CA1 au moyen d'une électroporation à cellule unique, qui consiste à introduire le plasmide uniquement dans les neurones postsynaptiques à l'aide de pulses électriques et assure un niveau d'expression plus physiologique qu'en cas d'une infection virale. Comme dans les explorations précédentes (Jurado et al., 2013, Park et al., 2004), l'expression de TeNT a altéré l'expression correcte de la PLT. Pourtant, dans les quelques neurones VAMP4 KD que nous avons pu enregistrer, shVAMP4 a été capable d'abolir la manifestation appropriée de la PLT. Pour conclure sur ce résultat, une expérience de sauvetage doit être effectuée.

Cependant, si cette tendance expérimentale serait confirmée, cela signifierait que l'exocytose des endosomes induite par VAMP4 apporterait une certaine charge PLT-associée à la membrane plasmique. Autrement, le phénomène observé pourrait être le résultat de certains effets en amont dans le trafic endosomal, en raison du caractère chronique de la régulation négative de VAMP4.